FUNCTIONAL CHARACTERIZATION OF LT-HSC METABOLIC ACTIVITY DEPENDENT ON AHR ACTIVITY

by

Everett R. Tate

A Dissertation Submitted in

Partial Fulfillment of the

Requirements for the Degree of

Doctor of Philosophy

in Environmental Health Sciences

at

The University of Wisconsin-Milwaukee

December 2019

ABSTRACT

FUNCTIONAL CHARACTERIZATION OF LT-HSC METABOLIC ACTIVITY DEPENDENT ON AHR ACTIVITY

by

Everett R. Tate

The University of Wisconsin-Milwaukee, 2019

Under the Supervision of Michael D. Laiosa Ph.D

The cells of the immune system are descended from multipotent hematopoietic stem cells (HSCs) that emerge during development. Multipotency means that a single progenitor HSC can differentiate into any cell of the immune system. HSCs are required to do this for the lifetime of the organism through a process called self-renewal, and as such, any perturbation during development or in the bone marrow can have a trickle-down effect, affecting the self-renewal capacity or ability to terminally differentiate. The aryl hydrocarbon receptor (AHR) is a known regulator of HSCs. The AHR is a transcription factor required for the detoxification of numerous xenobiotics and is agonized by the ubiquitous environmental contaminant 2,3,7,8-tetrachlorodibenzo-*p*-dioxin (TCDD). The advent of AHR-/- animal models have furthermore demonstrated that the AHR has an important role in the regulation of HSCs.

The overall goal was to characterize the effect of AHR agonism on long-term HSCs (LT-HSCs) – the cells at the top of the HSC hierarchy required for long-term,

lifelong reconstitution. Our approach was to utilize a lethal irradiation reconstitution model to compete vehicle treated HSCs against developmentally exposed TCDD HSCs.

During the course of this investigation, we sought further characterization of the effects of developmental AHR activation and absence on HSCs. Our approach was to compare AHR agonism and absence in HSCs across anatomical locations and developmental time points, and probe the differences in reactive oxygen species production and mitochondrial mass.

Finally, given the inadequacies of using surface markers alone, we sought to further elucidate how flow cytometry could be used to gather a population of HSCs that is more enriched for LT-HSCs. For this, we reframed how LT-HSCs are identified using flow cytometry and leveraged existing knowledge about their physical characteristics.

Taken together, the data presented herein supports 3 conclusions; 1: Developmental AHR agonism with TCDD decreases the repopulating ability of LT-HSCs; 2: AHR agonism and absence exhibit different effects on HSCs depending on developmental time and anatomical location, and 3: sorting HSCs based on surface markers in combination with selecting for low mitochondrial membrane potential, low mitochondrial mass, and low reactive oxygen species production can enrich for LT-HSCs better than using surface markers alone.

TABLE OF CONTENTS

LIST OF FIGURES

LIST OF TABLES

LIST OF ABBREVIATIONS

1.	AHR	Aryl Hydrocarbon Receptor
2.	AHRE	Aryl Hydrocarbon Response Element
3.	APC	Allophycocyanin
4.	ARNT	AHR nuclear translocator
5.	bHLH	basic Helix Loop Helix
6.	CD	Cluster designation
7.	C-KIT	Stem cell factor receptor, CD117
8.	Cy	Cyanine
9.	DCF	2′,7′-dichlorofluorescein
10.	FITC	Fluorescein isothiocyanate
11.	GD	Gestational day
12.	HSC	Hematopoietic stem cell
13.	IACUC	Institutional Animal Care and Use Committee
14.	KO	Knockout, null phenotype, -/-
15.	LSK	Lineage negative, Sca+. cKIT+
16.	LT-HSC	Long-term hematopoietic stem cell
17.	MMP	Mitochondrial membrane potential
18.	MPP	Multipotent progenitor
19.	NAO	Nonyl-acridine orange
20.	PAH	Polycyclic aromatic hydrocarbon
21.	PAS	Period, ARNT, Single-minded homology domain

22.	PBS	Phosphate buffered Saline
23.	PCR	Polymerase chain reaction
24.	PE	Phycoerthrin
25.	qRT^2 PCR	Qualitative real-time, reverse transcriptase PCR
26.	Rh123	Rhodamine 123
27.	ROS	Reactive oxygen species
28.	Sca-1	Stem cell antigen 1
29.	SEM	Standard error of the mean
30.	TCDD	2,3,7,8-Tetrachloro-*p*-dioxin
31.	WT	Wild type

CHAPTER 1

GENERAL INTRODUCTION

I. Introduction

The Aryl hydrocarbon receptor (AHR) is a member of the bHLH-PAS (basic Helix-Loop-Helix – Period/ARNT/Single minded) family of proteins. Other members of this family are involved in environmental sensing of oxygen concentration and circadian rhythm. AHR is the only bHLH-PAS member known to interact with xenobiotics. The uniqueness of the AHR lends its membership to another classification as an orphan receptor. While knowledge gained about the role of the AHR has primarily been through toxicological interactions using the potent ligand 2,3,7,8-tetrachlorodibenzo-*p*-dioxin (TCDD) due to its high affinity, the advent of transgenic animal models has indicated that the AHR has numerous endogenous and developmental roles. AHR-null (*Ahr-/-*) mice and rats have developmental defects in hepatic, hematopoietic, and renal physiology (Bennett et al., 2018; Fernandez-Salguero et al., 1997; Harrill et al., 2013; Schmidt et al., 1996; Singh et al., 2011). Given these developmental effects, many studies have utilized developmentally-exposed models to analyze the action of AHR. These are based, in part, on knowledge that humans, even in utero, are exposed to numerous polycyclic and halogenated aromatic hydrocarbons – both of which can activate the AHR. Moreover, the discipline of developmental toxicology looks at how the finely orchestrated developmental timings and cell migrations can be perturbed by exogenous compounds. While pursuing the question of the developmental role of the AHR, we made the interesting observation that there were unexpected similarities between the AHR-null and TCDD exposed HSCs.

Given the surprising similarities between AHR-/- and TCDD-exposed HSCs, we modified our question about the specific role of the AHR in HSCs. The central question

my dissertation focused on was what role is the AHR *no longer able* to perform if it is being agonized by TCDD. This contrasts with many traditional toxicology studies of

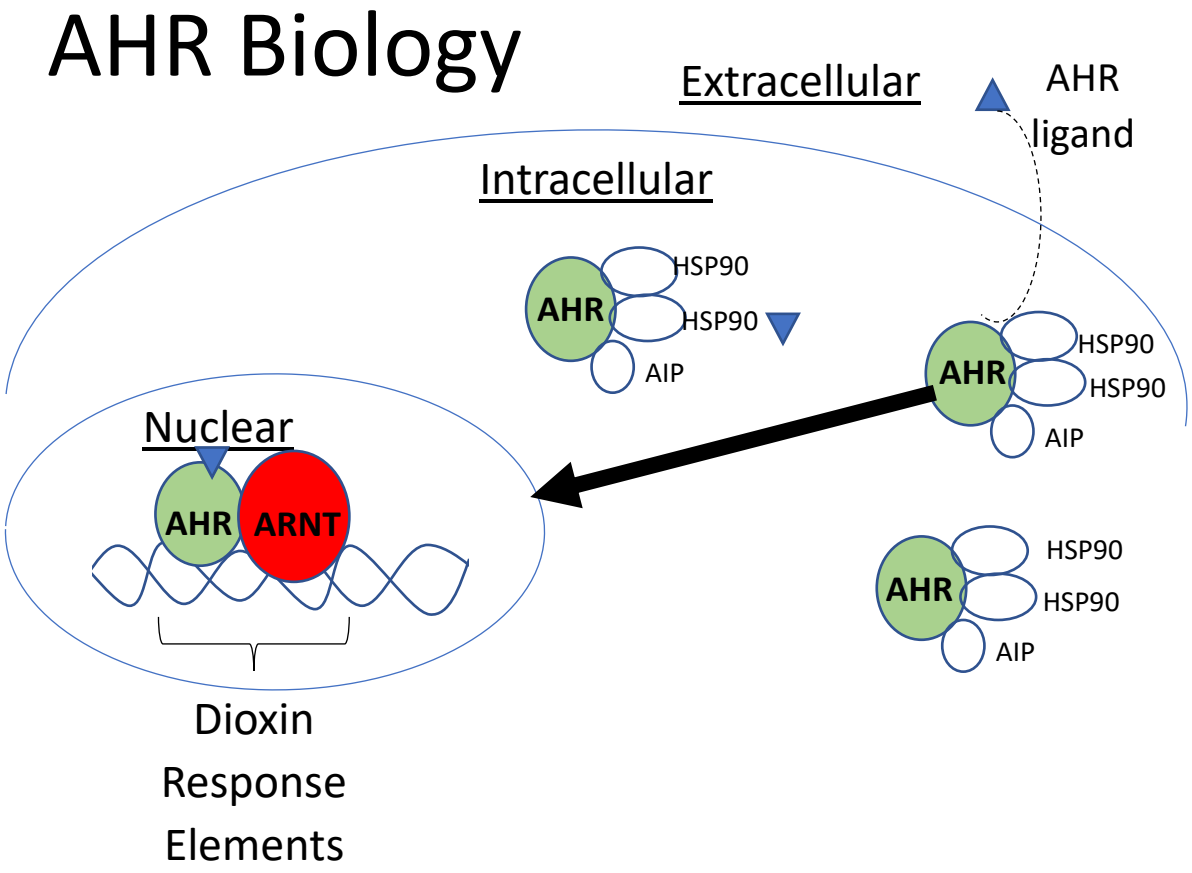

Figure 1. Canonical AHR agonism. The AHR is inactive in the cytoplasm and bound to heat-shock protein 90 (HSP90) and AHR interacting protein (AIP). When agonized, it gets translocated to the nucleus, and with its co-factor, AHR nuclear translocator (ARNT), binds to DNA and transcribes the dioxin response elements (DRE)

TCDD exposure that evaluate what happens to the AHR when it is agonized.

A. Historical perspective

Over 90% of human exposure to chlorinated polycyclic aromatic hydrocarbons is through food (JECFA 48, 2002). Dioxins encompass a broad group of compounds that

have similar structural characteristics of which chlorinated dibenzofurans and some polychlorinated biphenyls are members. While food is the primary source, dioxins are also produced as the result of combustion and can be found in cigarette smoke.

Western industrialization has led to numerous incidences of accidental exposure to dioxins which shed light on their toxicologic effects. An accidental exposure at a chemical plant in Nitro, West Virginia in 1949 left 122 workers with chloracne, a disfiguring eruption of cysts and pustules. Continued follow-up showed increased incidence of liver and blood diseases, however no association was found with increased cancer rates based on exposure to TCDD alone. If workers were exposed to TCDD at levels great enough to cause chloracne and exposed to an additional carcinogen, in this case 4-aminobiphenyl, there was increased mortality from soft tissue sarcoma, bladder cancer, and respiratory cancer (Collins et al., 1993).

TCDD produced as a byproduct of the herbicide 2,4-dichlorophenoxyacetic acid, known as Agent Orange, was liberally sprayed over forested areas in Vietnam from 1962-1967 and exposed a number of military personnel and native peoples to TCDD. Morbidity and mortality in the ‘Ranch Hand’ cohort is evaluated and published biennially and as such will not be discussed here (National Academies of Sciences, Engineering, and Medicine et al., 2018). 50 years later, TCDD continues to affect the native Vietnamese population by its persistence in soil and bioaccumulation in local food sources (Olson and Morton, 2019).

The Seveso, Italy industrial accident in 1976 released kilogram quantities of TCDD over a 6.9 sq. mi area. A 20 year follow up showed increased risk for lung cancer, lymphohematopoietic neoplasms and breast cancer (Pesatori et al., 2009).

Further retrospective analysis from three additional occupational exposures all demonstrated increased cancer incidence (Flesch-Janys et al., 1998; Hooiveld et al.,

Figure 2. Viktor Yushchenko – Former president of Ukraine showing the before and after effects of Dioxin poisoning. BBC News.

1998; Ott and Zober, 1996). Most recently, the attempted assassination of Ukrainian president Viktor Yushchenko with TCDD left him with chloracne (he has since recovered).

B. Evolutionary Perspective

An early paper written about the relationship between TCDD and the AHR postulated that exposing cells to this agonist could shed light of the role of the AHR in normal cell biology (Poland and Kende, 1976). This *non causa pro causa* (Lat: not the-cause for a cause) assumes that the AHR *must* be there to interact with dioxins; therefore, using TCDD is an appropriate avenue to study AHR in cell biology. Forty-

three years ago, this reflected our understanding of the AHR. Now, our understanding of the AHR extends well beyond toxicology, and into the disciplines of immunology and developmental biology. Further understanding emerges from comparative biologists that have yielded insights into AHR function in numerous species and have dated the AHR to the Cambrian explosion – 550 million years ago. This same investigation has also discovered that the function of binding PAHs and HAHs appears to have been acquired only in vertebrates (Hahn, 2002). *C. elegans* contains an AHR homolog that is insensitive to TCDD and is required for neuronal development (Qin and Powell-Coffman, 2004). The *D. melanogaster* AHR homologue, *Spineless (ss)*, acts to regulate the retinal cells required for color vision (Wernet et al., 2006). Similar to *C. elegans*, it also has a role in dendrite morphology (Kim et al., 2006b). The pleiotropic role of AHR in developing neuronal systems hints at an evolutionary raison d'être, and while this effect is less well studied in vertebrates, there are some interesting clues. AHR mRNA was found in the cortex, hippocampus, cerebellum and olfactory bulb in both mice and rats (Kainu et al., 1995; Kimura and Tohyama, 2017), and similar effects on hippocampal pathology were seen in both AHR null and TCDD exposed mice (Latchney et al., 2013). Moreover, perturbations of neuronal migration can be seen in mouse models using TCDD (Kimura et al., 2015, 2016). Given the developmental role of the AHR in invertebrates, it raises the critical question as to whether this role is maintained in vertebrates. Moreover, it raises the possibility that exogenous agonism could be removing it from such a role. Similar to *Drosophila* and *C. elegans,* AHR is highly expressed in developing mammalian sensory neurons (Juricek and Coumoul, 2018). Fascinatingly, this evolutionary role of AHR has been linked to some extent to human

pathology without using TCDD. Retinitis pigmentosa (RP) is a degenerative disease of the retina characterized by night blindness, progressive loss of peripheral vision followed by complete blindness. Two patients from a consanguineous Indian family presented with the characteristic symptoms of RP and whole exome sequencing revealed a spicing mutation in *AHR* which lead to a skipping of exon 9. Further analysis showed that the AHR in the RP patients had lost its transcriptional activity, thereby causing retinal degeneration (Zhou et al., 2018). Whether they had additional pathology aside of the RP was not reported, however given that AHR null mice exhibit considerable hepatic, reproductive, and immunological alterations, it draws the obvious contrast between a truncated protein (the RP patients) and having no protein altogether.

C. The Aryl Hydrocarbon Receptor and Immunity

In the absence of an agonist, the AHR is located in the cytoplasm as part of an AHR complex that includes heat shock protein 90 (HSP90), AHR interacting protein (AIP) and p23. Agonism by an exogenous or endogenous ligand leads to a conformational change that exposes the nuclear localization sequence and subsequent translocation to the nucleus. AHR dissociates from HSP90 and binds to AHR nuclear translocator via the PAS domain and binds to promoter regions of genes that contain the DNA sequence 5’ – GCGTG – 3’. This has been best characterized using TCDD mediated activation of the cytochrome P450 (CYP) family of xenobiotic metabolizing enzymes (Beedanagari et al., 2010). The xenobiotic response element (XRE – also Dioxin response element (DRE)) encodes the phase I metabolizing CYPs and also phase II glutathione transferases (Boverhof et al., 2006).

Studies using TCDD demonstrated an immunosuppressive effect that was linked to the induction of CD4+ regulatory T cells (Treg) (Funatake et al., 2005; Kerkvliet et al., 2002). The demonstration that AHR agonism can increase Treg cells later led to this being applied in mouse models of autoimmunity and other T-cell mediated autoimmune diseases (Funatake et al., 2005; Quintana et al., 2008; Ramirez et al., 2010; Veldhoen et al., 2008). Developmental exposure to TCDD can dampen the adaptive immune response to influenza virus (Vorderstrasse et al., 2004) but, the response against *Streptococcus penumoniae,* a common secondary infection after influenza, is enhanced with TCDD-induced AHR activation (Vorderstrasse and Lawrence, 2006). This could be due to specific AHR action in macrophages where it regulates proinflammatory signals (Kimura et al., 2009). Additionally enigmatic for the role of AHR in immune cells is how exposure to AHR agonists can improve autoimmune disease, as demonstrated with Crohn's (Benson and Shepherd, 2011), Type I diabetes (Kerkvliet et al., 2009), and a murine model of multiple sclerosis (Abdullah et al., 2019).

There is considerable evidence to support a physiological role of the AHR in the immune system absent of activation by environmental toxicants. The AHR may act as a pattern recognition receptor for bacterial infections (Moura-Alves et al., 2014). Moreover, AHR has been linked to B-cell development (Near et al., 1999; Vaidyanathan et al., 2017; Villa et al., 2017), and seems to have an anti-inflammatory role in dendritic cells (Quintana et al., 2015). In T-cells, the AHR seems to have a unique role. AHR expression is upregulated in CD4+ cells after activation (Quintana et al., 2008), and seems limited specifically to the Th17 subset of CD4+ cells (Veldhoen et al., 2008). In

HSCs, AHR expression is down regulated in the more quiescent bone marrow HSCs in contrast to the proliferative fetal liver HSCs (Venezia et al., 2004).

Taken together, there are some conclusions that can be drawn from the above studies. AHR activation has a different effect based on immune cell maturity, and can interact with different signaling pathways based on cell type. The combinatorial effect of the role of the AHR in development and its ability to modulate immune cells indicates that exogenous activation during development of hematopoietic progenitor cells could forever alter the host immune system. Our aim was to evaluate the AHR at the intersection of the developmental and toxicological pathways; to specifically ask why and how the AHR acts in HSCs whether agonized or absent.

D. Developmental Biology and Stem Cells

Mammalian life begins as a diploid cell – 1 set of chromosomes each donated from the male and female. From the moment of fertilization, the cell divides rapidly until it reaches the 32-cell stage, referred to as the morula. The cells at this point are totipotent, meaning they can turn into either the cells of the developing embryo or the placenta. Around day 4 in humans, the 32 cells of the morula begin to move down a path towards a specific type of cell. The inner cell mass are the cells that will develop into an embryo. At this point, these cells are referred to as pluripotent – capable of becoming any type of cell in the body, however they are restricted from returning to totipotency. As development progresses, the differentiation potential of cells becomes even more restricted. Embryonic development is a tightly regulated process that follows

very specific rules on timing and movement of these cells. Thus, the time spent *in utero* is especially sensitive to environmental toxicants that can affect the process, timing, or movement of these cells. Because embryonic pluripotent cells will create every organ, tissue, and cell, a perturbation at this timepoint has the potential to be carried throughout the lifetime of the organism.

E. Hematopoiesis

Hematopoiesis etymologically is literally the making of blood cells (Gk. αἷμα, "blood" and ποιεῖν "to make"). In a human adult, this process is capable of creating an estimated 1 trillion cells per day (Ogawa, 1993). All hematopoietic lineages descend from a very small population of hematopoietic stem cells (HSC). In contrast to the pluripotent stem cells found in the embryo, HSCs are lineage restricted meaning that they can differentiate only into a closely related family of blood cells, referred to as multipotency. Comparatively however, HSCs maintain the stem-cell specific capacity for self-renewal. This crucial function of stem cells dictates that of two daughter cells produced, 1 or both can replace the original. In mammals, this allows for rapid proliferation in times of trauma or infection without depleting the actual ‘stock’ of HSCs. This function also serves an additional purpose. The high metabolic activity required to sustain rapid proliferation, by extension, leads to increased risk of DNA-damaging reactive oxygen species (ROS) being produced. Increasing evidence has supported the idea that mitochondria are active participants in the self-renewal/differentiation axis, and possibly even cell fate determinants. Loss of mitochondrial carrier homolog 2 (MCTH2) increases mitochondrial mass and oxidative phosphorylation (OXPHOS) which drives

HSC differentiation (Maryanovich et al., 2015). Altering the tuberous sclerosis complex-mammalian target of rapamycin (TSC-mTOR) pathway increases ROS in HSCs forcing an exit from quiescence (Chen et al., 2008). Deletion of forkhead transcription factor 3 (Foxo3a) causes increased ROS and an inability to maintain quiescence in HSCs, indicating its importance for self-renewal (Miyamoto et al., 2007). A regulator of cellular metabolism, Liver kinase B1 (LKB1), was found to inhibit mitochondrial biogenesis and force HSCs from quiescence then quickly into apoptosis when absent (Gan et al., 2010). In line with this, apoptosis due to elevated ROS can be induced in HSCs missing thioredoxin-interacting protein (TNXIP) (Jung and Choi, 2014). Sirtuin 3 (SIRT3) was found to be enriched in HSCs where it acts to reduce the stress response (Brown et al., 2013). Ataxia telangiectasia mutated (ATM) inhibits oxidative stress in HSCs and knockout models demonstrated a failure of HSC self-renewal (Ito et al., 2004). Interestingly, knocking out protein tyrosine phosphatase mitochondrial 1 (PTPMT1) reduces OXPHOS and increases glycolysis leaves self-renewal capacity intact, but the proliferation capacity completely inhibited (Yu et al., 2013). Chemical inhibition of PTPMT1 *ex vivo* has been used to expand HSCs (Liu et al., 2015). In contrast, mitochondrial disease mice (mito-mice) demonstrate impaired self-renewal but no change in proliferative capacity (Inoue et al., 2010). Of significant importance is that in each of the molecular models listed above, deletion of Foxo3, LKB1, PTPM1, ATM, or mito-mice, had little impact on lineage restricted progenitors, only HSCs (Chen et al., 2008; Gan et al., 2010; Ito et al., 2004; Miyamoto et al., 2007). Since lineage restricted progenitors have increased mitochondrial activity (Inoue et al., 2010) , they may have compensatory anti-oxidant elements expressed at higher levels. Taken together, low

ROS is necessary to maintain quiescence, and increased ROS favors differentiation. Apoptosis is a highly conserved and self-regulatory mechanism of programmed cell death that prevents the spread of faulty cellular 'machinery' to daughter cells. HSC apoptosis in the LKB1 and TNXIP models may indicate that this is a safety mechanism for aberrant HSCs. Investigations using immortalized mammary epithelial cells demonstrated that the 'age' of mitochondria drive the asymmetric diving process (Katajisto et al., 2015a), and while this remains unconfirmed in HSCs, one could *a priori* interpret the data demonstrating increased ROS forcing differentiation over self-renewal as evidence that HSCs intrinsically regulate their oxidative and metabolic health.

In the normal self-renewal state, the newly replaced progenitor HSCs then return to their quiescent metabolic state. Adult HSCs exist in a quiescent state in the bone marrow (BM) in contrast to fetal HSCs which proliferate rapidly and can be found in numerous anatomical sites before their final egress, before birth, to the bone marrow. Again, this shows the potential danger of the *in utero* environment. The protective self-renewal mechanism found in the adult BM is not found in fetal HSCs, hence damage sustained to the cells at this point will be carried through the lifetime of the organism.

I. First Wave of Developmental Hematopoiesis

Almost 100 years ago, it was reported that blood and endothelial progenitors arise in the yolk sac of developing vertebrates. Since embryonic hematopoiesis has been conserved throughout evolution, studying murine HSC development correlates closely with human HSC development – gestational day (GD) 7.5 in the mouse is approximately 16-20 gestation in humans (Tavian and Peault, 2005). In the mouse,

what is referred to as primitive hematopoiesis occurs in the yolk sac (YS) at GD 7.5. The etymology of ‘primitive’ was based historically on the appearance of the erythroblasts. Early erythroblasts were large and nucleated and termed ‘primitive’, whereas the enucleated erythroblasts produced later were termed ‘definitive’. It was believed that the cells produced in the yolk sac were transient, only produced to sustain the embryo until the definitive wave of hematopoiesis. However, a number of studies have indicated that the cells produced *de novo* from the yolk sac are anything but primitive, and indispensable for the functionality of the organism. Fate-mapping experiments indicated that YS-derived macrophage-like progenitors go on to form the tissue resident macrophages found in the liver (Kupffer cells), brain (microglia), lung (alveolar macrophages), and epidermis (Langerhans cells) (Alliot et al., 1999; Gomez Perdiguero et al., 2015). Additional findings using a mouse model devoid of macrophages but that left developmental HSC lineage intact lacked these tissue resident macrophages and moreover, exhibited a severe osteopetrotic phenotype, meaning that osteoclasts, the monocyte like cells responsible for remodeling our bone marrow, are also derived from the macrophage progenitors (Jacome-Galarza et al., 2019). Lymphoid lineage T- and B- cells have also been found in the GD9.5 YS (Yoshimoto et al., 2011, 2012). *Ncx1-/-* mice die at GD11 due to lack of cardiac contractions, however hematopoiesis from GD7 to GD9 is unaffected. A study using the *Ncx1-/-* model demonstrated that the anatomical site that HSCs are thought to emerge, called the aorta-gonad-mesonephros (AGM), is in fact seeded by hematopoietic progenitor cells from the YS (Lux et al., 2008). Additional lineage studies were

performed by activating *Rosa* reporters in YS cells that resulted in the detection of *Rosa* reporters in adult blood cells (Samokhvalov et al., 2007).

So, while YS hematopoietic cells may not be deserving of the term ‘primitive’, they consistently fail in the most crucial test of a hematopoietic stem cell. The gold standard definition of an HSC is its ability to reconstitute an entire blood system for life in an irradiated recipient. To date, no study has been published demonstrating the repopulating ability of hematopoietic cells in the YS; seemingly, they lack the ‘stem’ness component of HSCs.

II. Second Wave of Definitive Hematopoiesis

The second wave of hematopoietic cell generation begins with the onset of the embryonic heartbeat at GD 8.25. While this does overlap with the first wave, the hematopoietic progenitors produced at this point also lack the ‘stem’ness seen in the YS. So, while they retain the multipotency to produced erythroid, myeloid, and lymphoid lineage cells, they lack the capacity for self-renewal. Referring back to the *Ncx-/-* model in which fetal mice fail to initiate a heartbeat, the same multipotent progenitor cells that arose at GD 7.5 in the YS are still circulating at GD 10 (Lux et al., 2008). The first definitive, by virtue of having the ability to reconstitute the blood system of an irradiated host, appear at GD10.5 in the AGM region. The AGM region developmentally stems from the para-aortic splanchnopleure and is one of the sites that gives rise to HSCs *de novo*. However, the AGM is neither a site for proliferation nor differentiation. HSCs share a developmental lineage with endothelial cells and arise from specialized cells

called hemangioblasts that emerge from the dorsal aorta and express many of the same surface markers (Godin and Cumano, 2005). There is still a debate as to whether this is a single linear process, or whether the emergence from the AGM is the final step in an early maturation process. Rybtsov et al., while not disagreeing with the emergence of HSCs from the AGM, demonstrated that the HSC lineage cells are primed as early as GD 9.5 in the luminal and subluminal layers of the dorsal aorta (Rybtsov et al., 2011). Runx1 belongs to a family of DNA binding transcription factors and is transiently required for HSC emergence from the hemogenic endothelium. Interestingly, while both HSCs and endothelial cells express Runx1, data generated from *Runx1-/-* embryos indicated that the endothelium was unaffected but failed to make hemangioblast clusters (Chen et al., 2009). This correlates with additional findings that Runx1 is, by itself, able to undo the endothelial commitment by the HoxA3 transcription factor (Iacovino et al., 2011). Curiously, the intact endothelium with absent hemangioblast clusters described by Chen et al. is also seen when compounds are given to block the effect of nitric oxide synthase (*nos*), the protein that makes nitric oxide (NO) (North et al., 2009). NO plays an integral role in vascular tone and angiogenesis and the use of NO donors can rescue the impaired HSC generation seen in nos knockout mice Additional studies using the *Ncx1-/-* embryos indicated that the shear stress of blood traversing the aorta is what leads not only to HSC formation in the endothelium, but can induce Runx1 expression (Adamo et al., 2009). As NO can be induced by shear stress, the timing of the embryonic heartbeat in the mouse with the emergence of hemangioblast clusters is intriguing, but questions still remain.

III. Fetal Liver

The fetal liver is a unique anatomical location for HSCs. Both the human and murine fetal liver are the primary sites of HSC expansion, however it is unable to produce HSCs *de novo*. The anatomical source of HSCs that arrive in the fetal liver remains unclear. Temporally, HSCs are found in the fetal liver 1 gestational day (GD 11.5) after their emergence from the AGM. The early fetal liver is contains more erythroid progenitors than lymphoid, and it is likely that the initial definitive erythroid production is in fact seeded by the erythroid progenitor cells produced in the YS (Lux et al., 2008; Mikkola, 2006). YS HSC-precursors are unable to repopulate a blood system, hinting that the HSCs that emerge from the AGM are the HSC source in the fetal liver. HSCs expand until GD 16.5, and then begin their egress to the bone marrow before birth. The fetal liver microenvironment that sustains such growth remains elusive. Fetal liver HSCs are actively and symmetrically self-renewing, in contrast to the quiescent HSCs found in the bone marrow. This raises an obvious question as to whether the HSCs in the fetal liver are fundamentally different than HSCs in the bone marrow, or whether it's the composition of cytokines and growth factors produced that allow for expansion.

IV. Placenta

The placenta is the only organ that is grown and excreted, only to be grown again. It is required for nutrient uptake, oxygen exchange, waste elimination, has its own endocrine system, and modulates the maternal immune system. While HSCs can

be found in the placenta, it was assumed that they were AGM-originated and fetal liver-expanded. However, a question remained as to how the low numbers of HSCs produced in the AGM at GD 10.5 could lead to the large numbers of HSCs seen in the fetal liver at GD 12. In 2005, two groups independently verified that HSC activity in the placenta is concurrent with HSC emergence from the AGM (GD 10.5) (Gekas et al., 2005; Ottersbach and Dzierzak, 2005). In terms of anatomical circulation, the placenta is downstream of the dorsal aorta, and the fetal liver is downstream from the placenta, so it was presumed that the HSCs found in the placenta were AGM originated. However, support for *de novo* placental HSC generation came from studies using *Ncx1-/-* knockout mice which demonstrated cellular markers of HSCs in mice that failed to initiate a heartbeat. At its peak at GD 11.5-12.5, the HSC population in the placenta is 15 times greater than can be found anywhere else in the fetus, but is replaced shortly thereafter by the fetal liver (Gekas et al., 2005, 2010). Interestingly, further analysis indicated that placental HSCs had retained the capacity for multipotency at a time when the fetal liver is producing large amounts lineage restricted erythrocyte and megakaryocyte populations (Alvarez-Silva et al., 2003; Gekas et al., 2005). Taken together, this indicates that despite their similarity by HSC surface markers, the fetal liver and placental microenvironments provide different growth and differentiation cues. Assessing AHR agonism in these compartments could shed light on if the effects of TCDD on fetal HSCs are intrinsic to the HSCs themselves, or dependent on the surrounding milieu.

V. Bone Marrow

The bone marrow (BM) is the final transit for HSCs in mammals. Their residence in the bone marrow niche sustains hematopoiesis for the life of the organism. And it is here where the phenotype of HSCs fundamentally changes. In contrast to fetal HSCs that are rapidly dividing, BM HSCs maintain a state of quiescence. Similarly, fetal HSCs have the capacity to symmetrically self-renew, meaning they can proliferate without differentiating. However, long-term HSCs (LT-HSC) in the BM asymmetrically divide which means that of two daughter cells produced, one is already polarized to a terminally differentiated fate. Biophysically, placental connection to the maternal vasculature increases the oxygen level is which FL HSCs are expanding to ~8% (Abdollahi et al., 2011). This is in stark contrast to BM HSCs that are found in the poorly perfused BM regions that are thought to have ~1% oxygen (Parmar et al., 2007). Not only is the hypoxic environment tolerated by LT-HSCs but seems to be an absolute requirement for their health and longevity. ROS, a byproduct of oxidative phosphorylation amongst other things, seems to skew HSCs towards terminal differentiation as opposed to self-renewal (Jang and Sharkis, 2007). By surface marker phenotype, HSCs appear similar, however HSCs collected specifically from the lower oxygen areas of the bone marrow are more enriched for LT-HSCs (Parmar et al., 2007; Winkler et al., 2010). Hypoxia causes stabilization of hypoxia-inducible factor (HIF1a) which shifts cellular metabolism away from mitochondrial oxidative phosphorylation and towards glycolysis. Under hypoxic conditions, energy is produced from the fermentation of glucose, called glycolysis. While this produces considerably less energy than mitochondrial oxidative phosphorylation, it has a few advantages for quiescent cells.

First, it allows for LT-HSCs to maintain their quiescent state, demonstrated by the finding that HIF1a deletion results in the loss of quiescence (Suda et al., 2011). Limited energy availability means limited energy utilization, therefore all non-essential metabolic needs are drastically reduced. Secondly, relying on glycolysis means less free radical production from the mitochondria. ROS can have deleterious effects on HSC DNA with evidence supporting that damage induced at the top of the hematopoietic hierarchy will trickle down into terminally differentiated cells (Norddahl et al., 2011). Paradoxically, HIF1a is seems to be stabilized in LT-HSCs after they leave the hypoxic niche indicating that this is intrinsically regulated (Nombela-Arrieta et al., 2013; Piccoli et al., 2007).

The mass and activity of mitochondria in LT-HSCs remains an open question. A shift from mitochondrial oxidative phosphorylation would decrease the mitochondrial membrane potential (MMP), and subsequently, has been used to enrich for LT-HSCs in the bone marrow (Simsek et al., 2010a). A key proliferative surface marker, CD34, that is highly expressed on fetal HSCs but downregulated in adult HSCs, is upregulated parallel with mitochondrial biogenesis (Mantel et al., 2010a). The combined studies of Simsek et al and Mantel et al seem to indicate that LT-HSCs have abundant, albeit inactive, mitochondria. In agreement with this were studies of oxygen consumption in HSCs that indicated that while HSCs and multipotent progenitors have comparable mitochondrial mass, oxygen consumption, ATP production, and maximal respiratory capacity were markedly lower in HSCs (de Almeida et al., 2017). This stands in contrast to findings that demonstrate that HSCs with a low mitochondrial mass are better suited to reconstitute an irradiated recipient (Romero-Moya et al., 2013). Reconciliation may lie

in better characterization of the xenobiotic efflux pumps that can confound fluorescence results (de Almeida et al., 2017; Snoeck, 2017).

The question of reconciliation underlines a more complex issue in HSC biology. Whether its MMP, CD34, low mitochondrial mass, or any other combination of markers, the issue is not that one is right, and one is wrong, it's how the markers are being used to identify LT-HSCs. De Almeida et al used Lin-Sca+cKIT+(LSK) CD48- to enrich for LT-HSCs, whereas Simsek et al. used LSK CD34- Flk2-. Under this lens, the results aren't contradictory at all – rather, their respective data support their findings for HSCs *only with those combinations of markers*. This underlies the inherent difficulty in the field of HSC biology that no combination of surface markers will indisputably select for LT-HSCs. Therefore, we wanted to combine metabolic vital dyes in addition to surface markers to better define HSCs, and assess how the combinatorial effect can better inform the role of AHR agonism or absence in hematopoiesis throughout development.

F. Aryl Hydrocarbon Receptor and Hematopoietic Stem Cells

There are a number of studies that have demonstrated a role for AHR in hematopoietic development (Singh et al., 2011, 2014). Antagonists of the AHR have been shown to promote expansion of HSCs (Boitano et al., 2010; Gu et al., 2014). In agreement with this is the demonstration that not only are there more LSKs from AHR-/- mice, but that they proliferate faster than wild type LSKs (Gasiewicz et al., 2010; Singh et al., 2011). AHR expression was shown to change if cells were actively proliferating or quiescent (Singh et al., 2009). Taken together, it seems that the AHR has a role in

maintaining the quiescence vs proliferation balance in HSCs. HSCs are capable of sustaining blood supply throughout the lifetime of an organism, however these cells show a gradual shift away from lymphoid potential for unknown reasons (Sudo et al., 2000). In agreement with the role of AHR in maintaining quiescence, aged AHR-/- mice have decreased reconstitution capacity due to premature HSC exhaustion (Singh et al., 2014).

It's worth observing that the forced exit from quiescence and consequent HSC exhaustion in the molecular models is similar to the AHR-/- models. Given the apparent role in HSC quiescence, the question becomes does the AHR directly involve the mitochondria. TCDD induced ROS production accelerates keratinocyte differentiation by depleting the mitochondrial glutathione pool (Kennedy et al., 2012). Similar mitochondrial perturbations with TCDD were reported in epididymal spermatozoa (Fisher et al., 2005) and rat hepatocytes (Aly and Domènech, 2009). To the specificity of the AHR and not the xenobiotic response element battery of proteins, ROS production was shown to be dependent on the AHR, but not the phase 1 monooxygenases (Senft et al., 2002a, 2002b). An intriguing link between AHR and mitochondrial function was demonstrated by the direct protein-protein interaction of AHR and ATP5a1, a subunit of the ATP synthase complex (Tappenden et al., 2011).

G. Study Rationale

There is a curious similarity between the toxicology studies demonstrating that in HSCs, TCDD induces mitochondrial dysfunction and increases ROS, therefore forcing

exit from quiescence, and the developmental biology findings whereby AHR-/- HSCs seem to show virtually the same thing. This led us to question if the TCDD effect is not the result of AHR translocation to the nucleus and subsequent upregulation of the XRE genes, rather that it is removing the AHR from another, as yet unknown, function.

HSCs are required to maintain the blood system for the lifetime of the organism. As such, their lifetime health is intimately tied to the overall health of the organism. Perturbations to HSCs, whether in utero or in adulthood, can deplete the HSC pool causing premature exhaustion, or can affect lineage commitment resulting in immunosuppression or autoimmunity.

Our first aim was to evaluate the hypothesis that AHR agonism via TCDD was the result of AHR being removed from another role. To test this, we evaluated wild type, TCDD-exposed, and AHR-/- HSCs in fetal liver and placenta in addition to bone marrow. Given the different metabolic and proliferative capacity of HSCs between these tissues, we wanted to evaluate if AHR agonism would affect the dynamics and behaviors of HSC populations in a manner similar to AHR absence. What we found was that only in certain populations using various surface markers was there an effect from TCDD vs AHR-/-.

In the course of testing Aim 1, it was found that the combination of markers to indisputably identify HSCs is a barrier to answering our question. Contradictory findings of mitochondrial mass in HSCs illustrate this problem. This becomes even more confounding when you consider that we were evaluating two fetal HSC compartments against adult bone marrow. As a result of this, we sought out ways to better define HSCs within our own combinations of markers, in addition of physical characteristics.

What we found was that gating HSCs by size and intracellular complexity gave three populations (I, II, and III) of which the smallest and least complex (Population I) was enriched for HSCs. When compared against population III, population I had less ROS production, lower mitochondrial membrane potential, and lower mitochondrial mass.

Encouraged by these findings, we applied the same gating strategy to studies done for our first aim. Using the same markers between all three tissues in addition to applying our gating strategy allowed for a unique look at how AHR agonism or absence affected HSCs. What we found was that increased ROS in population I due to AHR agonism was dependent on the presence of the stem cell growth factor receptor (cKIT) in the fetal liver and bone marrow, however the ROS increases in AHR null mice were independent of surface marker combinations.

The results of these studies add to HSC and AHR biology. The ability to enrich for HSCs by using markers and physical characteristics has implications for clinical HSC-transplant biology. Similarly, our finding that the increases in ROS in AHR-/- were independent of surface marker combinations indicate that the effect of TCDD exposure may specifically target the stem cell population. That notwithstanding, it may also indicate why HSC exhaustion is seen with both AHR agonism and absence, and how it affects downstream lineage committed cells.

CHAPTER 2

MATERIALS AND METHODS

DMEM complete: Dulbecco's Modified Eagle Medium (Mediatech, Manassas, VA); supplemented with 10% fetal bovine serum (FBS; Invitrogen, Grand Island, NY), 1% L-glutamine (Invitrogen), 1% 1 M HEPES (Invitrogen), 0.01% 0.5 M 2-Mercaptoethanol (EMD, Gibbstown, NJ), 0.001 mg/gL gentamycin (Life Technologies), filter sterilized and stored at 4°C in the dark.

Serum-free DMEM: Dulbecco's Modified Eagle Medium (Mediatech); supplemented with 1% L-glutamine (Invitrogen), 1% 1 M HEPES (Invitrogen), 0.01% 0.5 M 2-Mercaptoethanol (EMD, Gibbstown, NJ), 0.001 mg/mL gentamycin (Life Technologies), filter sterilized and stored at 4°C in the dark.

FACs buffer: Fluorescence activated cell sorting buffer; consisting of Hank's buffered saline solution (HBSS; Corning Cell Gro, Herndon, VA), supplemented with 0.5% FBS (Invitrogen) and 0.1% sodium azide (J.T. Baker/Avantor, Center Valley, PA), then stored at 4°C in the dark.

RBC lysis buffer concentrate: Red blood cell lysis buffer, consisting of 155mM NH_4Cl, 12mM $NaHCO_3$, 0.1mM EDTA.

Experimental animals

All animal procedures were conducted according to NIH *Guide for the Care and Use of Laboratory* Animals and with the approval of the Institutional Animal Care and Use Committee (IACUC) at the University of Wisconsin-Milwaukee. C57BL/6J (B6) and B6.129-*AHR*^{tm1Bra}/J (AHR) mice used for analysis were obtained directly from the Jackson Laboratory Bar Harbor Maine, or were offspring from original Jackson mice.

NOD.Cg-*Kit*$^{W\text{-}41J}$ *Tyr* $^{+}$ *Prkdc*^{scid} *Il2rg*^{tm1Wjl}/ThomJ (NBSGW) mice were ordered from Jackson laboratory.

After overnight pairings, the presence of a vaginal mucus plug was used as evidence of mating and designated as gestational day 0.5. For breeding resulting in live birth offspring, mice were placed together for 4-7 days and checked for the presence of vaginal plug each morning. However, for time-sensitive breeding, animals were placed together between 3 p.m. and 5 p.m. and the presence of a vaginal plug was determined between 7 a.m. and 9 a.m. the next morning to ensure fetuses were as close to developmental age as possible.

For breeding resulting in live birth offspring after gestational exposure to TCDD, all multiparous mothers were used. This change in protocol came about due to high percentage of neonatal deaths, possibly due to a lack of mothering experience.

All mice were housed in micro isolator cages in a specific pathogen free facility at the University of Wisconsin-Milwaukee, provided food and water ad libitum, and maintained on a 12:12 hour light cycle.

Genotyping of Transgenic Mouse Strains

Tissue samples were collected as ear punches from adult mice and tail samples from fetal mice. Ear tissues are digested with rotation at 55°C overnight and 190 µL DirectPCR Lysis Reagent (ViaGen Biotech, Los Angeles, CA) plus 10 µL Proteinase k (ViaGen Biotech). Fetal tail tissues for digested in 160 µL DirectPCR lysis buffer plus 40 µL proteinase k for 20 minutes with intermittent vortexing in a locking cap 1500 µL microcentrifuge tube (Eppendorf, USA). Proteinase K in samples tubes was then

inactivated for 1 hr at 85°C. Primers were thawed over ice. Reaction samples were mixed, each containing 12.5µL MyTaq, 0.5µL each primer, 9.5µL DNA free water, and 2µL of genomic DNA. Samples were run in thermal cycler according to specifications listed on table 3 PCR samples to run on a 2% agarose gel for 45 minutes.

TCDD

TCDD (Cambridge Isotopes, Andover, MA) was diluted in 1,4-dioxane (Sigma-Aldrich, St. Louis, MO) to a working stock concentration of 0.2 mg/mL. Appropriate volume of 1,4-dioxane was subsequently transferred to a sterile 15 mL conical tube and the liquid was evaporated in a chemical fume hood. The remaining TCDD residue was then suspended in olive oil (Filippo Berio, Hackensack, NJ) to a concentration of 3µg/mL. For dosing of vehicle control mice, olive oil was added to a tube from which an equal volume of 1,4-dioxane had been evaporated.

For experiments where LSKs were isolated from GD 14.5 fetal livers, pregnant mice in the treatment group were exposed to either 3µg tcdd/kg of body weight by oral gavage on gestational day is 0.5 and 7.5, or olive oil vehicle control on the same days. Doses were given 7 days apart to ensure a relatively constant level of tcdd throughout because the half-life of tcdd and a C57BL/6 mouse is approximately one week (Gasiewicz et al., 1983; Miniero et al., 2001; Weber and Birnbaum, 1985).

Mitochondrial and reactive oxygen species profiling of cells using flow cytometry

Analysis of mitochondrial mass was acquired with MitoTracker Deep Red 5nM (ThermoFisher Cat no. M22426) and nonyl-acridine orange 10uM (Invitrogen Cat no. A1372). Mitotracker deep red is a nonproton gradient sensitive dye that accumulates in

mitochondria. Nonyl acridine orange binds to cardiolipin in all mitochondria regardless of their energetic state.

Analysis of membrane potential was acquired using JC-10 5uM (Sigma Cat no. MAK159) and Tetramethylrhodamine ethyl ester (TMRE) 200nM (Sigma Cat no. 87917). JC-10 is a cationic, lipophilic dye that forms red fluorescent aggregates (λex = 540/λem = 590 nm) in polarized mitochondria. In cells with non-polarized mitochondria, JC-10 remains in its monomeric, green fluorescent form (λex = 490/λem = 525 nm). TMRE is a positively charged rhodamine-based dye that fluoresces red (λex = 549/λem = 574 nm) after it localizes in polarized mitochondria.

ROS analysis was performed using 2',7'-dichlorodihydrofluorescein diacetate (H2DCFDA) 1uM (Thermofisher Cat no. D399). H2DCFDA passively diffuses into cells where it is de-esterified and turns to highly fluorescent 2′,7′-dichlorofluorescein (DCF) in the presence of ROS.

Fetal Liver HSC Isolation and Cell Sorting

Pregnant C57BL/6J or AHR mice were euthanized by CO2 asphyxiation according to the AVMA guidelines on euthanasia on GD 14.5. Dissections in tissue harvest were carried out within a two-hour window each day to minimize time of day fluctuations in HSC numbers. Fetuses were removed to culture dishes containing cold DMEM complete media.

For all fetal HSC experiments, fetal livers were removed from individual fetuses, mechanically dispersed in DMEM complete, and passed through sterile Nitex nylon mesh (80µL, Wildco, Yulee, FL) to form single cell suspensions. After centrifugation at

300 G for 5 minutes, RBC lysis buffer was added for 5 minutes. 3 mLs of DMEM

Table 1. Monoclonal antibodies, clones and fluorochromes used in flow cytometry

Antibody	Clone	Fluorochromes Conjugates
B220	RA3-6B2	PE
CD3	145-2C11	PE-CF594
CD4	RM4-5	PE-Cy5
CD11b	M1/70	Alexa488
CD19	1D3	FITC
CD45	30-F11	PE
CD45.1	NDS58	PE
CD45.2	104	FITC
CD45R/B220	RA3-6B2	Biotin→ SA PE-TR
CD8	53-6.7	PE-Cy7
CD150	TC15-12F12.2	PE-Cy5
CD48	HM48-1	PE-Cy7
cKIT	2B8	Alexa647
GR-1	RB6-8C5	APC-Cy7
LY-76	TER119	Biotin→ SA PE-TR
LY6G/LY6C/GR-a	RB6-8C5	Biotin→ SA PE-TR
Sca-1	E13-161.7	PE

FITC=fluorescein isothiocyanate
PE=phycoerythrin
Cy=cyanine
APC=allophycocyanin
TR=Texas Red
SA=Streptavidin

complete was added, cells were spun down at 300g for 5 minutes, and pellet was re-suspended in DMEM serum-free media.

Cells were sorted on a BD FACSAria III, DIVA version 6.1.3, equipped with four laser (violet 407 nM, blue 488 nM, yellow/green 561 nM and red 633 nM) and 4-way sorting capacity. Just prior to cell sorting, 10µL of the vital die Sytox blue (Life Technologies), 1 mM, diluted 1:80, was added to label nuclei from dead or dying cells with permeable membranes. Sytox blue negative cells were electronically gated on the 407 Violet B detector. Subsequently, doublets were excluded using FSC height x width and SSC height x width discrimination. FITC cells were detected on the Blue B detector with a 502LP mirror and a 530/30 filter. PE, PE-Texas red, PE-Cy5, and PE-Cy7 stained cells were detected on the yellow-green D detector with a 582/15 filter set. APC and APC-Cy7 stained cells were detected on the Red B detector with a 660/20 filter set.

Antibodies for Lymphocyte Staining

Primary fluorochrome-conjugated monoclonal antibodies were used in flow cytometry analysis and cell sorting. All antibodies were used at titrated concentrations and were purchased from BD Biosciences unless otherwise noted. Biotin-conjugated antibodies used for the lineage cocktail included CD3 (clone 145-2c11), LY-76 (clone TER119), CD45R/B220 (clone RA3-6B2), CD11b (clone M1/70), and LY6G/LY6C/GR-1 (clone RB6-8C5) coupled with streptavidin–fluorescein isothiocyanate (streptavidin-FITC). Lineage-negative cells were further identified with phycoerythrin (PE)-conjugated Sca1 (clone E13-161.7) and Alexa647-conjugated c-Kit (clone 2B8; Life Technologies).

A list of all fluorochromes used is shown in table 1.

Blood and Tissue Harvest and Analysis

Tissue samples were harvested from mice at various time points. After euthanasia, spleens were removed from individual mice, mechanically dispersed in PBS, supplemented with a 0.5% fetal bovine serum and 0.1% sodium azide, and passed through a sterile Nitex nylon mesh to form single cell suspensions. The cells were then depleted of red blood cells with lysis buffer.

Femurs and Tibias were removed and placed in DMEM on ice. A 25g needle and DMEM was used to aspirate bone marrow. Bone marrow aspirate was lysed in a hypotonic buffer for 5 minutes at room temperature and the resulting pellet was washed 3 times with DMEM. Surface markers for lineage, CD150, and CD48 were added for 30 minutes. Cells were washed again, and streptavidin was added for 30 minutes.

Competitive Irradiation Chimeras

On GD 14.5, fetal liver hematopoietic progenitors were harvested for the limiting dilution experiment as described above. After depletion of red blood cells (RBCs), cells from vehicle-exposed CD45.1 fetuses were counted and mixed with an equivalent number of fetal liver cells from the vehicle- or TCDD-exposed CD45.2+ dams.

Four hours before reconstitution, host CD45.1+ mice were lethally irradiated with 11 Gy to eliminate all host hematopoietic cells. Subsequently, 1,000,000 fetal liver cells (500,000 CD45.1 cells plus 500,000 CD45.2 cells) were injected into each host recipient mouse by intravenous (IV) injection. Mice were then maintained for 8 weeks to allow complete blood system reconstitution. At 8 weeks, the primary competitive chimera recipients were euthanized by CO2 asphyxiation followed by cervical dislocation as described above, with the exception that the procedure was performed at the Blood

Research Institute between 0900 and 1000 hours. Bone marrow obtained from one femur as well as the thymus and the spleen were analyzed for the percent of chimerism. Bone marrow from the other femur was harvested under sterile conditions, depleted of RBCs, and counted, and 1 × 106 cells were used in a secondary IV transfer into individual naïve CD45.1+ irradiated host recipient mice. Transfers into the secondary recipients were performed by IV injection of cells from individual mice into each individual recipient to track any potential outliers throughout the full 16-week experiment. Eight weeks after the transfer, the secondary recipients were euthanized, and lymphoid tissues were analyzed for chimerism as with the primary recipients.

For analysis of competitive mixed chimeras, ≥ 100,000 viable lymphocytes from bone marrow, thymus, or spleen were acquired, and chimerism was analyzed by comparing the frequency of CD45.1 and CD45.2. Additional analysis of cell subset distribution was determined by first gating on CD45.1 or CD45.2, then analyzing lineage markers Sca1 and c-Kit (bone marrow) or CD4, CD8, and B220 (thymus and spleen).

RNA Preparation and Quantitative RT-PCR

On GD 11.5, hematopoietic cells pooled from individual litters of vehicle- or TCDD-exposed fetuses were isolated and sorted directly into Trizol (Life Technologies) using c-Kit and DCF fluorescence to discriminate between hematopoietic progenitor cells with

long- and short-term self-renewal potential, respectively. RNA was purified, quantified and processed as previously described (Ahrenhoerster et al. 2014). RNA was subjected to reverse transcription using a Tetro cDNA Synthesis kit (Bioline) with both anchored-

Gene name	Accession number	Name Accession 5'->3'	Forward 5'->3' Reverse
Hairy enhancer of split (Hes-1)	NM_008235.2	tgccagctgatataatggagaa	ccatgataggctttgatgacttt
Delta-like 1 (DL1)	NM_001190703	agcaaacgtgacaccaagtg	taagtgttggggcgatcttc
Jagged 1 (Jag1)	NM_013822	gtgccctggtgtccattc	taggaccgctggcagatg
Notch4	NM_010929	cctgcctgaagagggagag	cagaaatccaggggcaca
Notch1	NM_008714	cagaacaccaatggcagcta	acagttgcgacctgtatagcc
GTP cyclohydrolase (GTPCH1)	NM_008102	gccgcttactcgtccattct	gaacaaggtgatgctcacaca
Superoxide dismutase (SOD2)	NM_013671	tgctctaatcaggacccattg	gtagtaagcgtgctcccacac
Carnitine palmitoyltransferase2 (CPT2)	NM_009949	cagcacagcatcgtaccca	tcccaatgccgttctcaaaat
Pyruvate kinase (PKM2)	NM_001253883	gaagccacacagtgaagcag	tgtgttccaggaaggtgtca
Fatty acid synthase (FASN)	NM_007988.3	ccctgaccaaggtgctgt	gttgtggaagtgcaggttagg
Carnitine palmitoyltransferase1 (CPT1)	NM_013495	tcttcactgagttccgatggg	acgccagagatgccttttcc
Tuberous sclerosis 1 (TSC1)	NM_001289575	atggcccagttagccaacatt	cagaattgagggactccttgaag
CD36	NM_001159555	cgggccacgtagaaaacact	cagccaggactgcaccaata
HPRT	NM_013556.2	gtcaacgggggacataaaag	caacaatcaagacattctttcca

Table 2. Gene name, accession number and primer sequence used for qRT2 PCR

oligo(dT) 18 priming and random hexamer priming options and was stored at –20°C until the day of the assay. Primers were selected using Universal ProbeLibrary v.2.5 for Mouse (Roche) and checked for specificity using Primer-BLAST (http://www.ncbi.nlm.nih.gov/tools/primer-blast/). cDNA was used as a template in a 20-µL reaction consisting of 10 µmol of forward and reverse primers and 10 µL SensiFAST SYBR No-ROX (Bioline). Relative expression change was determined using the 2–ΔΔCT method with standardization to housekeeping genes. Samples were run in triplicate wells with at least two independent litters per treatment analyzed. Cycling

conditions were 95°C for 2 min, followed by 45 cycles at 95°C for 5 sec, 60°C for 10 sec, and 72°C for 10 sec.

Statistical analysis

Statistical significance was determined in denoted on graphs and tables as a single asterisk for $p \leq 0.05$, two asterisks for $p \leq 0.01$ or 3 asterisks for $p \leq 0.001$.

GraphPad Prism (GraphPad software, LaJolla, CA) was utilized for analysis of variance with Dunnett's t post-hoc tests, and graphical representation of all other data.

CHAPTER 3

EFFECTS OF DEVELOPMENTAL ACTIVATION OF THE ARYL HYDROCARBON RECEPTOR BY 2,3,7,8-TETRACHLORODIBENZO-*p*-DIOXIN ON LONG-TERM SELF-RENEWAL OF MURINE HEMATOPOETIC STEM CELLS

Adapted with permission from:

Laiosa MD, Tate ER, Ahrenhoerster LS, Chen Y, Wang D. 2016. Effects of developmental activation of the aryl hydrocarbon receptor by 2,3,7,8-tetrachlorodibenzo-p-dioxin on long-term self-renewal of murine hematopoietic stem cells. Environ Health Perspect 124:957–965

ABSTRACT

Background: Human epidemiological and animal studies suggest that developmental exposure to contaminants that activate the aryl hydrocarbon receptor (AHR) lead to suppression of immune function throughout life. The persistence of immune deficiency throughout life suggests that the cellular target of AHR activation is a fetal hematopoietic stem cell (HSC).

Objectives: The aim of this study was to identity the effects of transplacental exposure to an AHR agonist on long-term self-renewal of fetal hematopoietic stem cells.

Methods: Pregnant C57BL/6 or AHR+/- mice were exposed to the AHR agonist 2,3,7,8-Tetrachlorodibenzo-*p*-dioxin (TCDD). On gestational day 14 (GD14), HSCs from wild type or AHR deficient fetuses were analyzed for changes in reactive oxygen species (ROS). Finally, HSCs from fetuses transplacentally exposed to TCDD were mixed 1:1 with HSCs from congenic controls and used to reconstitute lethally irradiated recipients for analysis of long-term self-renewal potential.

Results: Our findings suggest that the effects of TCDD on the developing hematopoietic system were mediated by direct AHR activation in the fetus. Furthermore, developmental AHR activation by TCDD increased ROS in fetal HSCs, and the elevated ROS was associated with a reduced capacity of the TCDD-exposed fetal cells to compete with control cells in a mixed irradiation/reconstitution assay.

Conclusions: Our findings indicate that AHR activation by TCDD in the fetus during pregnancy leads to impairment of long-term self-renewal of hematopoietic stem cells.

INTRODUCTION

Hematopoiesis is literally the making of blood cells. In an adult human, it is estimated that 1 trillion cells per day are made by this process (Ogawa, 1993). The multiple lineages of the blood system descend from a very small population of hematopoietic stem cells (HSC). These multipotent cells retain the capacity for self-renewal meaning that, of two daughter cells produced, 1 will terminally differentiate while the other will replace the parent. This process fulfills two needs for the organism. It allows for rapid proliferation of the blood system without depleting the stock of HSCs and limits their exposure to the reactive oxygen species (ROS) that would be produced during rapid expansion.

There is evidence to support the idea that increased ROS is enough to force HSCs from their quiescent state. Both alteration of the tuberous sclerosis complex-mammalian target of rapamycin (TSC-mTOR) pathway (Chen et al., 2008) and deletion of forkhead transcription factor 3 (Foxo3a) (Miyamoto et al., 2007) will increase ROS in HSCs and force their exit from quiescence. It is worth noting that in both molecular models, there was little impact observed on the lineage restricted progenitors, indicating that for HSCs alone, elevated ROS favors differentiation over self-renewal and low ROS is necessary requirement of quiescence.

HSCs emerge during development from the aorta-gonad-mesonephros (AGM) shortly after the initiation of the heartbeat in mice, however both in humans and mice, migrate to the fetal liver (FL) to undergo expansion. While this is one of the primary sites of hematopoiesis, the FL does not produce HSCs *de novo*. In contrast to the quiescent

HSCs found in bone marrow, FL HSCs are actively symmetrically self-renewing for expansion until their egress to the bone marrow before birth. The protective self-renewal mechanism found in the adult BM is not found in fetal HSCs, hence damage sustained to the cells at this point will be carried through the lifetime of the organism.

The Aryl hydrocarbon receptor (AHR) is a member of the bHLH-PAS (basic Helix-Loop-Helix – Period/ARNT/Single minded) family of proteins. Knowledge gained about the role of the AHR has primarily been through toxicological interactions using the potent ligand 2,3,7,8-tetrachlorodibenzo-*p*-dioxin (TCDD) due to its high affinity for the AHR. The advent of transgenic animal models has indicated that the AHR has numerous endogenous and developmental roles aside of xenobiotic metabolism, especially in regard to hematopoiesis. AHR-/- models have indicated that not only is there an increased number of HSCs, but that they also proliferate faster than wild type (Gasiewicz et al., 2010; Singh et al., 2011). Additionally, HSCs from aged AHR-/- mice demonstrate a decreased reconstitution ability, likely due to HSC exhaustion (Singh et al., 2014). A study of mice exposed to TCDD as adults demonstrated that AHR agonism had adverse effects on long-term self-renewal (Sakai et al., 2003). While TCDD has been shown to increase ROS in some cell types, the link between developmental agonism of AHR increasing ROS thereby affecting HSCs has yet to be shown.

To address this question, pregnant mice were exposed to a low oral dose of TCDD, and we found that maternal TCDD exposure increased ROS in fetal HSCs. Using ROS as a marker of hematopoietic stem cell differentiation, we then sorted cells for gene expression analysis and found differential expression of Notch and ROS regulatory genes in TCDD-exposed HSCs. Finally, we performed an

irradiation/competitive reconstitution experiment using fetal liver progenitor cells from vehicle-exposed fetuses and fetuses that had been exposed to TCDD transplacentally. We found that cells derived from the TCDD-exposed fetuses were significantly reduced in all immune tissues when competing against hematopoietic progenitors from the controls.

RESULTS

Effects of Developmental TCDD Exposure on Reactive Oxygen Species in Fetal Hematopoietic Progenitor Cells

Based on the findings of others that HSCs are less ROS producing than differentiated cells, we wanted to assess how developmental exposure to TCDD would affect the fetal HSC population. Intracellular ROS was measured in GD 11.5 and GD 14.5 fetuses by using H_2DCF-DA, which is oxidized to highly fluorescent DCF in the presence of oxidative stress. We used these time points because taken together, they represent the initial arrival of HSCs in the fetal liver (11.5), and at the end of their expansion (14.5). Additionally, GD 11.5 represents the point at which HSCs acquire long-term self-renewal (Ciriza et al., 2013). Analysis of hematopoietic c-Kit+ progenitor populations indicated that DCF fluorescence was elevated in the TCDD-exposed fetuses (Figure 3A – middle panel) in addition to being elevated in the AHR-/- fetuses (Figure 3A – right panel). Figure 3B demonstrates that if AHR is either agonized or absent in fetal hematopoietic progenitors, the fluorescence intensity of DCF increased by almost 75% indicating higher levels of intracellular ROS. Moreover, by taking a ratio of the percentage of c-Kit+DCF hi cells to the c-Kit+DCF int, it is evident that developmental

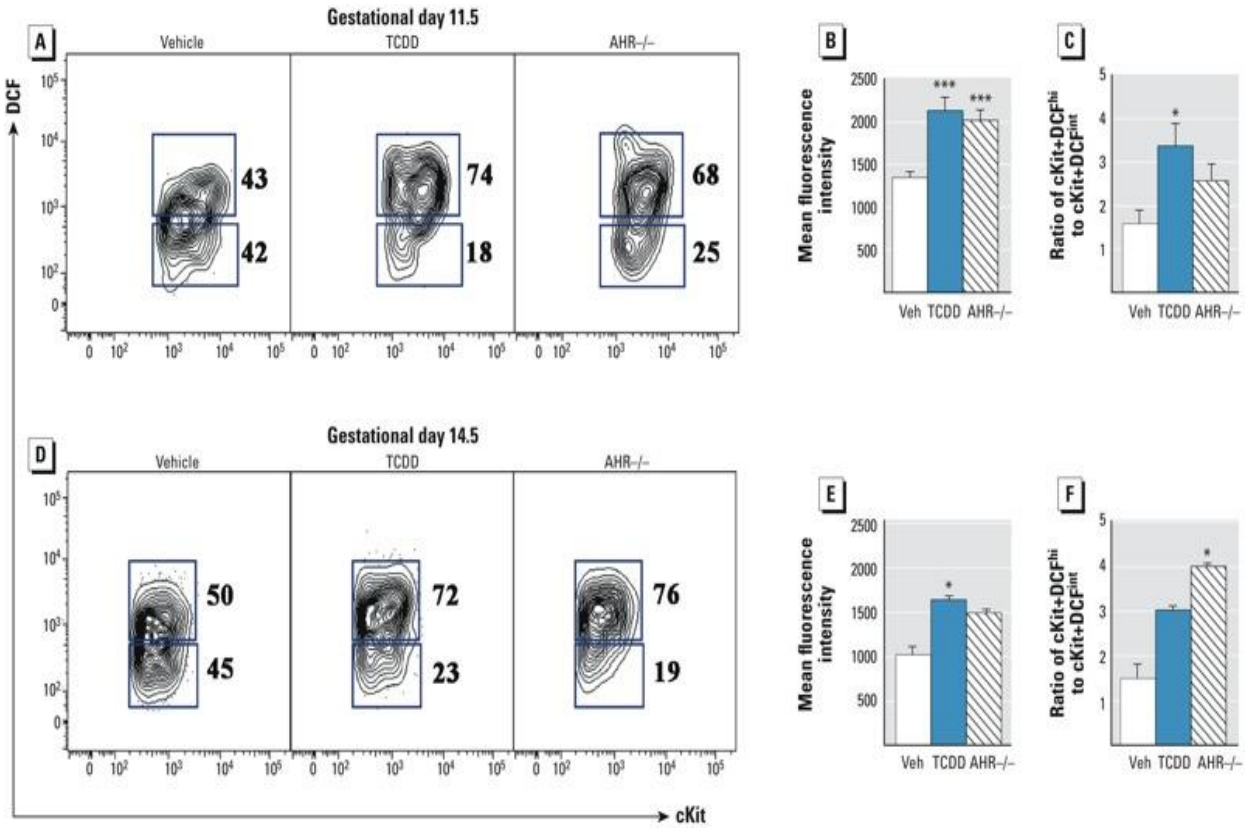

Figure 3

Effects of developmental tetrachlorodibenzo-*p*-dioxin (TCDD) exposure and fetal aryl hydrocarbon receptor (AHR) expression on reactive oxygen species in fetal hematopoietic progenitors. (*A*) Representative c-Kit versus dichlorofluorescein (DCF) flow cytometry plots on gestational day (GD) 11.5 for vehicle (Veh), TCDD, and $AHR^{-/-}$. The number to the right of each c-Kit^{+}DCF gate indicates the percentage of cells within each population. (*B*) Mean fluorescence intensity of total DCF in c-Kit^{+} cells. (*C*) The percentage of GD 11.5 c-Kit^{+} cells in the DCF^{hi} gate is compared with the percentage of cells in the DCF^{int} gate to illustrate that TCDD both increased the overall DCF profile and changed the distribution of the cells within the bimodal distribution. (*D*) On GD 14.5, li^{n}–c-$Kit^{+}Sca1^{+}$ (LSK) cells were further analyzed for c--Kit versus DCF as shown in Figure 2A. (*E*) Mean fluorescence intensity of total DCF in LSK cells on GD 14.5. (*F*) Ratio of DCF^{hi} cells to DCF^{int} cells in the GD 14.5 LSK population. Data in the bar graphs are the mean ± SEM with $n = 8$ individual fetuses per C57BL/6 group from two separate litters and 4 $AHR^{-/-}$ fetuses. The experiment was repeated twice. Statistical significance determined by Tukey's t-test after analysis of variance (ANOVA) is denoted with * for $p \leq 0.5$ or *** for $p \leq 0.001$ compared with vehicle.

AHR activation increased the distribution of hematopoietic progenitors with high

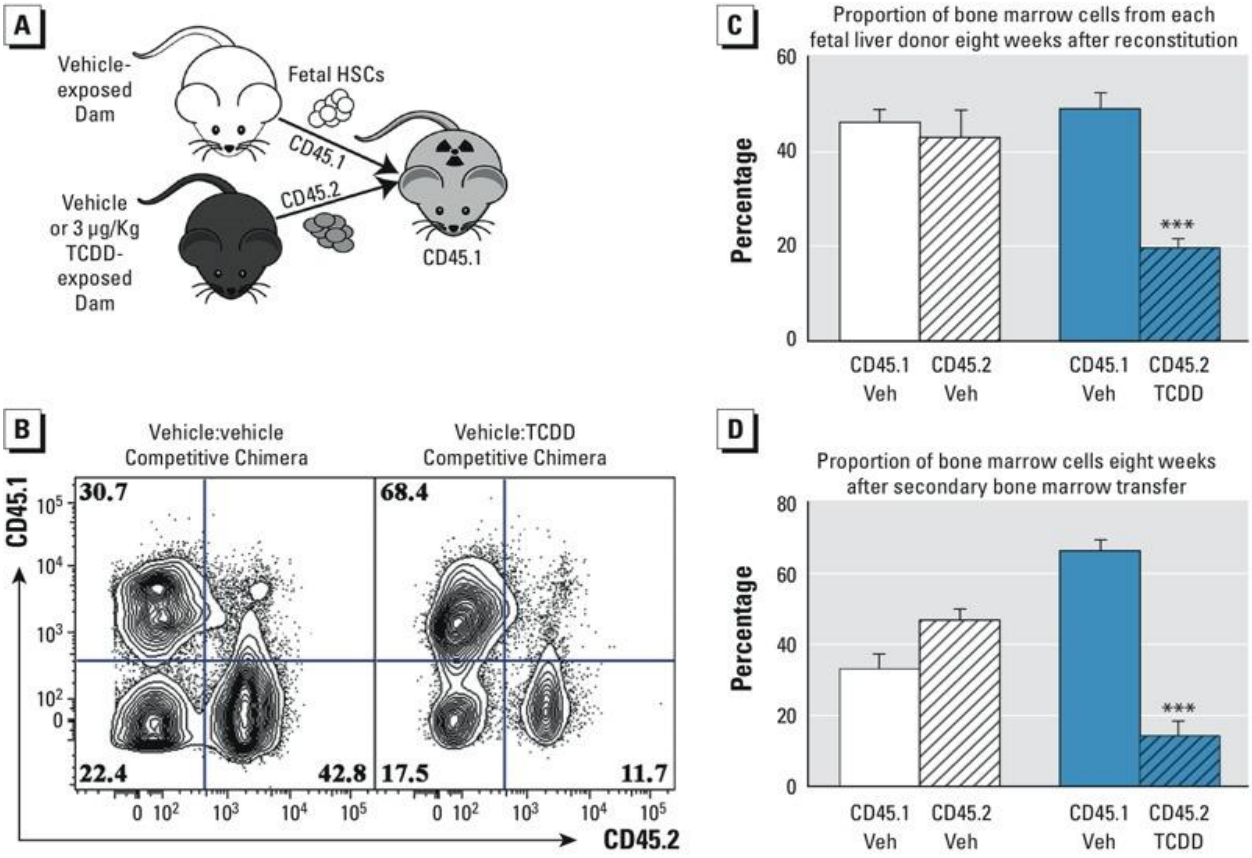

Figure 4

Effects of transplacental tetrachlorodibenzo-*p*-dioxin (TCDD) exposure on the long--term self-renewal potential of fetal liver hematopoietic stem cells. (*A*) Schematic model of the experimental design for the primary reconstitution experiment. (*B*) Representative flow cytometry plot of bone marrow from the primary chimera. Numbers in each quadrant of the flow cytometry plots represent the percentage of bone marrow cells identified by the antibody specific for CD45.1 or CD45.2 congenic surface proteins. (*C*) Percent of bone marrow cells from each donor in the primary and secondary recipients. White bars represent control competitive chimeras, and blue bars represent the chimeras where vehicle (Veh) cells were competed with cells obtained from TCDD-exposed fetuses. Solid bars represent $CD45.1^+$ cells, and $CD45.2^+$ cells are denoted with diagonal slash-filled bars. Data are the mean ± SEM with 5 mice per group. The experiment was repeated twice. (*D*) Percent of bone marrow cells from each donor after the secondary bone marrow transfer. *** Indicates statistical significance by analysis of variance (ANOVA) followed by Tukey's test; $p < 0.001$ compared with the congenic cells from the same chimera.

intracellular ROS relative to progenitors with a lower intracellular oxidative state ($p \leq 0.05$) (Figure 3C). Similar effects with ROS were observed in GD 14.5 (Figure 3D)

however, due to the vehicle hematopoietic progenitors having higher ROS levels, the effects are less pronounced than GD 11.5 (Figure 3E).

Effects of Developmental TCDD Exposure on Long-Term Self-Renewal Capacity of Hematopoietic Stem Cells

Self-renewal is a crucial function of HSCs as it ensures a supply of cells for the lifetime of the organism. The penultimate test of long-term self-renewing functional capacity is accomplished by their ability to reconstitute a lethally irradiated host. Additional cell types are capable of reconstitution in the short term (12 weeks in mice), thus long-term functional capacity must either exceed 12 weeks, or done by serial transplantation. Since we wanted to assess TCDD-exposed vs wild-type, they were both injected into a lethally irradiated host mouse. As demonstrated in Figure 4A, this was done by sorting GD 14.5 fetal liver HSCs from wild type CD45.1 and TCDD-exposed GD 14.5 CD45.2. Eight weeks after the initial reconstitution, the contribution of each donor was analyzed in the bone marrow and spleen of the recipients, and the remaining bone marrow was transferred into a secondary recipient. This was necessary to test the long-term self-renewal and mitigate any confounding effect from short-term reconstituting cells. We found that the HSCs from the TCDD-exposed fetuses failed to compete effectively in both the primary and secondary transplants (Figure 4B). Surprisingly, even in the primary competition, wild type reconstitution was 152% greater than TCDD (Figure 4C), which was further outcompeted in the secondary transfer where control HSCs were 381% greater than TCDD-exposed (Figure 4D).

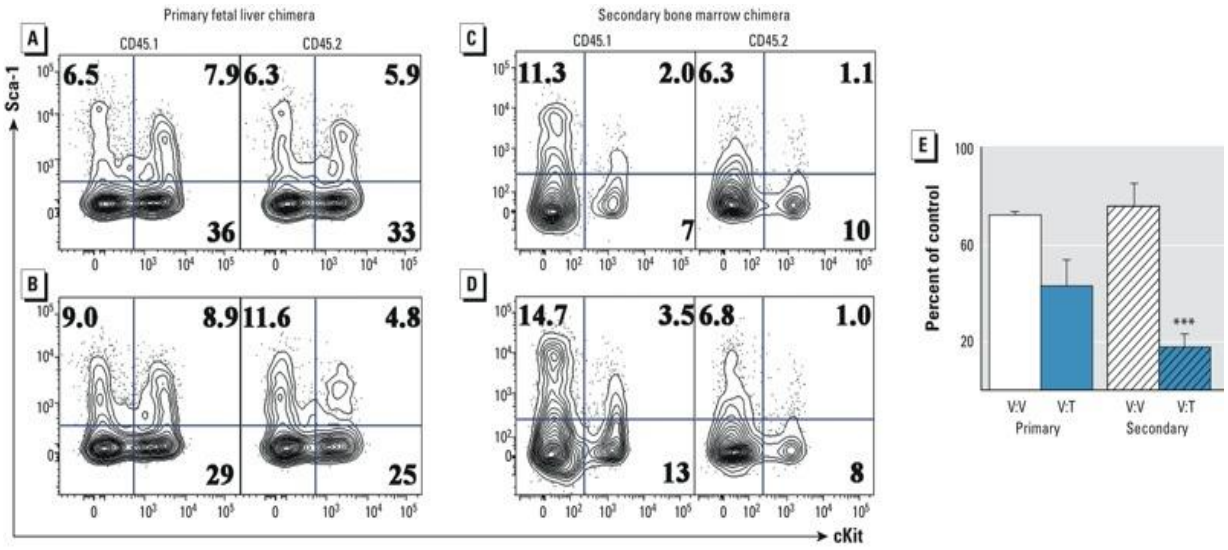

Figure 5

Effects of developmental tetrachlorodibenzo-*p*-dioxin (TCDD) exposure on bone marrow hematopoietic progenitor cells after long-term competitive reconstitution. (*A*) c-Kit versus Sca1 flow cytometry plots from the primary vehicle-to-vehicle (V:V) competitive chimeras with $CD45.1^{+}lin^{-}$ cells in the left panel and $CD45.2^{+}lin^{-}$ cells in the right panel. The percentage of lin^{-} cells is specified by the number in each quadrant. (*B*) Flow cytometry plots from the primary vehicle to TCDD competitive chimeras. (*C*) Representative c-Kit versus Sca1 flow cytometry plots from the - vehicle-to-vehicle secondary bone marrow chimera. (*D*) Flow cytometry plots from the secondary vehicle to TCDD (V:T) competitive chimeras. (*E*) Relative frequency of li^{n}–$c\text{-}Kit^{+}Sca1^{+}$ (LSK) hematopoietic progenitor cells in the CD45.2 population of cells compared with the CD45.1 competitor cells from the primary and secondary chimeras. White bars compare vehicle-to-vehicle chimeras, and blue bars compare the vehicle with TCDD chimeras. Solid bars are from the primary chimeras, and secondary chimeras are represented by bars containing slashes. The percentage of the control was calculated by dividing the frequency of $c\text{-}Kit^{+}Sca1^{+}$ cells in the $CD45.2^{+}lin^{-}$ population by the same population of $CD45.1^{+}lin^{-}$ cells. Data represents the mean ± SEM from $n = 5$ chimeras, and the experiment was repeated once. *** Denotes statistically significant by analysis of variance (ANOVA) followed by Tukey's test; $p < 0.001$ compared with the congenic cells from the same chimera.

We wanted to further assess if this was an effect specifically to the HSC compartment, and bone marrow was analyzed for the frequency of HSCs within their respective CD45.1 or CD45.2 delineations. HSCs were defined as an absence of lineage markers and expression of Sca1 and c-Kit (LSK). When vehicle was competed

against itself, there was little difference in the frequency of LSKs (Figure 5A). However, when vehicle treated was competed against TCDD-exposed, there was a nearly 50% decrease in the frequency of LSKs after the 8wk initial transfer (Figure 5B). Analysis of the bone marrow of the secondary transfer showed nearly an 80% against vehicle competitors (Figure 5E). This inability to compete with the self-renewal and differentiation program also carried into peripheral lymphoid tissues as well.

Effects of in Utero TCDD Exposure on Cellular Differentiation–Induced Gene Expression Changes

With these results in hand, we wanted to further investigate the difference in expression of certain genes to assess how they might be affected by TCDD exposure. Specifically, we sorted GD 11.5 Lin-c-Kit+ fetal hematopoietic progenitor cells by their DCF profile as indicated in Figure 3. We wanted to assess gene expression changes based on ROS given the widely-held belief that self-renewal potential is lost in higher ROS-producing cells. Given previous reports that elevated ROS signals a transition to short-term self-renewal and multilineage differentiation, comparing gene expression changes in c-Kit+ DCF int with those in c-Kit+ DCF hi was considered to be an innovative approach to determining the effects of in utero TCDD exposure on this putative developmental transition. The vehicle comparison demonstrates what ought to happen in these transitions; the TCDD comparison, a reflection of AHR agonism. The genes we chose to investigate were a cross-section of pathways, including Notch, cellular metabolism, and oxidative stress.

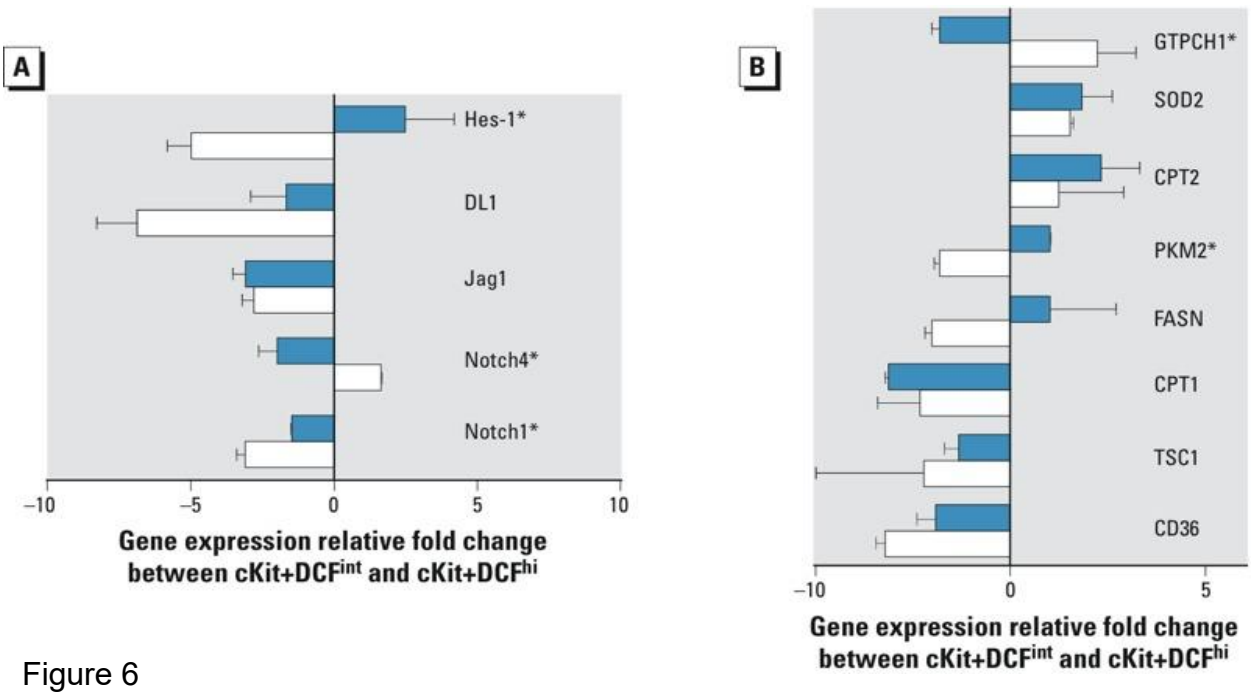

Figure 6

Impact of developmental tetrachlorodibenzo-p-dioxin (TCDD) exposure on -differentiation-induced changes in gene expression in hematopoietic progenitor cells. A) Gene expression changes associated with Notch signal transduction between c--Kit+DCFint and c-Kit+DCFhi cells from control fetuses (white bars) and TCDD--exposed fetuses (blue bars). (B) Gene expression changes associated with cellular metabolism (CD36, TSC1, CPT1, CPT2, FASN, PKM2) and oxidative stress (SOD2, GTPCH1) in c-Kit+DCFint and c-Kit+DCFhi cells from control fetuses (white bars) and TCDD-exposed fetuses (blue bars). Data are presented as the mean ± standard deviation of replicate wells from a single quantitative polymerase chain reaction (qPCR) reaction with the experiment performed on two independent litters of mice. *p ≤ 0.05, statistical significance between the two treatments (Student's t-test).

As indicated in Figure 6A, Notch and Notch-dependent signal transduction is markedly skewed when comparing vehicle in c-Kit+ DCF int to c-Kit+ DCF hi to TCDD-exposed cells of the same sorting strategy. The expression of Notch1 and Notch-dependent transcription factor Hes-1 were decreased in contrast to Notch4 which was slightly increased. In comparison, TCDD-exposed progenitors showed a less abrupt decrease in expression of Notch1, while the effects on Hes-1 and Notch4 were opposite to the vehicle treated progenitors. Additionally, TCDD significantly increased both

pyruvate kinase expression and fatty acid synthase. Finally, eNOS regulator GTP-cyclohydrolase was decreased in comparison to vehicle where it was upregulated.

DISCUSSION

As HSCs are required to fulfill both the roles of self-renewal and multilineage differentiation, assessing the danger of developmental environmental exposures is urgently needed. Our studies highlight how developmental insults to the fetal hematopoietic system can persist throughout life. Thus, we believe that we are the first to report experimental evidence that is consistent with a direct effect of prenatal TCDD exposure on impairment of hematopoietic stem cell long-term self-renewal.

Our conclusion that *in utero* TCDD exposure has a direct effect on hematopoiesis is based on work done in our lab demonstrating the effects of AHR agonism and absence in T-cell differentiation (Ahrenhoerster et al., 2014). We further demonstrated that AHR-/- fetal HSCs were resistant to the effects of TCDD, suggesting that agonism of the AHR is the primary mechanism by which TCDD affects HSCs.

AHR agonism via developmental exposure to TCDD increased oxidative stress in fetal HSCs. HSCs in the bone marrow meet their low energetic demands by glycolysis, and it is widely held that this is to limit potentially DNA-damaging ROS production (Simsek et al., 2010a). Similarly, increased ROS production seems to favor differentiation (Chen et al., 2008; Gan et al., 2010; Ito et al., 2004; Miyamoto et al., 2007). Additional studies have indicated that the self-renewal process is intrinsically regulated with older mitochondria being sent with the daughter cell that will terminally

differentiate (Katajisto et al., 2015b). During development however, the energetic balance is less well understood. Fetal HSCs are rapidly proliferating and metabolically active compared to bone marrow HSCs. This highlights the danger of the *in utero* environment specifically in regard to ROS production – the protective quiescence of the bone marrow is not established in these cells. The detriment to self-renewal of high ROS in HSCs was done with bone marrow, and it was necessary to demonstrate that this effect could be seen in fetal HSCs as well (Sakai et al., 2003).

To further evaluate the implications of the elevated oxidative state, we sorted fetal hematopoietic progenitors according to DCF, and therefore ROS, levels and conducted a focused analysis of gene expression changes dependent on the developmental stage of the cells and on TCDD exposure. We investigated pathways relating to Notch signaling, cellular metabolism, and oxidative stress. Notch genes were chosen due to studies done by others indicating that Notch activity leads to differentiation (Duncan et al., 2005) and Hes-1 has been shown to be a target gene of the AHR (Thomsen et al., 2004). Our findings of decreased Notch and Hes-1 expression (Figure 4A) are consistent with the literature supporting a loss of self-renewal in the higher ROS producing progenitors. The decrease in Notch1 was attenuated in the TCDD-exposed progenitors, whereas the effects on Hes-1 and Notch4 were opposite to control. Taken together, the altered expression patters of Notch pathway genes in the TCDD-exposed in addition to the increase in ROS could be interpreted as being indicative of premature differentiation of the HSC pool. The long-term consequence being that it would deplete the total number of long-term self-renewing cells before they make their way to the bone marrow.

In addition to the effects of TCDD on the Notch pathway, we wanted to assess potential changes to glycolytic and fatty acid pathways, in addition to genes related to oxidative stress. Interestingly, TCDD increased pyruvate kinase (PKM2) in progenitors going from DCF int to DCF hi, in contrast to controls where PKM2 expression was decreased. Pyruvate kinase catalyzes the last step within glycolysis and is thus responsible for net ATP production during glycolysis. As it can be found expressed in rapidly proliferating cells due to the high rate of nucleic acid synthesis, it could suggest that TCDD-induced ROS increase is favoring proliferation of self-renewal. Additionally noteworthy is the changes in GTP-cyclohydrolase I (GTPCH). GTPCH is the rate limiting enzyme in tetrahydrobiopterin (BH4) synthesis, which is required for endothelial nitric oxide synthase (eNOS) to produce nitric oxide (NO). Intracellular BH4 deficiency induces superoxide creation from eNOS, thus increasing oxidative stress (Vásquez-Vivar, 2009). NO donors have been shown to increase the number of HSCs *in vivo* (Michurina et al., 2004), which is consistent with our finding that GTPCH expression is increased in control fetal HSCs that are undergoing symmetric self-renewal. Conversely, TCDD decreases the expression to GTPCH, potentially indicating that TCDD-induced ROS forces cells to differentiate rather than self-renew. Finally, decreased GTPCH, and thus decreased BH4, can induce superoxide, potentially indicating a source for the increased oxidative stress in TCDD-exposed HSCs. Superoxide dismutase (SOD2) was relatively unchanged in control vs TCDD, however this reflects only the mitochondrial isoform, not the cytoplasmic.

Combined, we have identified a few potential mechanisms that could account for the loss of self-renewal in TCDD-exposed fetal HSCs. Our data demonstrating changes

in the Notch pathway of TCDD-exposed progenitors in addition to the increase in DCF fluorescence are suggestive of forced maturation of the fetal HSC pool. When combined with the competitive reconstitution data, this is indicative of a depletion of the number of long-term HSCs. Alternatively, changes in GTPCH expression in TCDD-exposed fetal progenitors could indicate that the HSCs are no longer expanding but prematurely differentiating. Additionally, superoxide production from uncoupled eNOS could be a source of oxidative stress.

A possible interpretation of our data is that the cytoplasmic-localized AHR complex has a normal function in maintaining low levels of ROS in HSCs. Additional support for this idea comes from recent studies have demonstrated that AHR directly interacts with ATP synthase (Tappenden et al., 2011). Thus, in the presence of a potent agonist such as TCDD, AHR is removed from this role prematurely. Our own data and data reported by others have shown that baseline levels of ROS are elevated in the absence of the AHR, lending further credence to the idea of AHR as a negative regulator of proliferation.

Perturbation of the developing hematopoietic system can be a harbinger for later-life blood diseases including cancer, autoimmunity, and immune suppression. While it cannot be determined from the present study whether exposure to other AHR agonists during development would produce a similar outcome, given the broad array of environmental toxicants that can affect AHR, our findings should initiate further study into how environmental exposures can affect the developing hematopoietic system.

CHAPTER 4

FUNCTIONAL ANALYSIS OF THE AHR IN HEMATOPOEITIC STEM CELLS DURING DEVELOPMENT

ABSTRACT

Background: The aryl hydrocarbon receptor (AHR) has an unknown function in the regulation of hematopoietic stem cells (HSC). Animal models where AHR is absent show skewing towards myeloid lineage and increased proliferation of HSCs. 2,3,7,8-Tetrachlorodibenzo-*p*-dioxin (TCDD) is a well known and potent AHR agonist that can decrease long-term reconstitution ability of HSCs. Both AHR-/- and TCDD-exposed have been shown to increase ROS in HSCs in the fetal liver and bone marrow.

Objectives: The aim of this study was to identity how AHR agonism and absence affects HSCs across multiple anatomical locations in the developing fetus in addition to the adult bone marrow.

Methods: Adult and pregnant C57BL/6 or AHR+/- crossed to AHR-/- mice were exposed to the AHR agonist 2,3,7,8-Tetrachlorodibenzo-*p*-dioxin (TCDD). On gestational day 11 (GD 11) and 14 (GD14), HSCs from wild type or AHR deficient fetuses were analyzed for changes in reactive oxygen species (ROS), mitochondrial mass, and for changes in population distribution between the bone marrow, fetal liver, and placenta.

Results: Our findings suggest that the effects of TCDD on the developing hematopoietic system were mediated by direct AHR activation in the fetus. Furthermore, developmental AHR activation by TCDD or AHR absence increased ROS and mitochondrial activity and mass in HSCs, however these effects differed based on anatomical location.

Conclusions: Our findings indicate that the AHR differentially modifies HSCs depending on anatomical location.

INTRODUCTION

Comparison of hematopoietic stem cells across age in mice

Hematopoietic stem cells are a unique population that emerge during embryonic development, retain multipotency, and are maintained through the lifetime of the organism. They have the ability to self-renew or to differentiate into multiple blood cell lineages based on the needs of the organism. Differentiation is a tightly regulated process, and disruption at the initial steps can have profound downstream effects. Murine hematopoietic stem cell (HSC) development takes place in two waves, referred to as primitive and definitive hematopoiesis. Primitive HSC's first appear in the extraembryonic yolk sac around gestational day 7.5. Primitive hematopoiesis gives rise to erythroid progenitors and megakaryocytes and are not thought to be capable of reconstituting an entire blood system of an irradiated recipient. Definitive hematopoiesis begins with the onset of a heartbeat, around gestational day 8.5. They emerge from the aorto-gonad-mesonephros (AGM), then migrate to the fetal liver where they expand 1000-fold. Shortly before birth around gestational day 18.5, these hematopoietic stem cells (HSC) make their way to the bone marrow. While the murine fetal liver is the main site of embryonic HSC expansion, it is incapable of *de novo* generation, thus is seeded with HSCs from extraembryonic sites (Kumaravelu et al., 2002). A number of studies have indicated that the placenta contains an HSC pool, which unlike the fetal liver, is

capable of *de novo* generation. (Bárcena et al., 2009; Dzierzak and Robin, 2010; Gekas et al., 2005; Robin et al., 2009). Evidence for this comes from Gekas et all 2005, who demonstrated that HSCs can be found in the placenta before they are found in the fetal liver, at gestational day 10.5. The expansion of HSCs in the placenta around gestational day 12 is comparable to the expansion of the fetal liver. Interestingly, at gestational day 13.5, the placental HSC pool rapidly decreases which is timed with the greatest expansion of HSCs in the fetal liver, lending credence to the idea that placental HSCs seed the fetal liver. During these anatomical transitions, the cells also undergo metabolic changes to fulfill their proliferative and anabolic demands. With the findings that the same metabolic process uses are an absolute requirement for the maintenance of hematopoietic stem cells, it is worth pursuing what exogenous factors can affect this transition, thereby affecting the HSC pool for the lifetime of the organism (Ito et al., 2012; Simsek et al., 2010b).

The aryl hydrocarbon receptor is a member of the bHLH-PAS (basic Helix-Loop-Helix, Period/ARNT/Single minded) family of transcription factors. While it was initially thought to be involved in xenobiotic metabolism, knock out animals demonstrated that the AHR is involved in far more physiological processes (Gasiewicz et al., 2010). Additional studies using TCDD, a potent activator of the AHR, demonstrated that a developmental exposure can affect the immune system for the life of the organism. While epidemiological studies with Vietnam veterans and of the population in Seveso, Italy have looked at the effect on adults, there exists a need to understand how persistent, low-level exposures during development affect the immune system (Liem et al., 2000).

Our approach was to evaluate and compare HSCs from the fetal liver (FL), placenta (P), and bone marrow (BM) in mice developmentally exposed to TCDD vs AHR-/- to answer determine the effect of AHR agonism or absence on HSCs within these different anatomical locations. Despite a number of different studies demonstrating the effects on HSCs, no one has compared the bone marrow, fetal liver, and placenta side by side in the context of the AHR and its effect on HSCs. These analyses were further refined using a gating strategy that separated HSCs based on small and large size. The advantages of our analytical method allowed for a side-by-side comparison of HSCs across different hematopoietic anatomical locations and developmental time points. Our aim was to elucidate how the AHR influences population dynamics, ROS production, and mitochondrial mass and energetics in HSCs in different anatomical locations throughout development. Our findings have the potential to enhance existing knowledge of the AHR in HSCs.

RESULTS

Influence of the aryl hydrocarbon receptor

on hematopoietic stem cell populations

We first thought to evaluate LSK populations and how agonism of the AHR using TCDD or the absence of the AHR could affect the distribution of cells in the bone marrow, GD 14.5 fetal liver, and GD 14.5 placental populations. Based on our findings that reliance on surface markers alone are inadequate for identification of HSCs (unpublished data – Chapter 5), we sought to apply a different gating strategy in order

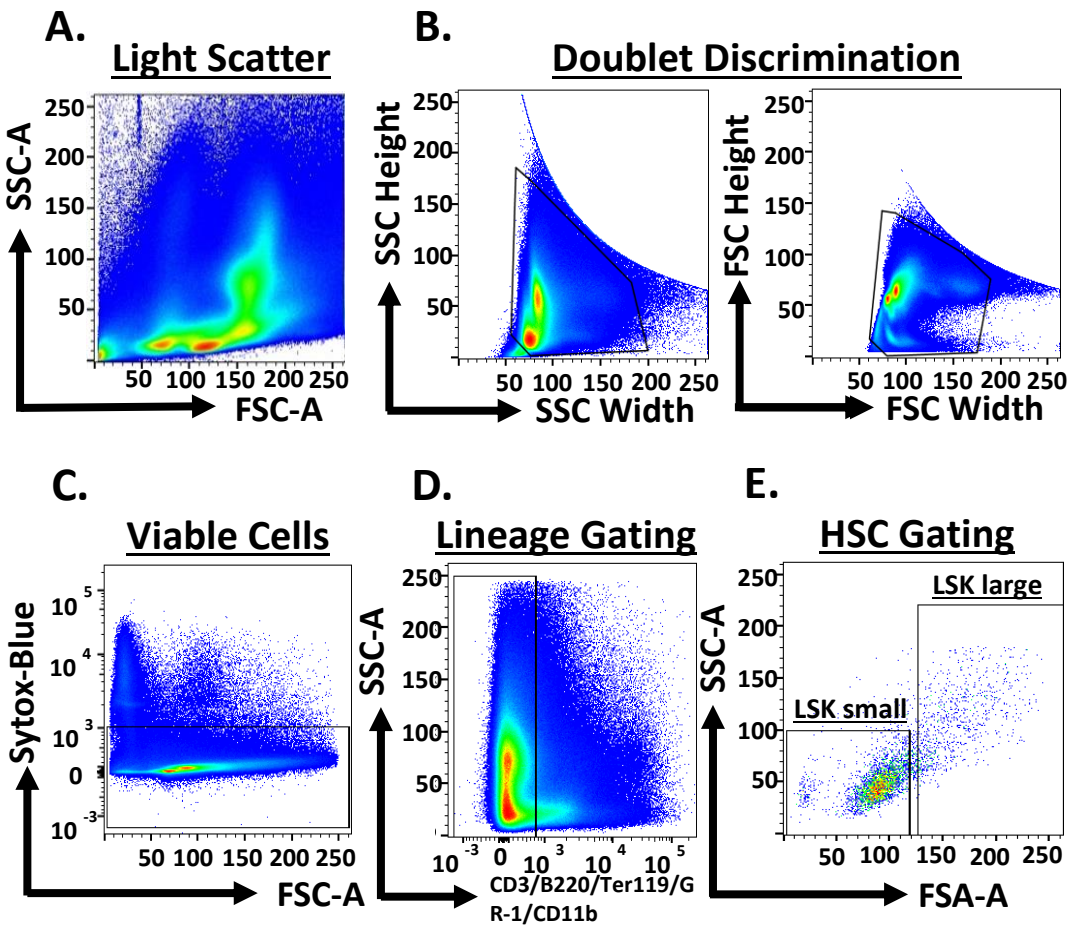

Figure 7

Gating strategy for identification of LSKs. The whole bone marrow plot is seen in (A). Doublets are subsequently removed in (B) then live cells selected in (C). Lineage negative cells are selected in (D), and LSKs (Lin-Sca+cKIT+) are divided into small and large as shown in (E).

to elucidate if the AHR can affect HSCs in various stages in development. As such, LSK populations were separated into a large and a small group based on their size and intracellular complexity as demonstrated in Figure 7.

Evidence indicates that glycolysis and low respiration are requirements for HSCs in the bone marrow (Snoeck, 2017; Takubo et al., 2013), however there is a paucity of data regarding how this applies to HSCs in the fetal liver and placenta . To determine if

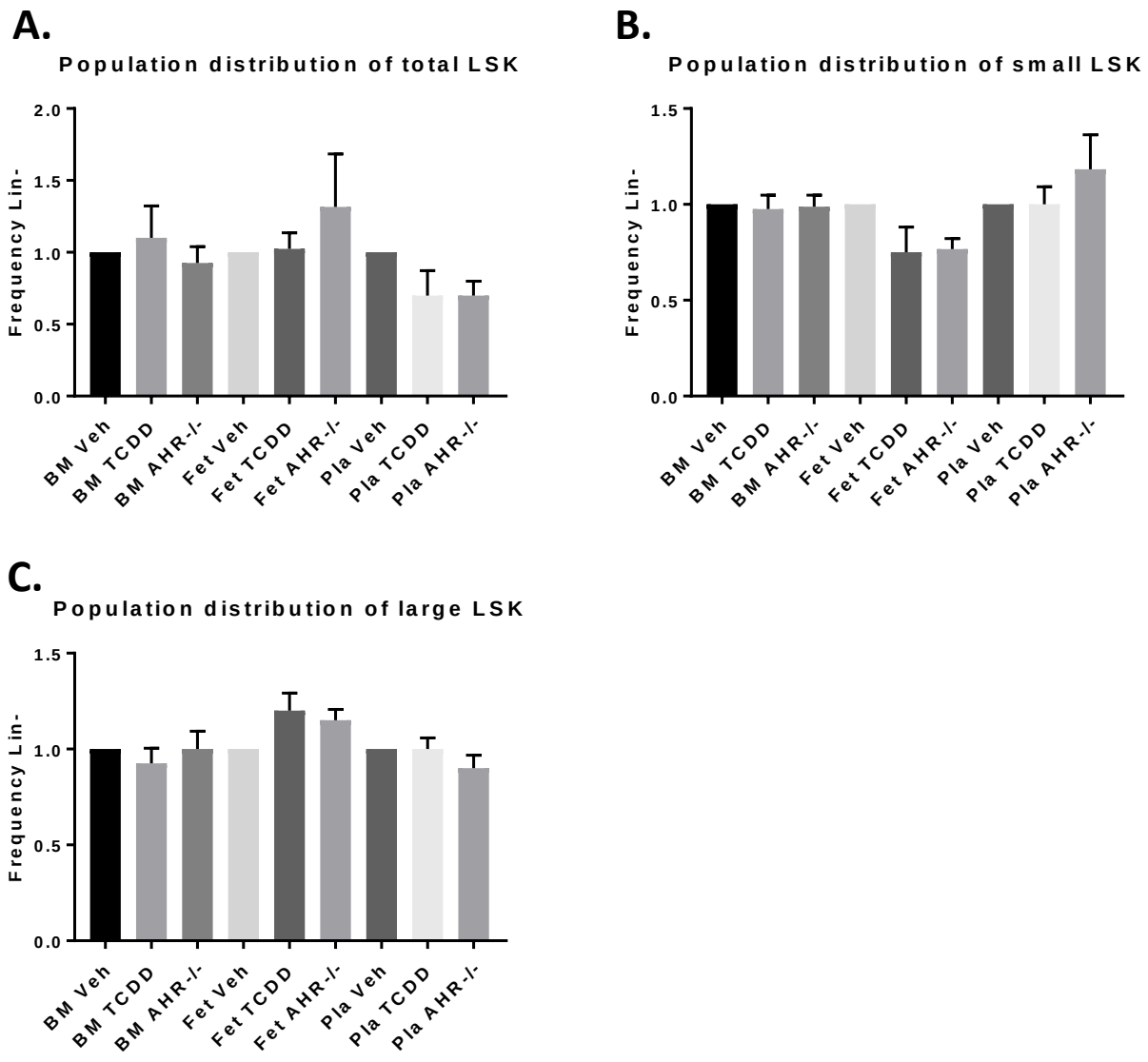

Figure 8

Distribution of HSC within anatomical locations of vehicle, TCDD exposed, and AHR null mice. Populations were selected for lineage negative (Lin-) (B220, CD3e, CD11b, GR-1, Ter-119), then cKIT+ and Sca1+ (LSK). Dead or dying cells were removed with SYTOX exclusion. LSKs were subsequently divided into small and large populations – the former having less side and forward scatter, the latter having more. A. Total LSK distribution. B. LSK large population distribution. C. LSK small distribution. Data shown is fold increase over the vehicle for that tissue. Adult mice were between 6-8 weeks old, gestational day analysis was by timed breeding and presence of mucus plug. N=10 samples over 3 experiments.

HSCs are affected in one anatomical location over another, we first compared the population distribution of LSKs in the BM, P, and FL as whole population, and after

applying our gating strategy. To determine population distribution, the lineage negative (B220, CD3e, CD11b, GR-1, Ter-119) is gated first, and further gating of cKIT, then Sca1 (LSK) were measured as a frequency of the Lin- population. Looking at the total population of LSKs across BM, there is a minor increase in LSKs in the TCDD exposed and no change in the BM AHR-/-. In contrast, FL LSKs show little variation with TCDD, but an increase in LSKs in AHR-/- (Figure 8A). The total population of LSKs in the placenta decreases in both TCDD-exposed and AHR-/-. Large LSKs show little variation in both the BM and P, but increase in population in the TCDD-exposed and AHR-/- FL. This stands in contrast to small FL LSKs that decrease in number, whereas bone marrow is unchanged (Figure 8B). Small placenta LSKs are increased, indicating a greater density of LSKs in that tissue vs vehicle.

Reactive oxygen species in hematopoietic stem cells indicates differences depending on aryl hydrocarbon receptor agonism or absence

To analyze ROS in HSCs, we used the oxidant sensing fluorescent probe 2-7 dichlorodyhydrofluorescein diacetate (H_2DCF-DA). H_2DCF-DA (DCF) is a non-polar dye and is converted by cellular esterases to the polar derivative DCFH. The fluorescent form of dichlorofluorescein (DCF) is the result of ROS oxidization of the non-fluorescent DCFH. DCF was used as a probe to compare redox activity in LSKs amongst three different anatomical locations in addition to TCDD-exposed and AHR-/- (Figure 9). To do this, we analyzed a single cell suspension after first adding markers specific for cell surface proteins that indicate LSKs. H_2DCF-DA was added to the suspension 10 minutes prior to analysis, and the result was measured by FACS for an additional 5

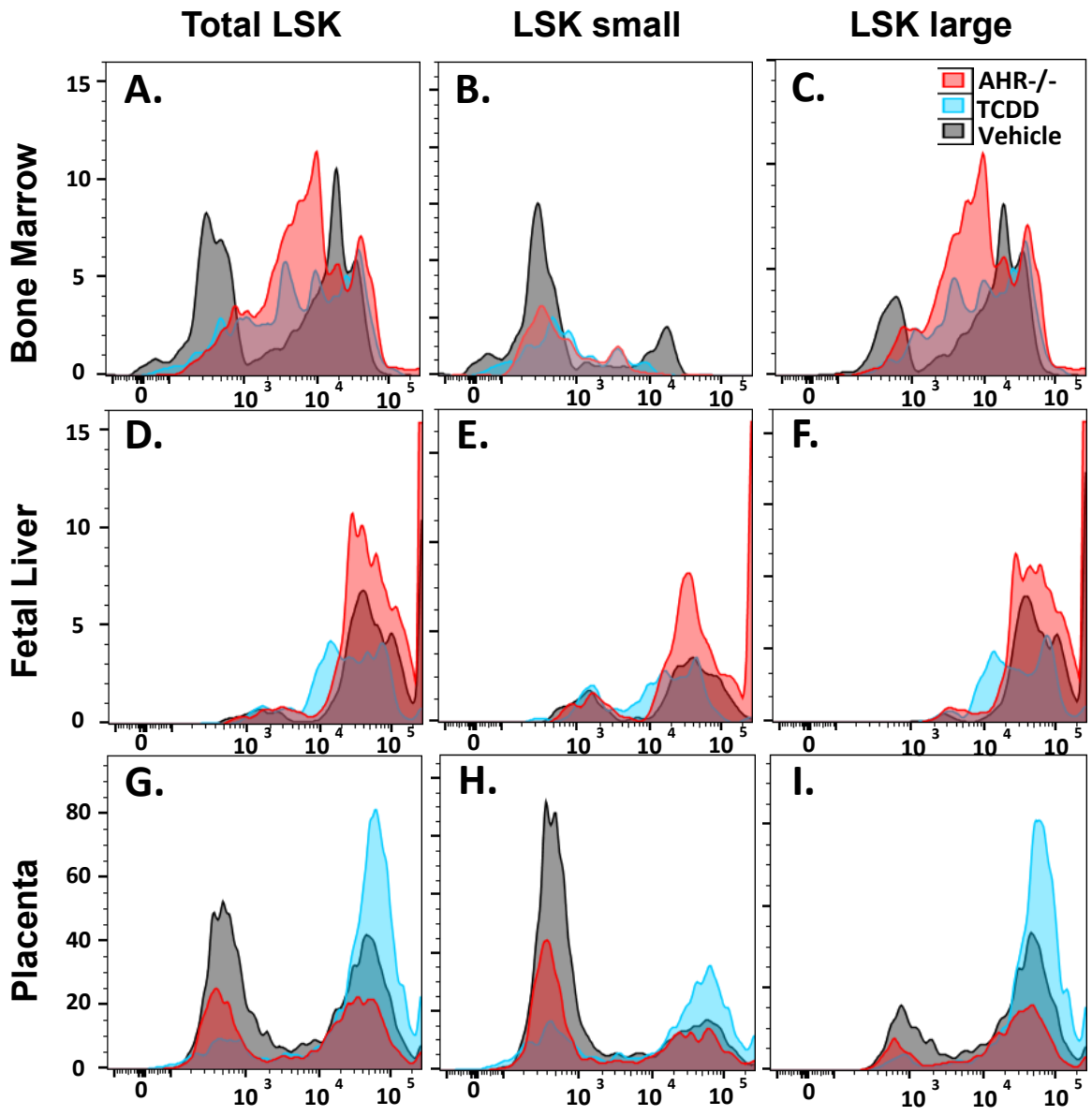

Figure 9

Histogram analysis of DCF fluorescence in bone marrow, fetal liver, and placental LSKs. A-C. Histogram fluorescence overlay in bone marrow total population (A), LSK small (B), and LSK large (B). D-F. Histogram fluorescence overlay in fetal liver total population (D), LSK small (E), and LSK large (F). G-I. Histogram fluorescence overlay in total placental LSK (G), LSK small (H), LSK large (I). N=8 samples over 2 experiments.

minutes. Looking at the entire LSK population, both bone marrow and placenta are unchanged versus vehicle, however the FL LSKs indicate a considerable increase in ROS production in both TCDD-exposed and AHR-/- (Figure 10A). While little is changed

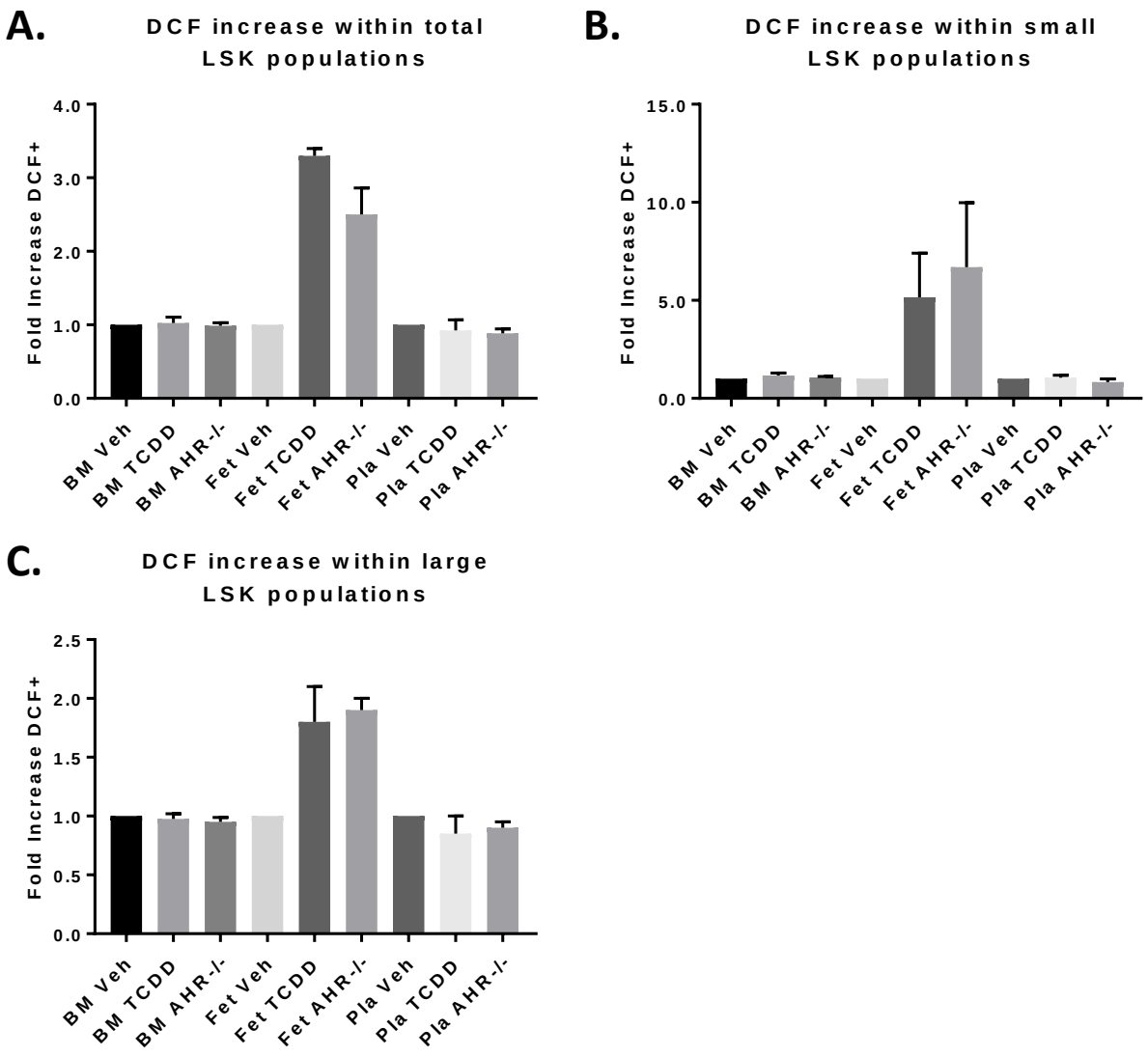

Figure 10

Distribution of DCF high populations within anatomical locations of vehicle, TCDD exposed, and AHR null mice. A. Total LSK in DCF high gate. B. LSK small in DCF high gate. C. LSK large in DCF high gate. Data shown is fold increase over the vehicle for that tissue. Adult mice were between 6-8 weeks old, gestational day analysis was by timed breeding and presence of mucus plug. N=8 samples over 2 experiments.

in the bone marrow and placenta when applying our LSK gating strategy, small LSKs in the fetal liver are >5 fold increased for ROS (Figure 10B) in contrast to ~1.8 fold change in large FL LSKs (Figure 10C).

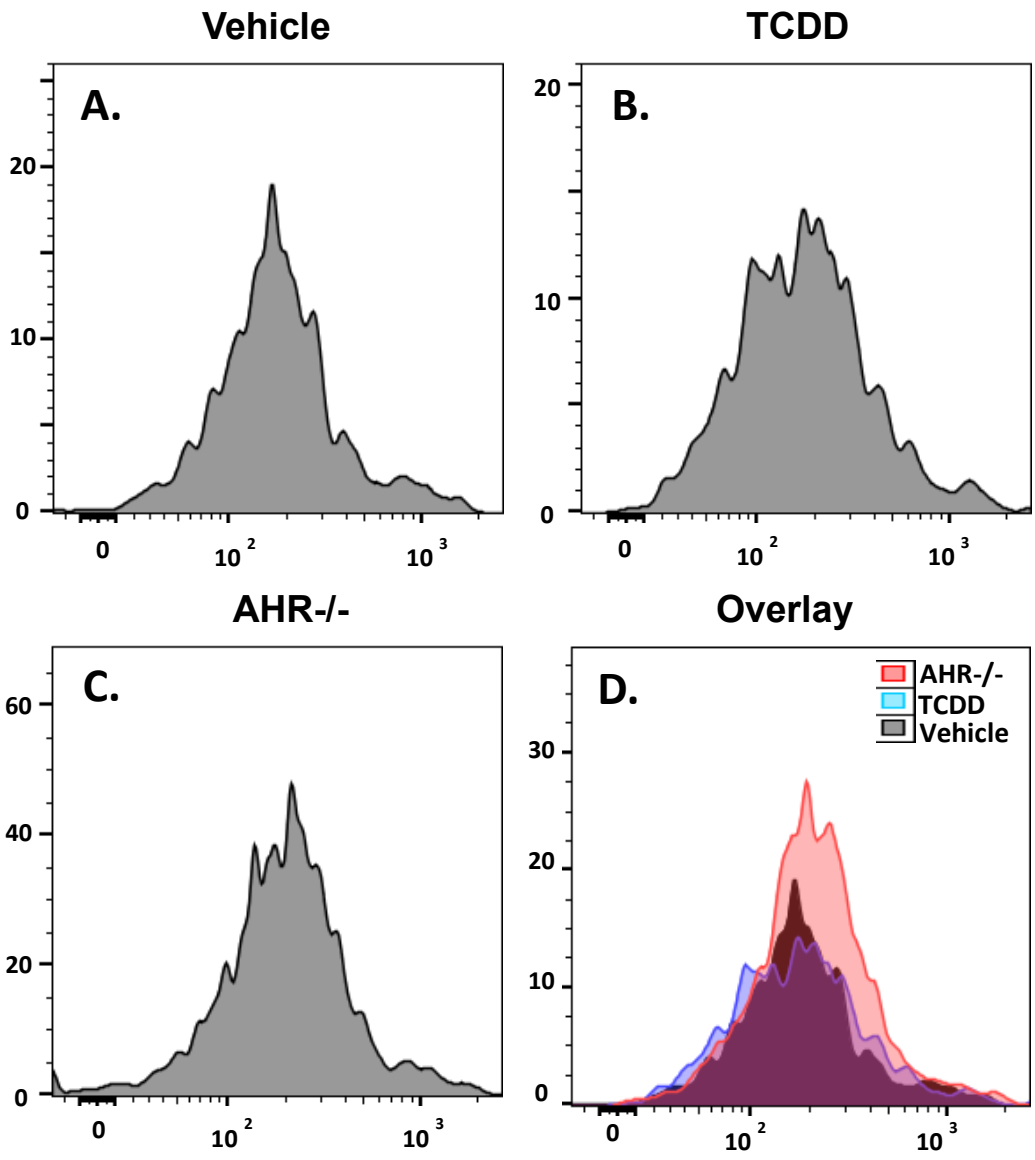

Figure 11

Histogram analysis of rhodamine 123 fluorescence in bone marrow LSKs. A. Vehicle treated; B. Developmentally TCDD exposed; C. AHR-/-. Spectral overlay of fluorescence is shown in D. N=3

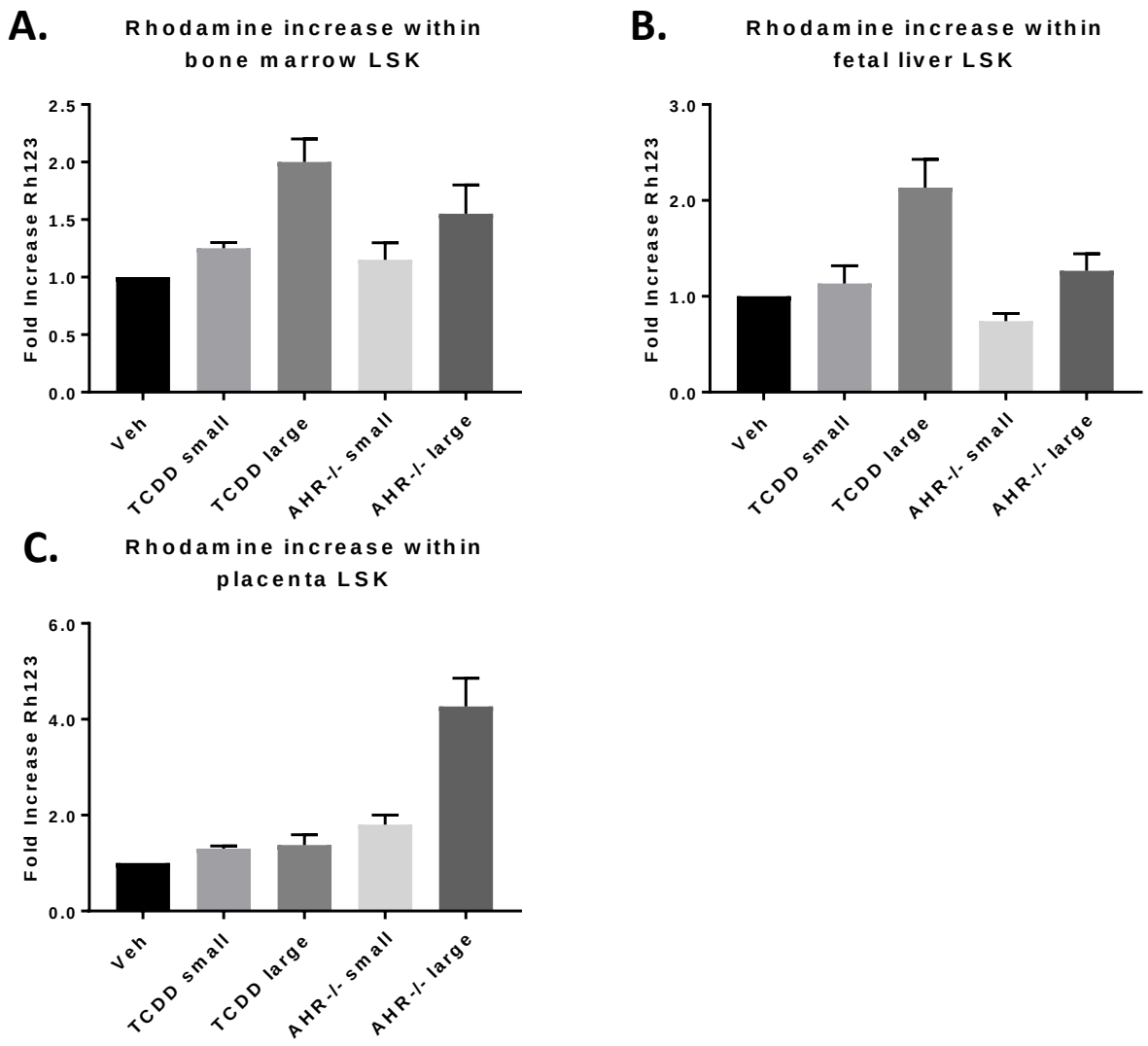

Figure 12

Distribution of Rh123 fluorescence within anatomical locations of vehicle, TCDD exposed, and AHR null mice. A. Total LSK Rh123 fluorescence in bone marrow. B. Fetal Rh123 fluorescence in LSK large and LSK small. C. Placental LSK Rh123 fluorescence in LSK large and LSK small. Data shown is fold increase over the vehicle for that tissue. Adult mice were between 6-8 weeks old, gestational day analysis was by timed breeding and presence of mucus plug. N=4

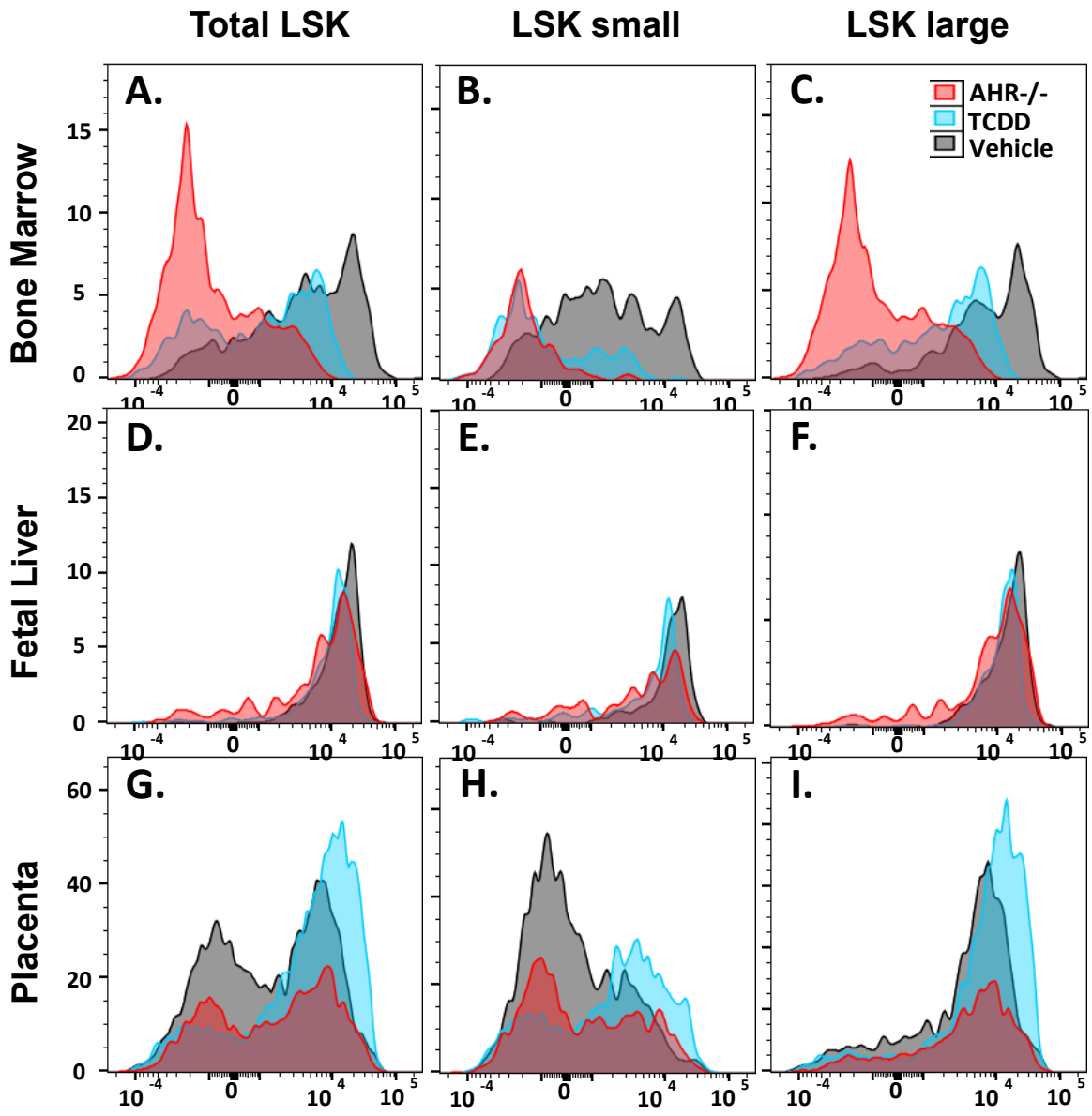

Figure 13

Histogram analysis of Mitotracker fluorescence in bone marrow, fetal liver, and placental LSKs. A-C. Histogram fluorescence overlay in bone marrow total population (A), LSK small (B), and LSK large (B). D-F. Histogram fluorescence overlay in fetal liver total population (D), LSK small (E), and LSK large (F). G-I. Histogram fluorescence overlay in total placental LSK (G), LSK small (H), LSK large (I). N=8 samples over 2 experiments.

Mitochondrial membrane potential and mass differ based on presence of aryl hydrocarbon receptor

It has been demonstrated that the mechanism driving asymmetric cell division in HSCs is the removal of aged mitochondria (Ito et al., 2006; Katajisto et al., 2015a). Moreover, it has been demonstrated that an increase in mitochondrial mass correlates with a decreased self-renewal capacity (Mortensen et al., 2011; Piccoli et al., 2005). Given our observed increase in ROS production in LSKs, we wanted to elucidate the role of mitochondria as the potential source of ROS. The transmembrane potential between the mitochondrial inner and outer membranes is required to drive ATP synthesis, and can be probed using rhodamine 123 (Rh123) to indicate differences in mitochondrial membrane polarization (MMP). Rhodamine 123 is sequestered in functioning mitochondria but can also be washed out once mitochondria lose their membrane potential, so we also utilized an additional mitochondrial dye call Mitotracker which is retained in active mitochondria after membrane potential is lost.

Dividing LSKs into small and large follows the logic that actively proliferating and functional cells will have a greater size (forward scatter) and more intracellular complexity (side scatter), and moreover, a greater likelihood of utilizing oxidative phosphorylation (OXPHOS) to meet their energetic needs. While Rh123 fluorecence in LSKs is largely bell-shaped (Figure 11 A-C), overlaying the histograms indicates how AHR-/- is more sharply peaked demonstrating a narrower curve and shifted to the right of vehicle (Figure 11D). With this in mind, it is not unexpected that in the bone marrow, there is a more pronounced increase in MMP in both the large TCDD and AHR-/- LSKs (Figure 12A). FL LSKs indicated similar increases in both small and large LSKs with

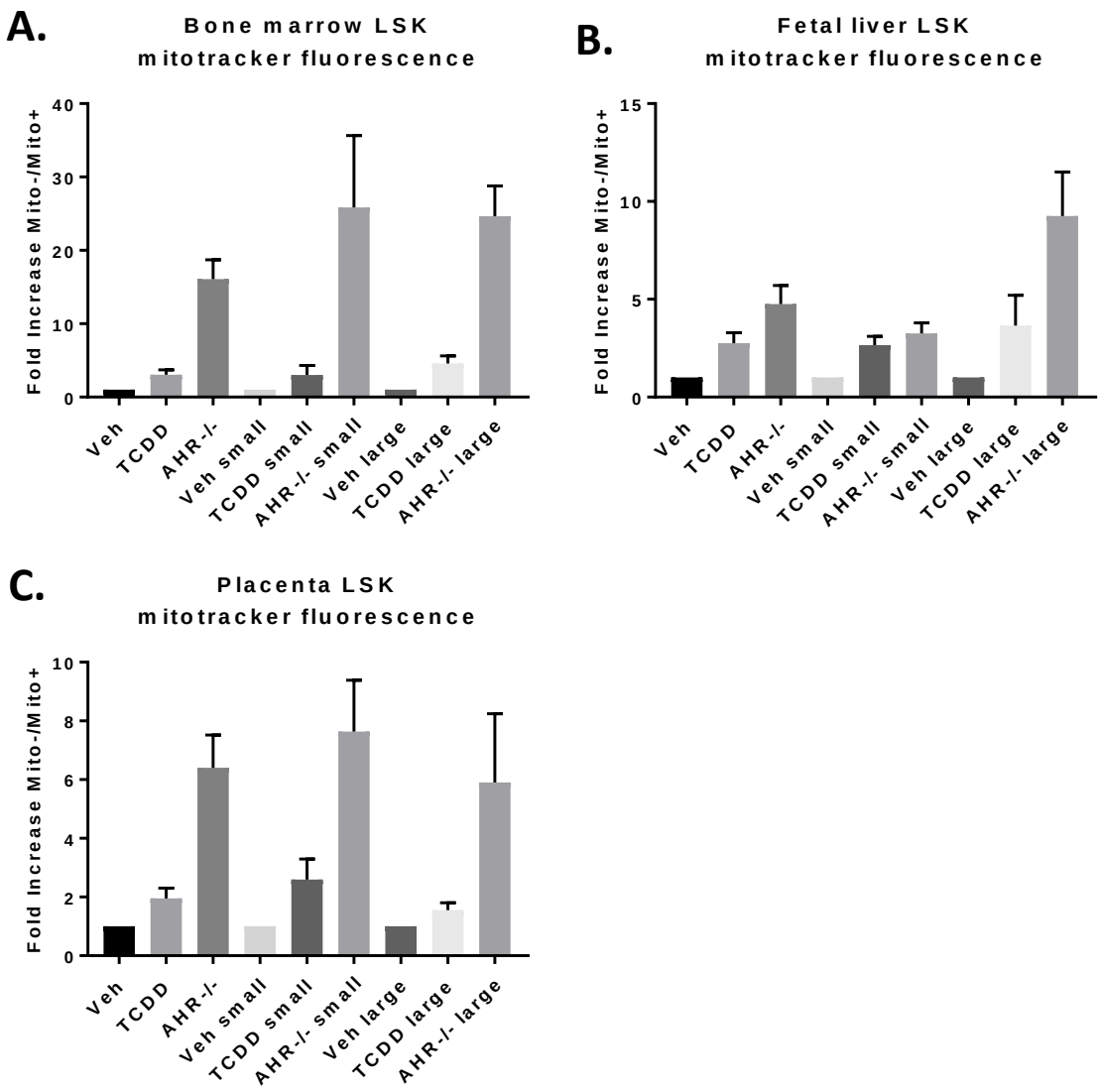

Figure 14

Distribution of mitotracker fluorescence within niches of vehicle, TCDD exposed, and AHR null mice. A. Bone marrow Mitotracker fluorescence. B. Fetal LSK Mitotracker fluorescence. C. Placental LSK Mitotracker fluorescence. Data shown is the ratio of fold increase of Mitotracker signal. Adult mice were between 6-8 weeks old, gestational day analysis was by timed breeding and presence of mucus plug. N=4

AHR agonism, and large AHR-/- FL LSKs are increased relative to control (Figure 12B).

In contrast, large placenta AHR-/- LSKs demonstrate >4-fold increase in Rh123

fluorescence with TCDD-exposure only indicating a 30% increase in MMP (Figure 12C).

Using Mitotracker in addition to Rh123 gives a better picture of functioning mitochondria since Mitotracker is not washed out of mitochondria if membrane permeabilization is lost. The data was calculated by evaluating the ratio of negative (low fluorescence) to positive (higher fluorescence), then shown as the fold change over control. The histogram overlays in Figure 13A and 13G demonstrate how varied the LSK population can be depending on anatomical location. Strikingly, the ratio of LSKs in Mitotracker low vs Mitotracker high is highest in the AHR-/- bone marrow (Figure 14A), which, in contrast to Rh123, trends with the placenta (Figure 14C). Fetal liver LSKs indicate a more pronounced decrease only in the large LSKs (Figure 14B), however it should be noted that developmental TCDD exposure decreases mitotracker fluorescence, and in theory, mitochondrial mass, in all anatomical locations. Given these differences in mitochondrial mass, it raises the possibility that the AHR might not be only a regulator of mitochondrial activity in HSCs, but potentially a regulator of mitochondrial mass as well.

Comparison of aryl hydrocarbon receptor agonism in hematopoietic stem cells by gestational age

The placenta is the primary hematopoietic tissue at GD11 before transit to the fetal liver, and changes in population or ROS at these time points could shed light on

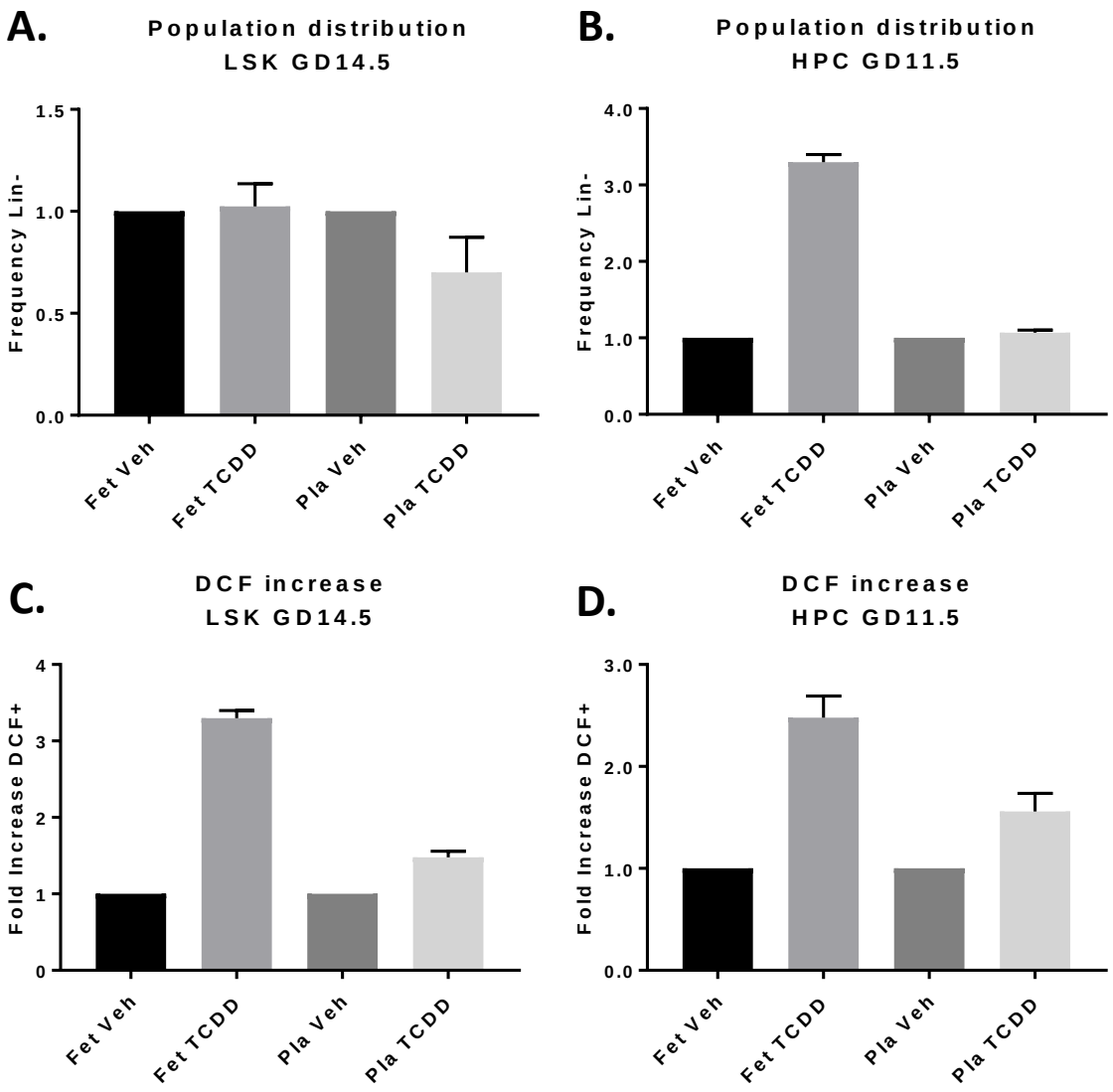

Figure 15

Distribution of LSK population in vehicle and TCDD exposed mice by gestational day. A. LSK population in gestational day (GD) 14 fetal liver and placenta. B. HPC (Lin-cKIT+CD45+) population in GD11 fetal liver and placenta. C. LSK GD14 DCF fluoresence. D. HPC GD11 fluorescence. Data shown is fold increase over the vehicle for that tissue. Adult mice were between 6-8 weeks old, gestational day analysis was by timed breeding and presence of mucus plug. N=10

how or if AHR agonism is more active at one hematopoietic site than another.

Moreover, we wanted to ask if the changes in LSKs were specific to the cells

themselves, or could be influenced by the surrounding milieu. To answer this, we

wanted to compare population distribution and ROS production in GD14 and GD11 fetal liver and placenta LSKs. Comparing these time points gives a unique window into two vital anatomical locations and developmental stages. Because surface markers differ based on timing, we used Lin-cKIT+CD45+ as an indicator for hematopoietic progenitor cell (HPC) at GD11. While there is little variation in LSK population at GD 14, HPCs at GD 11 show almost a 3-fold increase in population (Figure 15B) when compared against vehicle, whereas placental LSKs decrease at GD 14 (Figure 15A) and are unchanged at GD 11 (Figure 15B). Additionally, we wanted to evaluate ROS in HSC populations at these developmental locations and found that TCDD increased ROS at both GD 14 (Figure 15C) and GD 11 (Figure 15D).

DISCUSSION

The comparison of bone marrow, fetal liver, and placenta allows for a unique window into the differences and similarities between AHR agonism and absence. Given the initial expansion of HSCs during development, perturbations can have deleterious effects years, if not decades, later. TCDD has been shown to have a direct effect on hematopoiesis during these critical windows (Ahrenhoerster et al., 2014; Laiosa et al., 2015), and was similarly found to increase oxidative stress. It is widely held that HSCs limit ROS production to limit damage to DNA (Simsek et al., 2010b) and additional studies have demonstrated that increased ROS can favor differentiation over self-renewal (Chen et al., 2008; Ito and Suda, 2014; Miyamoto et al., 2007). Interestingly, AHR-/- HSCs share many similar characteristics to these studies. It was shown that

there is a faster proliferation rate and more LSKs in AHR-/- mice (Gasiewicz et al., 2010; Singh et al., 2011). Coupled with the findings that AHR-/- HSCs increase ROS in a manner similar to TCDD (Laiosa et al., 2015) and that the overall result is a depletion of Long-term HSCs, it is worth considering the concept that the AHR regulates a metabolic state in HSCs, and whether it is absent or agonized with TCDD, it is unable to fulfill such a task.

To further evaluate the implications of the AHR regulating metabolism in LSKs, we sought to compare these populations in the bone marrow, fetal liver, and placenta to assess similarities and differences. Additionally, based on our understanding of other work done in our lab, we separated LSKs into small and large compartments. We investigated first by total change in distribution in each compartment. Looking at the total LSK population (Figure 8A) a non-significant increase was noted in the bone marrow of TCDD exposed, whereas the fetal liver indicated no change and the placenta was decreased. The normal transit of HSCs in development is from the placenta to the fetal liver, so it's speculative to say that the developmental checkpoint that moves HSCs from the placenta to the fetal liver could be accelerated if the AHR is absent from its as yet unclear role in HSCs. Moreover, the finding that there are more large LSKs in the fetal liver (Figure 8C) could indicate that the cells are either undergoing rapid proliferation or are in the process of terminal differentiation. While we have shown previously that AHR-/- and TCDD increase ROS in fetal LSKs, we wanted to evaluate this difference side by side with bone marrow and placenta LSKs. Consistent with our previous results, ROS was increased almost exclusively in the fetal liver (Figure 10 A-

C). Interestingly, this effect was exaggerated in the small LSKs which showed a 5-fold increase in ROS (Figure 10B) versus a 1.8-fold increase in large LSKs (Figure 10C).

From this, we wanted to evaluate mitochondria more directly, so we used two vital dyes – one that evaluates the mitochondrial membrane potential (MMP), thus indicating active mitochondria; and the other that will fluoresce only once it is inside active mitochondria. The former, rhodamine 123 (Rh123), indicated that both AHR agonism and absence caused an increase in MMP, with TCDD having an exaggerated effect vs. AHR-/- in the bone marrow and fetal LSKs (Figure 12 A-B) and a more pronounced effect in AHR-/- placental LSKs. We used an additional mitochondrial vital dye called Mitotracker that fluoresces only in active mitochondria and since it is not dependent on MMP, may be a better indicator of mitochondrial mass. There was a dramatic decrease in the bone marrow and placenta of mitochondrial mass of both large and small LSKs (Figure 14 A-C) in AHR-/-, while this effect was limited to large LSKs in the fetal liver (Figure 14B). Taken together, it indicates that both AHR agonism and absence have the ability to decrease mitochondrial mass, with a more dramatic effect noted in the absence of AHR. The finding that the effect is >20-fold in the bone marrow (Figure 14A) in contrast to ~5-fold in the fetal liver (Figure 14B) and placenta (Figure 14C) is consistent with this notion since fetal LSKs are relatively newer compared to aged bone marrow LSKs. This could also explain the Rh123 staining since if there are fewer mitochondria, the effect of polarization would be disproportionately exaggerated.

Gestational day 14 in the fetal liver is an important site of expansion for HSCs, however the fetal liver lacks the ability for *de novo* generation. The placenta is an equally important site of HSC expansion, albeit at an earlier time point (Dzierzak and

Robin, 2010; Gekas et al., 2005). With this in mind, we wanted to compare HSC distribution and ROS in gestational day 11 and 14 fetal liver and placentas. While we did not see a notable increase in LSKs after developmental exposure to TCDD (Figure 15A), we did see an effect at GD 11 (Figure 15B) in the fetal liver with no effect in the placenta. The finding that the population increase is limited to the fetal liver and not found in the placenta could indicate that the effect on LSKs is due to AHR-dependent changes on surrounding cells in that location, or, conversely, that the developmental cue to migrate was accelerated prematurely. Similarly, the increases in ROS are greatest in the fetal liver at both developmental time points (Figure 15 C-D).

Combined, we have highlighted some important differences in AHR agonism or absence during HSC development. AHR-dependent changes can be seen in HSC distribution as early as GD11, when HSCs are first starting to migrate to the fetal liver. The ones that have made it there already demonstrated increased ROS production. Taken together, this indicates that the change is specific to HSCs independent of the surrounding milieu. That the increase in ROS is only seen in the fetal liver is also highly significant since HSCs, in contrast to their quiescent counterparts in the bone marrow, are highly active. When combined with the GD11 findings, it seems to indicate that TCDD has the greatest effect on actively proliferating cells. It has been reported that HSCs have lower mitochondrial mass (Romero-Moya et al., 2013; Simsek et al., 2010b), while others have pointed to this as an artifact of xenobiotic efflux pumps in HSCs (de Almeida et al., 2017). The curious finding that AHR-/- has such a disproportionate shift with more LSKs indicating low Mitotracker fluorescence indicates that if this is due to xenobiotic efflux pumps, then AHR-/- LSKs must either have more,

or a greater activity of these pumps. Otherwise, AHR-/- LSKs do in fact have a lower mitochondrial mass, an equally interesting finding since the older bone marrow LSKs in AHR-/- mice had a greater shift than the newer fetal liver and placental LSKs. Mitophagy is the self-regulation of mitochondrial numbers which, in HSCs, is biased towards the suppression of active mitochondria (Ho et al., 2017). An increase in mitophagy or a decrease in mitochondrial biogenesis could explain why there is a 20-fold decrease in AHR-/- LSKs indicating lower mitochondrial mass in the bone marrow in contrast to the ~5-fold decrease in the fetal liver and placenta.

This work was performed to elucidate how AHR agonism or absence could affect LSKs at developmental hematopoietic stages. By comparing different tissue types at different ages, our aim was to strengthen the hypothesis that the HSC effects of AHR agonism with TCDD are the result of removing the AHR from a metabolic regulatory role in HSCs. While the similarities between AHR agonism and absence were not as clear cut as we had expected, we did report some findings that are relevant to HSC biology. Regardless of Mitotracker results reflecting efflux pumps or mitochondrial mass, the finding that TCDD fluorescence is between AHR-/- and vehicle leads one to question if, given a longer duration of exposure to TCDD, would they then more resemble the AHR-/-? We showed that LSKs are largely positive for Mitotracker in the vehicle treated HSCs, however we and others have indicated that LSKs are not proliferating as rapidly in AHR agonism or absence which leads to a tentative hypothesis that the LSKs in TCDD-exposed and AHR-/- are the result of newer cells with an enhanced mitophagy process or increased expression of xenobiotic efflux pumps.

Of equal importance is our finding of the inverse relationship in HSC expansion between GD14 and GD11. GD14 LSKs are increased with TCDD in the fetal liver, but decreased in the placenta, whereas at GD 11, are decreased in the fetal liver and increased in the placenta. Taken with the consideration that AHR agonism causes an increase in LSK numbers, the finding that this happens at another anatomical site, and at another developmental time point, is highly significant. This could indicate that the effect of AHR agonism is independent of any interactions with surrounding cells, and is solely intrinsic to HSCs. Moreover, the fact that we saw the expansion at an earlier point in hematopoiesis could indicate that the number of LSKs is already expanded before their transit to the fetal liver.

The role of the AHR as a receptor for xenobiotics may overshadow its role as a regulatory protein for metabolism in stem cells. A better understanding of the unique role of the AHR in HSCs may allow us to potentially mitigate its later-life hematological consequences.

CHAPTER 5

FUNCTIONAL CHARACTERIZATION OF LONG-TERM HEMATOPOETIC STEM CELLS

ABSTRACT

Background: Identification of LT-HSCs remains elusive. Characterizations of LT-HSCs by measuring proliferation or by surface markers reveal a more enriched, but still heterogenous population of multipotent hematopoietic stem cells.

Objectives: The aim of this study was to identify if a gating strategy based on size and intracellular complexity were applied first, followed by conventional surface markers, if it would yield a population more enriched for Long-Term HSCs.

Methods: Bone marrow from C57BL/6 mice was isolated and stained using conventional surface markers. HSCs were assessed for changes in reactive oxygen species production and mitochondrial membrane potential over time by collecting the sample continuously for 15 minutes at 37c.

Results: Our findings suggest that by discriminating samples by both size and intracellular complexity yields a more enriched population for LT-HSCs. Furthermore, the differences in these populations could be demonstrated by mitochondrial mass staining, mitochondrial membrane potential staining, and ROS production.

Conclusions: A more enriched population of LT-HSCs can be gathered using combinations of surface markers in addition to physical characteristics.

INTRODUCTION

Hematopoietic stem cells are specialized tissue specific progenitors that reside in low oxygen microenvironments of the bone marrow and possess the dual function of long-term self-renewal potential along with multi-lineage differentiation potential into every blood cell circulating throughout the body. Given their fundamental importance for blood and immune system function, advances in hematopoietic stem cell identification, isolation, and potential in vitro enrichment are needed to improve efficacy of blood cell product generation for a spectrum of clinical applications. However, a current limitation to conducting these critical basic science studies is partially attributed to the combination of the lack of an accepted consensus on what single or combination of markers can be used to identify both human and murine HSCs. This, combined with the need for specialized UV LASER-equipped fluorescence activated cell sorters which are less commonly available throughout the research community, adds an additional level of difficulty. Our aim was to perform flow cytometric analysis of ROS production using a kinetic acquisition method. We found this to be a better method for the multiparametric analysis of multiple populations *in situ* due to the low numbers of cells collected.

LT-HSCs have been shown to reside in specialized low-oxygen microenvironments of the bone marrow called ‘niches’ (Nombela-Arrieta et al., 2013; Suda et al., 2011). Because of this hypoxic environment, LT-HSCs rely on anaerobic glycolysis rather than oxidative phosphorylation (OXPHOS) to meet their low energy demands. LT-HSCs exist in a state of quiescence and are thought to divide as few as 5 times over the lifetime of the mouse (Wilson et al., 2008) This is due to their tremendous proliferative potential once they escape quiescence. This state of quiescence is thought

to be an evolutionary adaption to prevent the accumulation of DNA mutations that would promote malignancy (Lobo et al., 2007). Thus, the hypoxic microenvironment limits DNA-damaging reactive oxygen species (ROS) production by both promoting anaerobic glycolysis in the LT-HSC and by limiting the exposure of these cells to higher oxygen concentrations. It has further been demonstrated that HSCs have reduced mitochondrial mass in contrast to their mitotically active differentiating progeny (Piccoli et al., 2005; Simsek et al., 2010b). The data showing ST-HSC and MPP have more mitochondrial-mass is consistent with the evidence indicating these cells are dependent on OXPHOS (Yu et al., 2013).

Given this evidence highlighting the importance of metabolism in LT-HSC, there also appears to be a crucial role for mitochondria in determining progenitor cell fate. Others have demonstrated that HSCs asymmetrically divide in order to remove the aged mitochondria from the self-renewing HSC population (Ito et al., 2006; Katajisto et al., 2015b). It was further shown that there is an increase in mitochondrial mass with the loss of self-renewing capacity (Piccoli et al., 2005). Additional studies targeting the lysosomal degradation process indicated that over-proliferation of mitochondria is detrimental to self-renewing capacity (Mortensen et al., 2011). Taken together, these studies provide evidence to substantiate the idea that having low mitochondrial mass is a requirement for a self-renewing HSC.

Our approach was to leverage the knowledge about mitochondria in LT-HSCs by profiling these cells flow cytometrically using a combination of vital dyes to define mitochondrial mass, membrane potential, reactive oxygen species (ROS) along with physical characterization using precisely defined light scattering gating strategies.

These analyses were further refined by utilizing a kinetic-based flow cytometric acquisition approach for ROS production. The advantages of our analytical method for identifying putative LT-HSC is the combination of multiparametric analysis of surface antigens that define HSC progenitor populations combined with *in situ* analysis of Redox state and mitochondria activity within a mixed population of bone marrow cells. Our findings have the potential to further enhance existing knowledge of LT-HSCs and ultimately enhance enrichment of this clinically relevant population.

RESULTS

Lin-CD150+CD48- stem cells are a heterogenous population in bone marrow

Hematopoietic stem cells actively scavenge reactive oxygen species or aim to limit their production in order to prevent oxidative damage to DNA that can impair long-term self-renewal potential and raise the risk of later-life malignancy. Therefore, rigorous analyses of ROS levels using fluorescent indicator dyes may be a useful biomarker for hematopoietic stem cells within a heterogeneous population of bone marrow cells. The vital dye H_2DCF-DA is a frequently used marker for ROS production. DCF-DA passes through cell membranes and is oxidized to highly fluorescent DCF in the presence of ROS. Moreover, DCF was used as an initial probe to assess redox activity given the expectation that OXPHOS-respiring energetically active cells are predicted to have elevated ROS compared to quiescent cells.

To determine the ROS levels of putative LT-HSCs, we first analyzed a single cell suspension comprised of whole bone marrow after first staining cells with antibodies

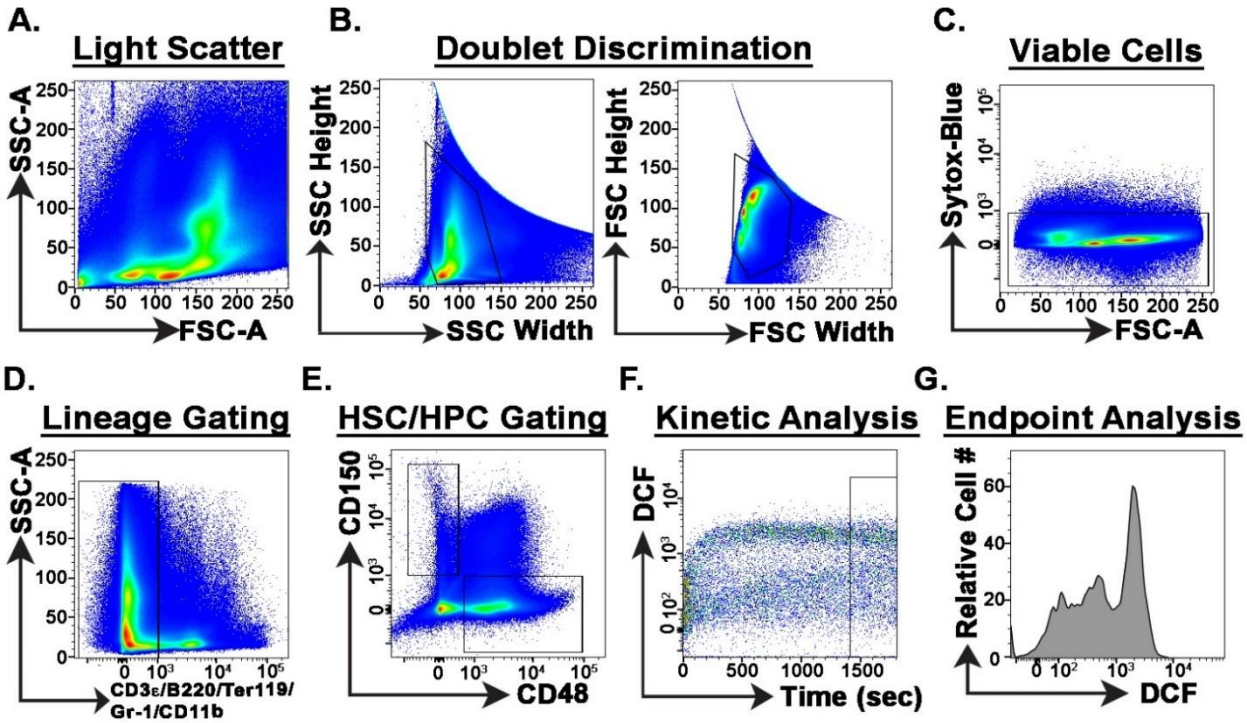

Figure 16

Gating strategy for identification of LT-HSCs in bone marrow. The whole bone marrow plot is seen in (A). Doublets are subsequently removed in (B) then live cells selected in (C). Lineage negative cells are selected in (D), and LT-HSCs (Lin-CD150+CD48-) are gated in (E). (F) shows the increase in DCF of the whole LT-HSC gated population with representative histogram shown in (G).

specific for cell surface proteins that delineate LT-HSCs (Lin-CD150+CD48-). Next, we analyzed the cells by flow cytometry using a kinetic approach to follow DCF fluorescence as a measure of ROS across heterogenous bone marrow cell populations. Specifically, cells were first gated based on size and granularity using width vs height doublet discrimination (Figure 16 A-C) followed by dead cell discrimination with the vital DNA dye Sytox blue (Figure 16D). Next cells lacking maturation defining lineage markers (CD3, B220, GR1, Ter119, Mac1) were gated followed by analysis of the putative hematopoietic stem cell markers CD48 and CD150 (HSC: lin-CD150+CD48-). Further, cells were acquired on the FACS for 15 continuous minutes to produce a kinetic trace of ROS production. Notably, both DCF levels throughout the kinetic

analysis (Figure 16F) and a histogram of the total DCF fluorescence in the last 5 minutes of the experiment (Figure 16G) reveal that cell surface identification of LT-HSCs alone identifies a heterogenous population with at least two distinct populations based on ROS levels. This is exemplified by the histogram of the final five minutes of the acquisition which reflects a bimodal distribution of DCF fluorescence and thus ROS (Figure 16G) in LT-HSCs.

Multiparametric and kinetic analysis of murine bone marrow populations

To analyze the distribution of LT-HSCs in bone marrow, we modified the gating strategy focused on physical characteristics of the cells before isolating by surface markers. Forward scatter is used as a measure of cellular size due to light diffraction around the cell and the light signal gathered from around the cell is relational to the diameter. The measurement of side scatter is representational of intracellular complexity. The scattering of the light signal is proportional to the number of cytoplasmic granules. Our strategy was to look at all live cells, then use height and width to remove cellular debris before gating on all lineage negative cells (Figure 17A). From this, heat mapping of bone marrow shows three distinct highly concentrated populations of cells (Figure 17B), which are further divided into gating strategies, labelled as I, II, and III. We then analyzed Lin-CD150+CD48- within each respective population. A priori, population I was predicted to contain the least differentiated and more primitive cells. Population II, being slightly larger, would contain more multipotent progenitor cells, and population III would contain cells already undergoing terminal differentiation. However, using these light scattering strategies, we find long-term HSCs

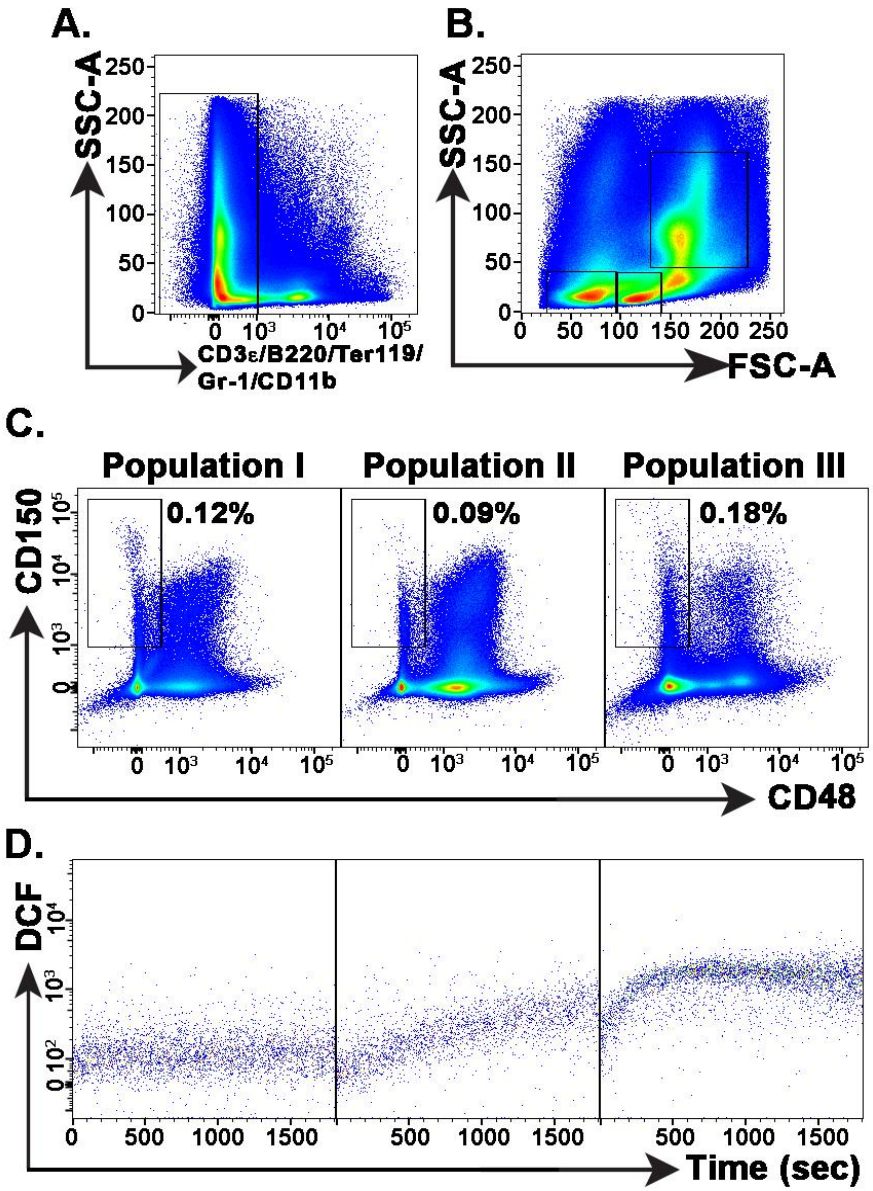

Figure 17

Segregation of LT-HSCs. After gating on Lin- population (A), the remainder of the bone marrow population was gated based on size and intracellular complexity, which we labelled at I, II, and III (B). From this, gated on LT-HSCs (C) and segregated the kinetic trace of DCF using this gating strategy (D).

(Lin-CD150+CD48-) in all three bone marrow populations (Figure 17C). Notably, when our kinetic study of ROS was added to the analysis, the differences in ROS production differed significantly between all Lin-CD150+CD48- cells. Population I contains cells with minimal DCF fluorescence increase (Figure 17D - left), whereas population II

shows a linear increase over time (Figure 17D - middle). Population III is a log higher fluorescence than population I (Figure 17D - right), however does not show the linearity seen in population II. Moreover, when compared against the bimodal distribution of fluorescence seen in Figure 16G, it appears that LT-HSCs in population I are the only population exhibiting low ROS.

Characterization of mitochondria in bone marrow populations

DCF is a non-specific indicator of ROS. Since a one electron oxidation is all that is required for DCF to fluoresce, cellular inducers of H2DCF to DCF can range from peroxynitrite to hydroxyl radical. Electroparamagnetic resonance imaging (EPR), an additional method of testing for more specific reactive species, are problematic due to the low number of LT-HSCs collected. Given these difficulties in the assessment and sourcing of ROS production, we sought to investigate mitochondria since it is a frequent source of ROS.

While others studies have demonstrated that self-renewing HSCs contain lower mitochondrial mass (Piccoli et al., 2005; Simsek et al., 2010b), we wanted to evaluate how this fit with our light-scatter based gating strategy. We first used Mitotracker, a cationic dye that passively diffuses across plasma membranes and undergoes a modification in active mitochondria that causes it to fluoresce and prevents its escape. Due to the timing and complexity of our experiments, we found this to be a better dye than rhodamine 123 which can be washed out of mitochondria when the membrane potential is lost. We additionally utilized nonyl acridine orange (NAO) which binds to

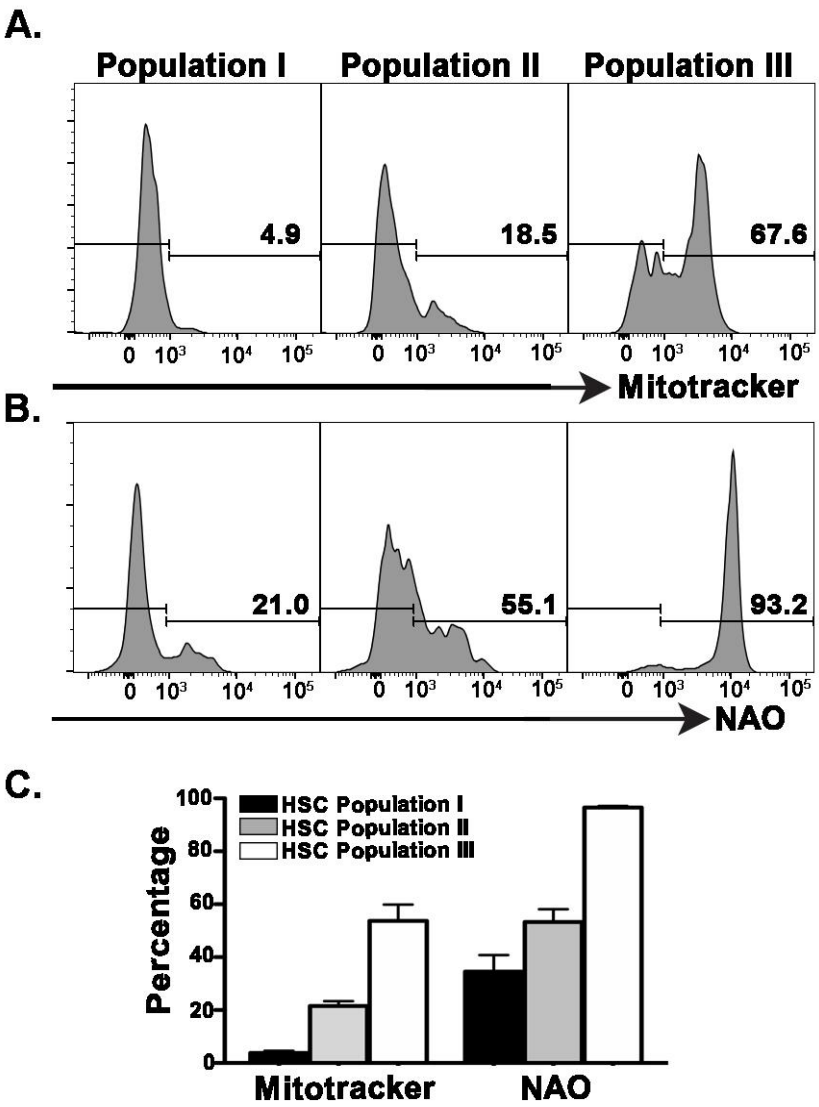

Figure 18

Staining of mitochondria in LT-HSC populations. (A) Mitotracker fluorescence in populations I, II, III, with the lowest florescence seen in populations I and II. (B) Nonyl acridine orange (NAO) fluorescence in populations I, II, and III with the lowest staining for mitochondria seen in population I. (C) Bar graph representation of positive populations using respective dyes.

cardiolipin in mitochondria independent of membrane potential and is thus a useful comparison when using mitochondrial vital dyes (Ferlini and Scambia, 2007; Garcia Fernandez et al., 2004). Mitotracker staining shows a similar distribution with low fluorescence in populations I and II (Figure 18A – left and middle), and a bimodal

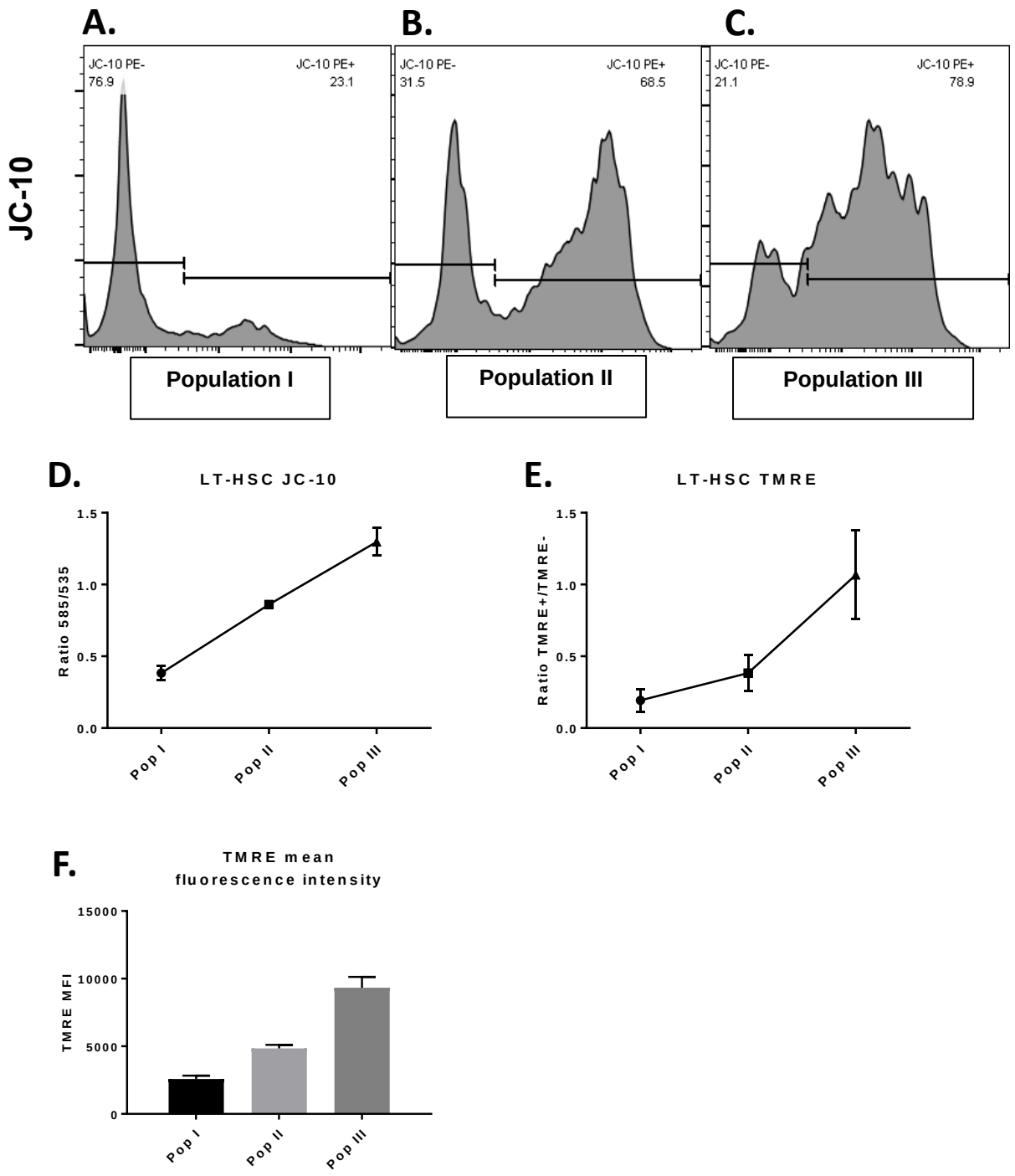

Figure 19

Analysis of mitochondrial membrane potential. JC-10 fluoresces to red in polarized mitochondria. In the absence of polarization, it remains green. (A, B C) JC-10 fluorescence in populations I, II, III respectively. (D) Ratio of aggregate to monomer. (E) Ratio of TMRE+ to TMRE-. (F) Mean Fluorescence intensity of TMRE in populations.

distribution in population III (Figure 18A - right). This could be indicative of the relative

mitochondrial activity in these populations since Mitotracker requires active mitochondria to undergo the change required for fluorescence. NAO staining shows a similar distribution to Mitotracker in population I (Figure 18A-B), which is further indicative of low mitochondrial mass in population I.

Mitochondrial membrane potential staining reflects activity of mitochondria within populations

One limitation of studying mitochondrial mass is that they do little to shed light on the functionality of mitochondria. Our findings based on our methods that population I contains lower mitochondrial mass lead us to investigate if mitochondrial membrane potential would show a similar trend. It has been demonstrated by others that as cells move towards differentiation, they rely more on oxidative phosphorylation than glycolysis (Chen et al., 2012). Moreover, it has also been shown that long-term self-renewing cells deliberately act to maintain inactive mitochondria (Katajisto et al., 2015b). To investigate mitochondrial activity, we used two lipophilic cationic dyes; JC-10 and tetremethylrhodamine ethyl ester (TMRE). TMRE will only fluoresce in mitochondrial with an active membrane potential. JC-10 passively enters the mitochondria and in the absence of mitochondrial membrane potential (MMP) remains in its monomeric form, however with an active (MMP) , JC-10 forms an aggregate (Cottet-Rousselle et al., 2011; Perry et al., 2011; Srivastava et al., 2015).

Analysis with JC-10 indicates that population I has the highest distribution of cells with low mitochondrial membrane potential (Figure 19A) when compared against the

bimodal distributions of populations II and III (Figure 19B-C). Aggregate to monomer ratio (Figure 19D) demonstrates increased mitochondrial polarization as size and complexity increases. The comparison of TMRE high to low populations (Figure 19E) yields a curve similar that generated using JC-10 (Figure 19D). Comparison of the mean fluorescence intensity (MFI) using TMRE (Figure 19F) further demonstrates the lack of active mitochondria in population I.

Competing LT-HSC populations indicate differences in reconstitution ability

Finally, we sought to investigate how LT-HSCs from population I and III would repopulate an immunocompromised mouse. For this we utilized NOD,B6.SCID Il2rg$^{-/-}$ Kit$^{W41/W41}$ (NBSGW) mice, colloquially referred to as the “badger” mouse due their distinct coloration and that they were developed at UW-Madison. NOD *scid* gamma (NOD.Cg-*Prkdc*^{scid} *Il2rg*^{tm1Wjl}/SzJ, NSG) mice are highly immunodeficient with the *scid* and *Il2rg* mutations contributing to lymphocyte maturation and NK cell maturation respectively. The stem cell factor receptor, *c-kit*, is expressed on hematopoietic stem cells and is required for functional hematopoiesis. The NBSGW strain thus is immunocompromised and because of the addition of the *c-kit* mutation, contains space within the bone marrow niche for donor cells.

We chose to utilize populations I and III (Figure 20A-E) as these indicated the greatest difference in ROS production (Figure 17D), mitochondrial mass (Figure 18A-B) and mitochondrial membrane potential (Figure 19A-C) within the whole Lin- CD150+CD48- surface marker population.

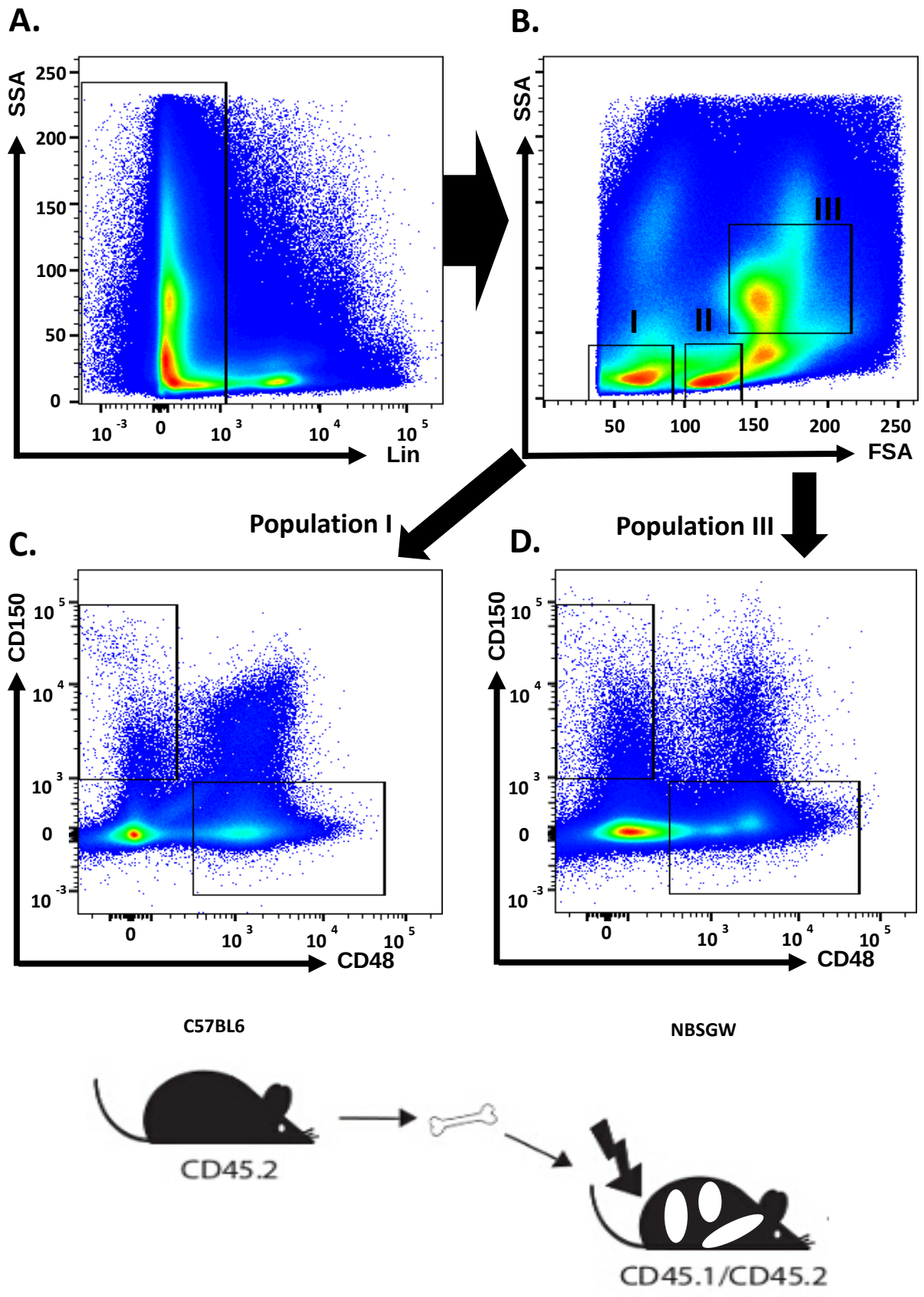
A.
B.
SSA
Lin
FSA
I
II
III
Population I
Population III
C.
D.
CD150
CD48
C57BL6
NBSGW
CD45.2
CD45.1/CD45.2

Figure 20

Sorting strategy for isolation of LT-HSCs. A. Lineage positive cells were excluded, and the size by complexity gating paradigm was structured (B). Lin-CD150+CD48- cells were sorted from populations I or III for injection into NBSGW mouse. E. NBSGW mice are on a CD45.1 background, hence C57BL6 were used. A limiting dilution was utilized with recipient mice receiving either 6000, 1000, or 600 LT-HSCs.

Our analysis based on our gating strategy indicates that the LT-HSCs collected from population I are indeed better at populating multiple lineages in the NBSGW model. While there was only a slight increase in CD45.2 cells in the whole bone marrow (Figure 21A), a more in-depth characterization of bone marrow cells showed a marked increase in B-cell precursor cells (Figure 21B).

We also wanted to analyze the spleen for T-cell populations since the NSBGW background contains the *scid* mutation which should lymphodeplete the recipient mouse. While there was an increase in the CD45.2+ population in the whole spleen (Figure 21C), both CD4+ and CD8+ populations are significantly increased in the mice that received the highest LT-HSC injection number from population I. By comparison, the same number of cells injected from population III failed to show any increase. While NBSGW mice are lymphodepleted, they maintain myeloid lineage cells, and we wanted to investigate if either population I or population III would contribute to this population as well. As shown in Figure 21E, there was an increase in granulocytes (GR-1+) only in the mice that received cells from population I.

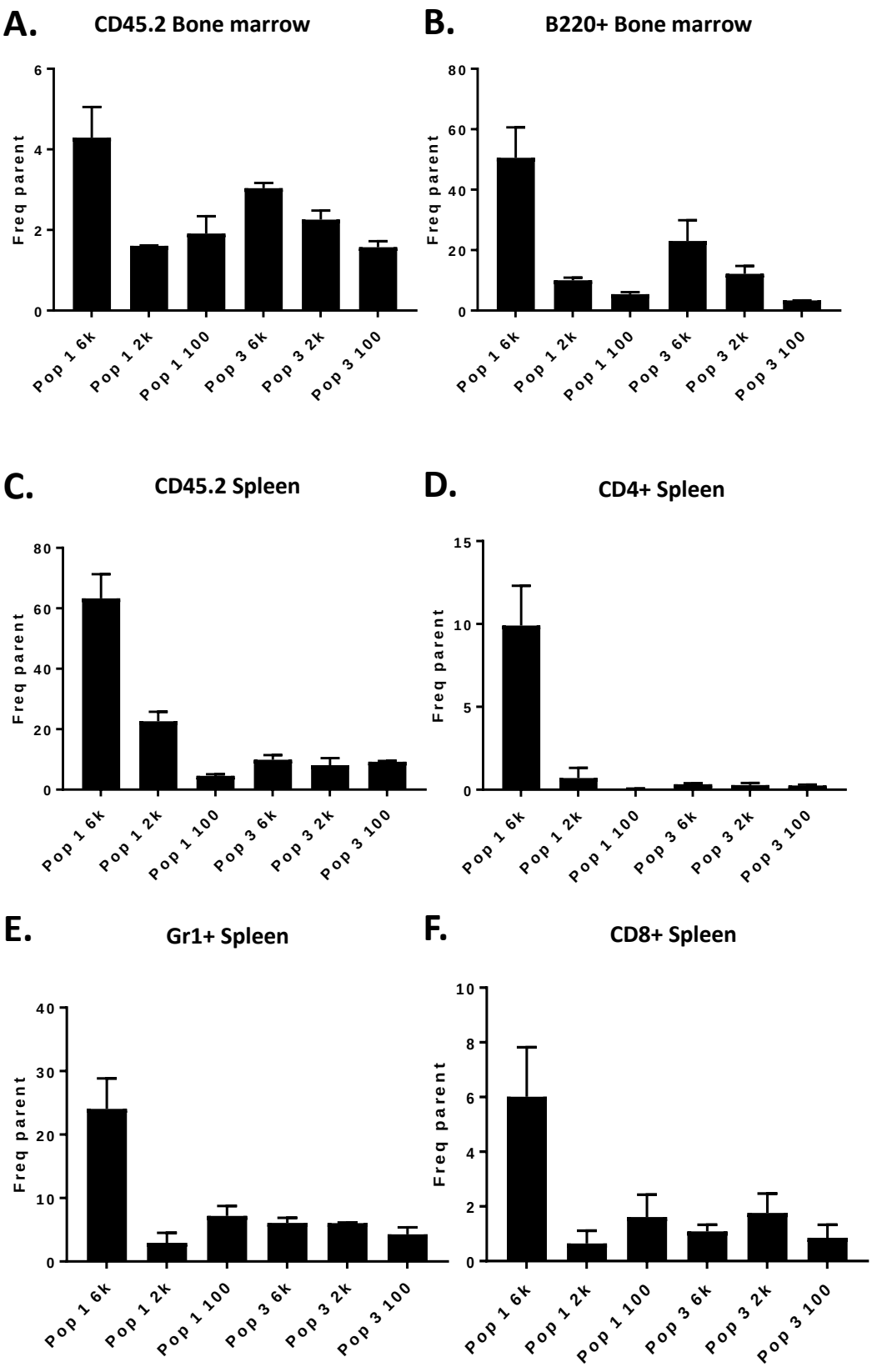
A.
CD45.2 Bone marrow
Freq parent
0
2
4
6
Pop 1 6k
Pop 1 2k
Pop 1 100
Pop 3 6k
Pop 3 2k
Pop 3 100
B.
B220+ Bone marrow
Freq parent
0
20
40
60
80
Pop 1 6k
Pop 1 2k
Pop 1 100
Pop 3 6k
Pop 3 2k
Pop 3 100
C.
CD45.2 Spleen
Freq parent
0
20
40
60
80
Pop 1 6k
Pop 1 2k
Pop 1 100
Pop 3 6k
Pop 3 2k
Pop 3 100
D.
CD4+ Spleen
Freq parent
0
5
10
15
Pop 1 6k
Pop 1 2k
Pop 1 100
Pop 3 6k
Pop 3 2k
Pop 3 100
E.
Gr1+ Spleen
Freq parent
0
10
20
30
40
Pop 1 6k
Pop 1 2k
Pop 1 100
Pop 3 6k
Pop 3 2k
Pop 3 100
F.
CD8+ Spleen
Freq parent
0
2
4
6
8
10
Pop 1 6k
Pop 1 2k
Pop 1 100
Pop 3 6k
Pop 3 2k
Pop 3 100

Figure 21

8 week analysis of chimeras. A. CD45.2 is represented as a percentage of all CD45+ cells. B. Bone marrow B-cell precursors (B220+). C-F. Analysis of speenic CD45.2 (C), CD4+ (D), GR-1+ (E), and CD8+ (F). B,D,E, and F are the frequency of that population that is also CD45.2.

DISCUSSION

In the current study, we sought to characterize LT-HSCs using combinations of physical characteristics, surface markers, mitochondrial phenotype and kinetic analysis of ROS production. ROS studies on isolated populations of cells requires that they first be sorted, a process which can damage cells. The advantage of testing ROS kinetics by flow cytometry is that it allows for the comparison of multiple populations. Using this method, we show that what is dogmatically referred to as an LT-HSC by SLAM surface markers (CD48 and CD150) is a highly heterogenous population with some cells showing very high ROS and others very low ROS. To investigate further, we devised a method of first separating LT-HSCs (Lin-CD150+CD48-) based on size and intracellular complexity. The results of these studies showed that LT-HSCs that are the smallest size and demonstrate the lowest intracellular complexity (population I) possess the characteristics that are thought to be specific for a long-term renewing hematopoietic stem cell. Due to the various complications of using one probe over another, we instead chose to test them against each other and found similar results. Both Mitotracker and nonyl-acridine orange staining demonstrated that LT-HSCs found in population I have the lowest mitochondrial mass. Similar results were seen when using the mitochondrial membrane potential probes JC-10 and TMRE. Our results are particularly striking when

compared against populations II and III, despite the whole population being investigated is labeled by surface marker as a LT-HSC.

While a number of studies have validated the use of SLAM markers to define murine long-term hematopoietic stem cells (Forsberg et al., 2005; Kiel et al., 2005; Kim et al., 2006a; Oguro et al., 2013; Yilmaz et al., 2006), the population remains functionally and phenotypically heterogenous. Kiel et al. demonstrated that 47% of LSK CD150+CD48- were capable of long term reconstitution (Kiel et al., 2005), in contrast to Nakauchi et al. that found 25% of CD34-LSK were LT-HSCs (Nakauchi, 2004). It is not that either study was flawed or incorrect, rather to illustrate that even when using 6 surface markers in the case of Kiel et al., the best we can generate is ~50% assuredness in LT-HSC population. Elegant studies have also been done using combinations of surface probes and mitochondrial stains which allowed for further characterization of the mitochondrial and metabolic phenotype of LT-HSCs (Simsek et al., 2010b; Vannini et al., 2016). The question of using mitochondrial mass as an indication of 'stem'ness remains unclear with some demonstrating lower mitochondrial mass in HSCs (Romero-Moya et al., 2013; Simsek et al., 2010b) and others indicating equal mass, but with lower activity (de Almeida et al., 2017). When evaluated collectively, the task becomes a matter of enrichment – how can we collect a heterogenous population of HSCs using existing markers that is more *enriched* for LT-HSCs.

The results are similar to the findings of those mentioned previously. who have demonstrated that surface marker labeling is insufficient to define a long-term self-renewing HSC. Our method was to use surface markers to label the heterogenous LT-

HSC population, and then separated based on physical characteristics. While there was no change in distribution of LT-HSCs, we further sought to characterize them using redox and mitochondrial probes.

While we hypothesize that size and intracellular complexity in addition to surface marker staining represents a more defined subset of long-term reconstituting cells, our results could also indicate that while LT-HSCs represent a heterogenous population, lymphoid-biased LT-HSCs are more likely to reside in one population over another.

CHAPTER 6

GENERAL DISCUSSION AND FUTURE STUDIES

Hematopoiesis, the process that produces all blood cells, is a finely-tuned balance of signals that determine whether a HSC will self-renew or differentiate, and further, differentiate into which type of blood cell. If the self-renewal/differentiation axis shifts towards the latter, then the HSCs will become prematurely exhausted. HSCs emerge during development, and perturbations during this window can have lifelong effects. The AHR is a transcription factor that, amongst other roles, contributes to the regulation of hematopoiesis. TCDD is a ubiquitous environmental contaminant and potent agonist of the AHR, thus exogenous agonism can affect the hematopoietic process.

In the research described here, we have shown two things. First, that surface marker staining of what are customarily LT-HSCs (Lin-CD150+CD48-) are different populations of cells in terms of size, intracellular complexity, reactive oxygen species production, and mitochondrial membrane potential, while possessing similar numbers of mitochondria. Secondly, by examining bone marrow, fetal and placental HSCs in vehicle, TCDD exposed, and AHR null mice, we were able to evaluate how AHR agonism and absence affects population dynamics and ROS production in multiple cell lineages.

A significant obstacle in the study of HSCs is how to identify an HSC. Methods have ranged from assessing cell cycle speed on the hypothesis that LT-HSCs ought to be cycling very rarely; to different combinations of surface markers. Despite decades of research, any sorted population of HSCs remains a heterogenous mix of long-, short-, and multipotent cells. It begs the question as to whether the customary descriptions of long-term, short-term, and multipotent, are, at best, broad classifications for what may

be more distinct subsets of cells. Our studies have shown that what we identify as LT-HSCs (Lin-CD150+CD48-) encompass numerous phenotypes of cells. Using a gating strategy the first segregated on size and intracellular complexity, we were able to phenotypically define LT-HSCs in each population, each with their own unique signature.

Nonyl-acridine orange (NAO) is a fluorescent probe that stains cardiolipin in mitochondria independent of membrane potential (Garcia Fernandez et al., 2004). In our investigations, we demonstrated that the smallest and least complex population of LT-HSCs exhibited low NAO fluorescence when compared against larger and more intracellularly complex populations. However, cardiolipin is used within to mitochondria to form and stabilize respiratory supercomplexes (Arnarez et al., 2016). Given that LT-HSCs are quiescent, it would be assumed that they have little need for highly energetic respiratory supercomplexes. Our data showed that based on this alone, LT-HSCs can be segregated into those containing high cardiolipin content, and those without. Similarly for probes used to assess mitochondrial membrane potential, again, the finding that LT-HSCs can be segregated into groups with an active membrane potential and those without. Our findings of LT-HSCs using our gating strategy show that population I, the smallest and least complex, are consistent with others who have demonstrated that HSCs contain the same number of mitochondria, however differ in terms of how they are utilized (Mantel et al., 2010b; Simsek et al., 2010b). Strikingly, what are defined by surface marker as LT-HSCs in population III are markedly different. Population III exhibits high membrane potential, high cardiolipin content, and high ROS-production – characteristics of differentiated cells, not HSCs.

Future examination into these populations should include analysis of the cell cycle. Presumably, population III would be cycling faster than population I, however this ought to be demonstrated empirically. Additionally worthwhile would be an examination of symmetric self-renewal vs. asymmetric self-renewal. LT-HSCs should produce a daughter cell that will terminally differentiate, and another that will replace the original. The rapid expansion of the HSC population in the placenta, and later in the AGM, suggest that HSCs are capable of symmetric self-renewal, that is, two daughter cells the replace the original absent of terminal differentiation. Whether the HSCs in population I and III are capable of symmetric and asymmetric self-renewal, or if 1 is more likely to produce a terminally differentiated daughter cell remains to be elucidated.

A thorough understanding of the role of AHR agonism or absence in HSCs must include the various sites and developmental time points of hematopoiesis. The fetal liver and placenta are sites of hematopoiesis before egress to the bone marrow shortly before birth, and by examining HSCs in each location can one get a better idea of the role of the AHR in HSCs. Similarly, a large pool of HSCs can be found in the placenta as early as gestational day 11 where there is an initial expansion before migration to the fetal liver. However, there are several methodological limitations in performing an analysis of this type. Whether one uses Lin-Sca1+cKIT+ or SLAM markers (Lin-CD150+CD48-) to identify HSCs, the result is a heterogenous mix with little understanding of how enriched one versus another is for LT-HSCs, and moreover, if this degree of enrichment changes between anatomical locations. Additionally, surface markers can change with developmental stage, Sca1 being expressed in GD14.5 LSKs, but relatively absent at GD11 (unpublished data). However, the greatest asset of flow

cytometry is the ability to look at numerous cell populations and combinations at the same time. Future work should use this ability specifically to ask, given any population of Lin- cells from the fetal liver represents a heterogenous mixture of HSCs, what combination of markers can be used to measure a specific effect of AHR agonism – whether by population change or ROS.

Our lab uses TCDD as the ultimate AHR agonist. However, the ever-increasing number of endogenous ligands should also be considered for future experiments as well. Having different affinities for AHR, and different metabolites, it is entirely possible that these would agonize AHR in unexpected ways. Moreover, the consequence of transient AHR agonism during development may yield more insights into the exact timing of how AHR perturbation affects HSC development.

With these findings in hand, we propose a modification to the current understanding of the AHR in HSCs. The vertebrate adaption of binding to exogenous compounds should not disguise the fact that the AHR, from its earliest days on earth, is required for, and during, development. The discoveries using potent AHR agonists could be interpreted another way – that AHR agonism is *removing* the AHR from this developmental role in stem cells. Discoveries using molecular knockout models point to this as well in HSCs, with increased proliferation, and more rapid aging. Our findings of increased HSC ROS in AHR-/- is especially noteworthy, since this could point towards the mechanism by which AHR serves as an intracellular metabolic sensor of mitochondrial activity. Lending additional strength to this argument are demonstrations of direct mitochondrial and AHR interaction (Hwang et al.; Tappenden et al., 2011, 2013). Using these findings to modify our idea, we propose that the AHR interacts

directly with mitochondria to act in such a way that it keeps mitochondrial activity at minimum; a requirement to maintain self-renewal in HSCs. If the AHR is removed either by knocking it out, or agonizing with TCDD, mitochondrial activity is increased, ROS is increased, and self-renewal becomes symmetric terminal differentiation. This affects the lifetime supply of HSCs required for the life of the organism.

Not covered in this research but equally important in AHR studies is its role as an endocrine disruptor. TCDD agonism can affect thyroid-, retinoid-, and estrogen-hormone signaling pathways (Rüegg et al., 2008; Swedenborg et al., 2009; Wahlström, 2008). It is worth noting that transcriptional activation of AHR and hormone receptors is very similar; both are found in the cytoplasm (or nucleus less commonly) bound to chaperones, both undergo a conformational change upon activation that leads to translocation, and both have respective binding partners in the nucleus. In theory then, AHR agonism can affect coactivator recruitment, or the metabolizing enzymes produced from the XRE can lead to premature degradation of hormone signals. This becomes especially relevant in the study of hematopoiesis since HSCs express receptors for androgens, estrogens, pituitary hormones, and gonadotropins (Abdelbaset-Ismail et al., 2016; Mierzejewska et al., 2015). So it ought to at least be considered that AHR agonism with TCDD is affecting the hematopoietic process in multiple and unexpected ways. Further research is needed to elucidate the hormonal regulation of hematopoiesis in development and the role of the AHR in this process.

Although we accounted for and considered many variables when designing our studies, the role of AHR in circadian rhythm may have been a confounding factor that could have affected our results. The PAS domain of the AHR belongs to a family of

environmental sensors that include many circadian proteins, and the clock genes, Circadian locomotor output cycles kaput (CLOCK) and Brain and muscle ARNT-like 1 (BMAL1), share structural similarities to AHR. Activated AHR can heterodimerize with BMAL1, which interferes with the normal CLOCK/BMAL1 function thereby affecting downstream genes related to circadian function (Xu et al., 2010). Moreover, additional studies have indicated that this AHR mediated alteration of circadian rhythm can affect metabolism (Jaeger et al., 2017). AHR and ARNT mRNA was found to rhythmically oscillate in murine HSCs and was perturbed by administration of TCDD (Garrett and Gasiewicz, 2006). Taken collectively, everything from the time of day the cells are harvested to collection and injection in a chimera could potentially be affected by circadian rhythm. How we mitigated this confounding potential was by starting our experiments around the same time every day, for every experiment.

References

Abdelbaset-Ismail, A., Suszynska, M., Borkowska, S., Adamiak, M., Ratajczak, J., Kucia, M., and Ratajczak, M.Z. (2016). Human haematopoietic stem/progenitor cells express several functional sex hormone receptors. J. Cell. Mol. Med. *20*, 134–146.

Abdollahi, H., Harris, L.J., Zhang, P., McIlhenny, S., Tulenko, T., and DiMuzio, P.J. (2011). The Role of Hypoxia in Stem Cell Differentiation and Therapeutics. J. Surg. Res. *165*, 112–117.

Abdullah, A., Maged, M., M, I.H.-I., I, A.O., Maha, H., Manal, A., and Hamza, H. (2019). Activation of aryl hydrocarbon receptor signaling by a novel agonist ameliorates autoimmune encephalomyelitis. PLOS ONE *14*, e0215981.

Adamo, L., Naveiras, O., Wenzel, P.L., McKinney-Freeman, S., Mack, P.J., Gracia-Sancho, J., Suchy-Dicey, A., Yoshimoto, M., Lensch, M.W., Yoder, M.C., et al. (2009). Biomechanical forces promote embryonic haematopoiesis. Nature *459*, 1131–1135.

Ahrenhoerster, L.S., Tate, E.R., Lakatos, P.A., Wang, X., and Laiosa, M.D. (2014). Developmental exposure to 2,3,7,8 tetrachlorodibenzo-p-dioxin attenuates capacity of hematopoietic stem cells to undergo lymphocyte differentiation. Toxicol. Appl. Pharmacol.

Alliot, F., Godin, I., and Pessac, B. (1999). Microglia derive from progenitors, originating from the yolk sac, and which proliferate in the brain. Brain Res. Dev. Brain Res. *117*, 145–152.

de Almeida, M.J., Luchsinger, L.L., Corrigan, D.J., Williams, L.J., and Snoeck, H.-W. (2017). Dye-Independent Methods Reveal Elevated Mitochondrial Mass in Hematopoietic Stem Cells. Cell Stem Cell *21*, 725-729.e4.

Alvarez-Silva, M., Belo-Diabangouaya, P., Salaün, J., and Dieterlen-Lièvre, F. (2003). Mouse placenta is a major hematopoietic organ. Development *130*, 5437–5444.

Aly, H.A.A., and Domènech, O. (2009). Cytotoxicity and mitochondrial dysfunction of 2,3,7,8-tetrachlorodibenzo-p-dioxin (TCDD) in isolated rat hepatocytes. Toxicol. Lett. *191*, 79–87.

Bárcena, A., Muench, M.O., Kapidzic, M., and Fisher, S.J. (2009). A new role for the human placenta as a hematopoietic site throughout gestation. Reprod. Sci. Thousand Oaks Calif *16*, 178–187.

Beedanagari, S.R., Taylor, R.T., and Hankinson, O. (2010). Differential regulation of the dioxin-induced Cyp1a1 and Cyp1b1 genes in mouse hepatoma and fibroblast cell lines. Toxicol. Lett. *194*, 26–33.

Bennett, J.A., Singh, K.P., Welle, S.L., Boule, L.A., Lawrence, B.P., and Gasiewicz, T.A. (2018). Conditional deletion of Ahr alters gene expression profiles in hematopoietic stem cells. PloS One *13*, e0206407.

Benson, J.M., and Shepherd, D.M. (2011). Aryl Hydrocarbon Receptor Activation by TCDD Reduces Inflammation Associated with Crohn's Disease. Toxicol. Sci. *120*, 68–78.

Boitano, A.E., Wang, J., Romeo, R., Bouchez, L.C., Parker, A.E., Sutton, S.E., Walker, J.R., Flaveny, C.A., Perdew, G.H., Denison, M.S., et al. (2010). Aryl Hydrocarbon Receptor Antagonists Promote the Expansion of Human Hematopoietic Stem Cells. Science *329*, 1345–1348.

Boverhof, D.R., Burgoon, L.D., Tashiro, C., Sharratt, B., Chittim, B., Harkema, J.R., Mendrick, D.L., and Zacharewski, T.R. (2006). Comparative toxicogenomic analysis of the hepatotoxic effects of TCDD in Sprague Dawley rats and C57BL/6 mice. Toxicol. Sci. Off. J. Soc. Toxicol. *94*, 398–416.

Brown, K., Xie, S., Qiu, X., Mohrin, M., Shin, J., Liu, Y., Zhang, D., Scadden, D.T., and Chen, D. (2013). SIRT3 reverses aging-associated degeneration. Cell Rep. *3*, 319–327.

Chen, C., Liu, Y., Liu, R., Ikenoue, T., Guan, K.-L., Liu, Y., and Zheng, P. (2008). TSC–mTOR maintains quiescence and function of hematopoietic stem cells by repressing mitochondrial biogenesis and reactive oxygen species. J. Exp. Med. *205*, 2397–2408.

Chen, C.-T., Hsu, S.-H., and Wei, Y.-H. (2012). Mitochondrial bioenergetic function and metabolic plasticity in stem cell differentiation and cellular reprogramming. Biochim. Biophys. Acta BBA - Gen. Subj. *1820*, 571–576.

Chen, M.J., Yokomizo, T., Zeigler, B., Dzierzak, E., and Speck, N.A. (2009). Runx1 is required for the endothelial to hematopoietic cell transition but not thereafter. Nature *457*, 887–891.

Ciriza, J., Thompson, H., Petrosian, R., Manilay, J.O., and García-Ojeda, M.E. (2013). The migration of hematopoietic progenitors from the fetal liver to the fetal bone marrow: Lessons learned and possible clinical applications. Exp. Hematol. *41*, 411–423.

Collins, J.J., Strauss, M.E., Levinskas, G.J., and Conner, P.R. (1993). The mortality experience of workers exposed to 2,3,7,8-tetrachlorodibenzo-p-dioxin in a trichlorophenol process accident. Epidemiol. Camb. Mass *4*, 7–13.

Cottet-Rousselle, C., Ronot, X., Leverve, X., and Mayol, J.-F. (2011). Cytometric assessment of mitochondria using fluorescent probes. Cytometry A *79A*, 405–425.

Duncan, A.W., Rattis, F.M., DiMascio, L.N., Congdon, K.L., Pazianos, G., Zhao, C., Yoon, K., Cook, J.M., Willert, K., Gaiano, N., et al. (2005). Integration of Notch and Wnt signaling in hematopoietic stem cell maintenance. Nat. Immunol. *6*, 314–322.

Dzierzak, E., and Robin, C. (2010). Placenta as a source of hematopoietic stem cells. Trends Mol. Med. *16*, 361–367.

Ferlini, C., and Scambia, G. (2007). Assay for apoptosis using the mitochondrial probes, Rhodamine123 and 10-N-nonyl acridine orange. Nat. Protoc. *2*, 3111–3114.

Fernandez-Salguero, P.M., Ward, J.M., Sundberg, J.P., and Gonzalez, F.J. (1997). Lesions of aryl-hydrocarbon receptor-deficient mice. Vet. Pathol. *34*, 605–614.

Fisher, M.T., Nagarkatti, M., and Nagarkatti, P.S. (2005). Aryl hydrocarbon receptor-dependent induction of loss of mitochondrial membrane potential in epididydimal spermatozoa by 2,3,7,8-tetrachlorodibenzo-p-dioxin (TCDD). Toxicol. Lett. *157*, 99–107.

Flesch-Janys, D., Steindorf, K., Gurn, P., and Becher, H. (1998). Estimation of the cumulated exposure to polychlorinated dibenzo-p-dioxins/furans and standardized mortality ratio analysis of cancer mortality by dose in an occupationally exposed cohort. Environ. Health Perspect. *106*, 655–662.

Forsberg, E.C., Prohaska, S.S., Katzman, S., Heffner, G.C., Stuart, J.M., and Weissman, I.L. (2005). Differential Expression of Novel Potential Regulators in Hematopoietic Stem Cells. PLoS Genet. *1*.

Funatake, C.J., Marshall, N.B., Steppan, L.B., Mourich, D.V., and Kerkvliet, N.I. (2005). Cutting edge: activation of the aryl hydrocarbon receptor by 2,3,7,8-tetrachlorodibenzo-p-dioxin generates a population of CD4+ CD25+ cells with characteristics of regulatory T cells. J. Immunol. Baltim. Md 1950 *175*, 4184–4188.

Gan, B., Hu, J., Jiang, S., Liu, Y., Sahin, E., Zhuang, L., Fletcher-Sananikone, E., Colla, S., Wang, Y.A., Chin, L., et al. (2010). Lkb1 regulates quiescence and metabolic homeostasis of haematopoietic stem cells. Nature *468*, 701–704.

Garcia Fernandez, M.I., Ceccarelli, D., and Muscatello, U. (2004). Use of the fluorescent dye 10-N-nonyl acridine orange in quantitative and location assays of cardiolipin: a study on different experimental models. Anal. Biochem. *328*, 174–180.

Garrett, R.W., and Gasiewicz, T.A. (2006). The Aryl Hydrocarbon Receptor Agonist 2,3,7,8-Tetrachlorodibenzo-p-dioxin Alters the Circadian Rhythms, Quiescence, and Expression of Clock Genes in Murine Hematopoietic Stem and Progenitor Cells. Mol. Pharmacol. *69*, 2076–2083.

Gasiewicz, T.A., Geiger, L.E., Rucci, G., and Neal, R.A. (1983). Distribution, excretion, and metabolism of 2,3,7,8-tetrachlorodibenzo-p-dioxin in C57BL/6J, DBA/2J, and B6D2F1/J mice. Drug Metab. Dispos. *11*, 397–403.

Gasiewicz, T.A., Singh, K.P., and Casado, F.L. (2010). The aryl hydrocarbon receptor has an important role in the regulation of hematopoiesis: Implications for benzene-induced hematopoietic toxicity. Chem. Biol. Interact. *184*, 246–251.

Gekas, C., Dieterlen-Lièvre, F., Orkin, S.H., and Mikkola, H.K.A. (2005). The Placenta Is a Niche for Hematopoietic Stem Cells. Dev. Cell *8*, 365–375.

Gekas, C., Rhodes, K.E., Vanhandel, B., Chhabra, A., Ueno, M., and Mikkola, H.K.A. (2010). Hematopoietic stem cell development in the placenta. Int. J. Dev. Biol. *54*, 1089–1098.

Godin, I., and Cumano, A. (2005). Of birds and mice: hematopoietic stem cell development. Int. J. Dev. Biol. *49*, 251–257.

Gomez Perdiguero, E., Klapproth, K., Schulz, C., Busch, K., Azzoni, E., Crozet, L., Garner, H., Trouillet, C., de Bruijn, M.F., Geissmann, F., et al. (2015). Tissue-resident macrophages originate from yolk sac-derived erythro-myeloid progenitors. Nature *518*, 547–551.

Gu, A., Torres-Coronado, M., Tran, C.-A., Vu, H., Epps, E.W., Chung, J., Gonzalez, N., Blanchard, S., and DiGiusto, D.L. (2014). Engraftment and lineage potential of adult hematopoietic stem and progenitor cells is compromised following short-term culture in the presence of an aryl hydrocarbon receptor antagonist. Hum. Gene Ther. Methods *25*, 221–231.

Hahn, M.E. (2002). Aryl hydrocarbon receptors: diversity and evolution. Chem. Biol. Interact. *141*, 131–160.

Harrill, J.A., Hukkanen, R.R., Lawson, M., Martin, G., Gilger, B., Soldatow, V., LeCluyse, E.L., Budinsky, R.A., Rowlands, J.C., and Thomas, R.S. (2013). Knockout of the aryl hydrocarbon receptor results in distinct hepatic and renal phenotypes in rats and mice. Toxicol. Appl. Pharmacol. *272*, 503–518.

Ho, T.T., Warr, M.R., Adelman, E.R., Lansinger, O.M., Flach, J., Verovskaya, E.V., Figueroa, M.E., and Passegué, E. (2017). Autophagy maintains the metabolism and function of young and old (hematopoietic) stem cells. Nature *543*, 205–210.

Hooiveld, M., Heederik, D.J., Kogevinas, M., Boffetta, P., Needham, L.L., Patterson, D.G., and Bueno-de-Mesquita, H.B. (1998). Second follow-up of a Dutch cohort occupationally exposed to phenoxy herbicides, chlorophenols, and contaminants. Am. J. Epidemiol. *147*, 891–901.

Hwang, H.J., Dornbos, P., Steidemann, M., Dunivin, T.K., Rizzo, M., and LaPres, J.J. Mitochondrial-targeted aryl hydrocarbon receptor and the impact of 2,3,7,8-tetrachlorodibenzo-p-dioxin on cellular respiration and the mitochondrial proteome. Toxicol. Appl. Pharmacol.

Iacovino, M., Chong, D., Szatmari, I., Hartweck, L., Rux, D., Caprioli, A., Cleaver, O., and Kyba, M. (2011). HoxA3 is an apical regulator of haemogenic endothelium. Nat. Cell Biol. *13*, 72–78.

Inoue, S.-I., Noda, S., Kashima, K., Nakada, K., Hayashi, J.-I., and Miyoshi, H. (2010). Mitochondrial respiration defects modulate differentiation but not proliferation of hematopoietic stem and progenitor cells. FEBS Lett. *584*, 3402–3409.

Ito, K., and Suda, T. (2014). Metabolic requirements for the maintenance of self-renewing stem cells. Nat. Rev. Mol. Cell Biol. *15*, 243–256.

Ito, K., Hirao, A., Arai, F., Matsuoka, S., Takubo, K., Hamaguchi, I., Nomiyama, K., Hosokawa, K., Sakurada, K., Nakagata, N., et al. (2004). Regulation of oxidative stress by ATM is required for self-renewal of haematopoietic stem cells. Nature *431*, 997–1002.

Ito, K., Hirao, A., Arai, F., Takubo, K., Matsuoka, S., Miyamoto, K., Ohmura, M., Naka, K., Hosokawa, K., Ikeda, Y., et al. (2006). Reactive oxygen species act through p38 MAPK to limit the lifespan of hematopoietic stem cells. Nat. Med. *12*, 446–451.

Ito, K., Carracedo, A., Weiss, D., Arai, F., Ala, U., Avigan, D.E., Schafer, Z.T., Evans, R.M., Suda, T., Lee, C.-H., et al. (2012). A PML–PPAR-δ pathway for fatty acid oxidation regulates hematopoietic stem cell maintenance. Nat. Med. *18*, 1350–1358.

Jacome-Galarza, C.E., Percin, G.I., Muller, J.T., Mass, E., Lazarov, T., Eitler, J., Rauner, M., Yadav, V.K., Crozet, L., Bohm, M., et al. (2019). Developmental origin, functional maintenance and genetic rescue of osteoclasts. Nature *568*, 541.

Jaeger, C., Khazaal, A.Q., Xu, C., Sun, M., Krager, S.L., and Tischkau, S.A. (2017). Aryl Hydrocarbon Receptor Deficiency Alters Circadian and Metabolic Rhythmicity. J. Biol. Rhythms *32*, 109–120.

Jang, Y.-Y., and Sharkis, S.J. (2007). A low level of reactive oxygen species selects for primitive hematopoietic stem cells that may reside in the low-oxygenic niche. Blood *110*, 3056–3063.

Jung, H., and Choi, I. (2014). Thioredoxin-interacting protein, hematopoietic stem cells, and hematopoiesis. Curr. Opin. Hematol. *21*, 265–270.

Juricek, L., and Coumoul, X. (2018). The Aryl Hydrocarbon Receptor and the Nervous System. Int. J. Mol. Sci. *19*.

Kainu, T., Gustafsson, J.A., and Pelto-Huikko, M. (1995). The dioxin receptor and its nuclear translocator (Arnt) in the rat brain. Neuroreport *6*, 2557–2560.

Katajisto, P., Dohla, J., Chaffer, C.L., Pentinmikko, N., Marjanovic, N., Iqbal, S., Zoncu, R., Chen, W., Weinberg, R.A., and Sabatini, D.M. (2015a). Asymmetric apportioning of aged mitochondria between daughter cells is required for stemness. Science *348*, 340–343.

Katajisto, P., Döhla, J., Chaffer, C., Pentinmikko, N., Marjanovic, N., Iqbal, S., Zoncu, R., Chen, W., Weinberg, R.A., and Sabatini, D.M. (2015b). Asymmetric apportioning of aged mitochondria between daughter cells is required for stemness. Science.

Kennedy, L.H., Sutter, C.H., Leon Carrion, S., Tran, Q.T., Bodreddigari, S., Kensicki, E., Mohney, R.P., and Sutter, T.R. (2012). 2,3,7,8-Tetrachlorodibenzo-p-dioxin-Mediated Production of Reactive Oxygen Species Is An Essential Step in the Mechanism of Action to Accelerate Human Keratinocyte Differentiation. Toxicol. Sci. *132*, 235–249.

Kerkvliet, N.I., Shepherd, D.M., and Baecher-Steppan, L. (2002). T lymphocytes are direct, aryl hydrocarbon receptor (AhR)-dependent targets of 2,3,7,8-tetrachlorodibenzo-p-dioxin (TCDD): AhR expression in both CD4+ and CD8+ T cells is necessary for full suppression of a cytotoxic T lymphocyte response by TCDD. Toxicol. Appl. Pharmacol. *185*, 146–152.

Kerkvliet, N.I., Steppan, L.B., Vorachek, W., Oda, S., Farrer, D., Wong, C.P., Pham, D., and Mourich, D.V. (2009). Activation of aryl hydrocarbon receptor by TCDD prevents diabetes in NOD mice and increases Foxp3+ T cells in pancreatic lymph nodes. Immunotherapy *1*, 539–547.

Kiel, M.J., Yilmaz, Ö.H., Iwashita, T., Yilmaz, O.H., Terhorst, C., and Morrison, S.J. (2005). SLAM Family Receptors Distinguish Hematopoietic Stem and Progenitor Cells and Reveal Endothelial Niches for Stem Cells. Cell *121*, 1109–1121.

Kim, I., He, S., Yilmaz, Ö.H., Kiel, M.J., and Morrison, S.J. (2006a). Enhanced purification of fetal liver hematopoietic stem cells using SLAM family receptors. Blood *108*, 737–744.

Kim, M.D., Jan, L.Y., and Jan, Y.N. (2006b). The bHLH-PAS protein Spineless is necessary for the diversification of dendrite morphology of Drosophila dendritic arborization neurons. Genes Dev. *20*, 2806–2819.

Kimura, E., and Tohyama, C. (2017). Embryonic and Postnatal Expression of Aryl Hydrocarbon Receptor mRNA in Mouse Brain. Front. Neuroanat. *11*, 4.

Kimura, A., Naka, T., Nakahama, T., Chinen, I., Masuda, K., Nohara, K., Fujii-Kuriyama, Y., and Kishimoto, T. (2009). Aryl hydrocarbon receptor in combination with Stat1 regulates LPS-induced inflammatory responses. J. Exp. Med. *206*, 2027–2035.

Kimura, E., Kubo, K.-I., Matsuyoshi, C., Benner, S., Hosokawa, M., Endo, T., Ling, W., Kohda, M., Yokoyama, K., Nakajima, K., et al. (2015). Developmental origin of abnormal dendritic growth in the mouse brain induced by in utero disruption of aryl hydrocarbon receptor signaling. Neurotoxicol. Teratol. *52*, 42–50.

Kimura, E., Ding, Y., and Tohyama, C. (2016). AhR signaling activation disrupts migration and dendritic growth of olfactory interneurons in the developing mouse. Sci. Rep. *6*, 26386.

Kumaravelu, P., Hook, L., Morrison, A.M., Ure, J., Zhao, S., Zuyev, S., Ansell, J., and Medvinsky, A. (2002). Quantitative developmental anatomy of definitive haematopoietic stem cells/long-term repopulating units (HSC/RUs): role of the aorta-gonad-mesonephros (AGM) region and the yolk sac in colonisation of the mouse embryonic liver. Development *129*, 4891–4899.

Laiosa, M.D., Tate, E.R., Ahrenhoerster, L.S., Chen, Y., and Wang, D. (2015). Effects of Developmental Activation of the Aryl Hydrocarbon Receptor by 2,3,7,8-Tetrachlorodibenzo-p-dioxin on Long-Term Self-Renewal of Murine Hematopoietic Stem Cells. Environ. Health Perspect.

Latchney, S.E., Hein, A.M., O'Banion, M.K., DiCicco-Bloom, E., and Opanashuk, L.A. (2013). Deletion or activation of the aryl hydrocarbon receptor alters adult hippocampal neurogenesis and contextual fear memory. J. Neurochem. *125*, 430–445.

Liem, A.K., Fürst, P., and Rappe, C. (2000). Exposure of populations to dioxins and related compounds. Food Addit. Contam. *17*, 241–259.

Liu, X., Zheng, H., Yu, W.-M., Cooper, T.M., Bunting, K.D., and Qu, C.-K. (2015). Maintenance of mouse hematopoietic stem cells ex vivo by reprogramming cellular metabolism. Blood *125*, 1562–1565.

Lobo, N.A., Shimono, Y., Qian, D., and Clarke, M.F. (2007). The Biology of Cancer Stem Cells. Annu. Rev. Cell Dev. Biol. *23*, 675–699.

Lux, C.T., Yoshimoto, M., McGrath, K., Conway, S.J., Palis, J., and Yoder, M.C. (2008). All primitive and definitive hematopoietic progenitor cells emerging before E10 in the mouse embryo are products of the yolk sac. Blood *111*, 3435–3438.

Mantel, C., Messina-Graham, S., and Broxmeyer, H.E. (2010a). Upregulation of nascent mitochondrial biogenesis in mouse hematopoietic stem cells parallels upregulation of CD34 and loss of pluripotency: a potential strategy for reducing oxidative risk in stem cells. Cell Cycle Georget. Tex *9*, 2008–2017.

Mantel, C., Messina-Graham, S., and Broxmeyer, H.E. (2010b). Upregulation of nascent mitochondrial biogenesis in mouse hematopoietic stem cells parallels upregulation of CD34 and loss of pluripotency: a potential strategy for reducing oxidative risk in stem cells. Cell Cycle Georget. Tex *9*, 2008–2017.

Maryanovich, M., Zaltsman, Y., Ruggiero, A., Goldman, A., Shachnai, L., Zaidman, S.L., Porat, Z., Golan, K., Lapidot, T., and Gross, A. (2015). An MTCH2 pathway repressing mitochondria metabolism regulates haematopoietic stem cell fate. Nat. Commun. *6*, 7901.

Michurina, T., Krasnov, P., Balazs, A., Nakaya, N., Vasilieva, T., Kuzin, B., Khrushchov, N., Mulligan, R.C., and Enikolopov, G. (2004). Nitric oxide is a regulator of hematopoietic stem cell activity. Mol. Ther. J. Am. Soc. Gene Ther. *10*, 241–248.

Mierzejewska, K., Borkowska, S., Suszynska, E., Suszynska, M., Poniewierska-Baran, A., Maj, M., Pedziwiatr, D., Adamiak, M., Abdel-Latif, A., Kakar, S.S., et al. (2015). Hematopoietic Stem/Progenitor Cells Express Several Functional Sex Hormone Receptors—Novel Evidence for a Potential Developmental Link Between Hematopoiesis and Primordial Germ Cells. Stem Cells Dev. 150303082601000.

Mikkola, H.K.A. (2006). The journey of developing hematopoietic stem cells. Development *133*, 3733–3744.

Miniero, R., De Felip, E., Ferri, F., and di Domenico, A. (2001). An overview of TCDD half-life in mammals and its correlation to body weight. Chemosphere *43*, 839–844.

Miyamoto, K., Araki, K.Y., Naka, K., Arai, F., Takubo, K., Yamazaki, S., Matsuoka, S., Miyamoto, T., Ito, K., Ohmura, M., et al. (2007). Foxo3a Is Essential for Maintenance of the Hematopoietic Stem Cell Pool. Cell Stem Cell *1*, 101–112.

Mortensen, M., Soilleux, E.J., Djordjevic, G., Tripp, R., Lutteropp, M., Sadighi-Akha, E., Stranks, A.J., Glanville, J., Knight, S., W. Jacobsen, S.-E., et al. (2011). The autophagy protein Atg7 is essential for hematopoietic stem cell maintenance. J. Exp. Med. *208*, 455–467.

Moura-Alves, P., Faé, K., Houthuys, E., Dorhoi, A., Kreuchwig, A., Furkert, J., Barison, N., Diehl, A., Munder, A., Constant, P., et al. (2014). AhR sensing of bacterial pigments regulates antibacterial defence. Nature *512*, 387–392.

Nakauchi, H. (2004). Isolation and Clonal Characterization of Hematopoietic and Liver Stem Cells. Cornea *23*.

National Academies of Sciences, Engineering, and Medicine, Health and Medicine Division, Board on Population Health and Public Health Practice, and Committee to Review the Health Effects in Vietnam Veterans of Exposure to Herbicides (Eleventh Biennial Update) (2018). Veterans and Agent Orange: Update 11 (2018) (Washington (DC): National Academies Press (US)).

Near, R.I., Matulka, R.A., Mann, K.K., Gogate, S.U., Trombino, A.F., and Sherr, D.H. (1999). Regulation of preB cell apoptosis by aryl hydrocarbon receptor/transcription factor-expressing stromal/adherent cells. Proc. Soc. Exp. Biol. Med. Soc. Exp. Biol. Med. N. Y. N *221*, 242–252.

Nombela-Arrieta, C., Pivarnik, G., Winkel, B., Canty, K.J., Harley, B., Mahoney, J.E., Park, S.-Y., Lu, J., Protopopov, A., and Silberstein, L.E. (2013). Quantitative imaging of haematopoietic stem and progenitor cell localization and hypoxic status in the bone marrow microenvironment. Nat. Cell Biol. *15*, 533–543.

Norddahl, G.L., Pronk, C.J., Wahlestedt, M., Sten, G., Nygren, J.M., Ugale, A., Sigvardsson, M., and Bryder, D. (2011). Accumulating Mitochondrial DNA Mutations Drive Premature Hematopoietic Aging Phenotypes Distinct from Physiological Stem Cell Aging. Cell Stem Cell *8*, 499–510.

North, T.E., Goessling, W., Peeters, M., Li, P., Ceol, C., Lord, A.M., Weber, G.J., Harris, J., Cutting, C.C., Huang, P., et al. (2009). Hematopoietic stem cell development is dependent on blood flow. Cell *137*, 736–748.

Ogawa, M. (1993). Differentiation and Proliferation of Hematopoietic Stem Cells. Hematop. STEM CELLS *81*, 2844–2853.

Oguro, H., Ding, L., and Morrison, S.J. (2013). SLAM family markers resolve functionally distinct subpopulations of hematopoietic stem cells and multipotent progenitors. Cell Stem Cell *13*, 102–116.

Olson, K.R., and Morton, L.W. (2019). Long-Term Fate of Agent Orange and Dioxin TCDD Contaminated Soils and Sediments in Vietnam Hotspots. Open J. Soil Sci. *9*, 1–34.

Ott, M.G., and Zober, A. (1996). Cause specific mortality and cancer incidence among employees exposed to 2,3,7,8-TCDD after a 1953 reactor accident. Occup. Environ. Med. *53*, 606–612.

Ottersbach, K., and Dzierzak, E. (2005). The murine placenta contains hematopoietic stem cells within the vascular labyrinth region. Dev. Cell *8*, 377–387.

Parmar, K., Mauch, P., Vergilio, J.-A., Sackstein, R., and Down, J.D. (2007). Distribution of hematopoietic stem cells in the bone marrow according to regional hypoxia. Proc. Natl. Acad. Sci. U. S. A. *104*, 5431–5436.

Perry, S.W., Norman, J.P., Barbieri, J., Brown, E.B., and Gelbard, H.A. (2011). Mitochondrial membrane potential probes and the proton gradient: a practical usage guide. BioTechniques *50*, 98–115.

Pesatori, A.C., Consonni, D., Rubagotti, M., Grillo, P., and Bertazzi, P.A. (2009). Cancer incidence in the population exposed to dioxin after the “Seveso accident”: twenty years of follow-up. Environ. Health *8*, 39.

Piccoli, C., Ria, R., Scrima, R., Cela, O., D’Aprile, A., Boffoli, D., Falzetti, F., Tabilio, A., and Capitanio, N. (2005). Characterization of Mitochondrial and Extra-mitochondrial Oxygen Consuming Reactions in Human Hematopoietic Stem Cells NOVEL EVIDENCE OF THE OCCURRENCE OF NAD(P)H OXIDASE ACTIVITY. J. Biol. Chem. *280*, 26467–26476.

Piccoli, C., D’Aprile, A., Ripoli, M., Scrima, R., Boffoli, D., Tabilio, A., and Capitanio, N. (2007). The hypoxia-inducible factor is stabilized in circulating hematopoietic stem cells under normoxic conditions. FEBS Lett. *581*, 3111–3119.

Poland, A., and Kende, A. (1976). 2,3,7,8-Tetrachlorodibenzo-p-dioxin: environmental contaminant and molecular probe. Fed. Proc. *35*, 2404–2411.

Qin, H., and Powell-Coffman, J.A. (2004). The Caenorhabditis elegans aryl hydrocarbon receptor, AHR-1, regulates neuronal development. Dev. Biol. *270*, 64–75.

Quintana, F.J., Basso, A.S., Iglesias, A.H., Korn, T., Farez, M.F., Bettelli, E., Caccamo, M., Oukka, M., and Weiner, H.L. (2008). Control of T(reg) and T(H)17 cell differentiation by the aryl hydrocarbon receptor. Nature *453*, 65–71.

Quintana, F.J., Yeste, A., and Mascanfroni, I.D. (2015). Role and therapeutic value of dendritic cells in central nervous system autoimmunity. Cell Death Differ. *22*, 215–224.

Ramirez, J.-M., Brembilla, N.C., Sorg, O., Chicheportiche, R., Matthes, T., Dayer, J.-M., Saurat, J.-H., Roosnek, E., and Chizzolini, C. (2010). Activation of the aryl hydrocarbon receptor reveals distinct requirements for IL-22 and IL-17 production by human T helper cells. Eur. J. Immunol. *40*, 2450–2459.

Robin, C., Bollerot, K., Mendes, S., Haak, E., Crisan, M., Cerisoli, F., Lauw, I., Kaimakis, P., Jorna, R., Vermeulen, M., et al. (2009). Human placenta is a potent hematopoietic niche containing hematopoietic stem and progenitor cells throughout development. Cell Stem Cell *5*, 385–395.

Romero-Moya, D., Bueno, C., Montes, R., Navarro-Montero, O., Iborra, F.J., López, L.C., Martin, M., and Menendez, P. (2013). Cord blood-derived CD34+ hematopoietic cells with low mitochondrial mass are enriched in hematopoietic repopulating stem cell function. Haematologica *98*, 1022–1029.

Rüegg, J., Swedenborg, E., Wahlström, D., Escande, A., Balaguer, P., Pettersson, K., and Pongratz, I. (2008). The transcription factor aryl hydrocarbon receptor nuclear translocator functions as an estrogen receptor beta-selective coactivator, and its recruitment to alternative pathways mediates antiestrogenic effects of dioxin. Mol. Endocrinol. Baltim. Md *22*, 304–316.

Rybtsov, S., Sobiesiak, M., Taoudi, S., Souilhol, C., Senserrich, J., Liakhovitskaia, A., Ivanovs, A., Frampton, J., Zhao, S., and Medvinsky, A. (2011). Hierarchical organization and early hematopoietic specification of the developing HSC lineage in the AGM region. J. Exp. Med. *208*, 1305–1315.

Sakai, R., Kajiume, T., Inoue, H., Kanno, R., Miyazaki, M., Ninomiya, Y., and Kanno, M. (2003). TCDD Treatment Eliminates the Long-Term Reconstitution Activity of Hematopoietic Stem Cells. Toxicol. Sci. *72*, 84–91.

Samokhvalov, I.M., Samokhvalova, N.I., and Nishikawa, S. (2007). Cell tracing shows the contribution of the yolk sac to adult haematopoiesis. Nature *446*, 1056–1061.

Schmidt, J.V., Su, G.H., Reddy, J.K., Simon, M.C., and Bradfield, C.A. (1996). Characterization of a murine Ahr null allele: involvement of the Ah receptor in hepatic growth and development. Proc. Natl. Acad. Sci. U. S. A. *93*, 6731–6736.

Senft, A.P., Dalton, T.P., Nebert, D.W., Genter, M.B., Hutchinson, R.J., and Shertzer, H.G. (2002a). Dioxin increases reactive oxygen production in mouse liver mitochondria. Toxicol. Appl. Pharmacol. *178*, 15–21.

Senft, A.P., Dalton, T.P., Nebert, D.W., Genter, M.B., Puga, A., Hutchinson, R.J., Kerzee, J.K., Uno, S., and Shertzer, H.G. (2002b). Mitochondrial reactive oxygen production is dependent on the aromatic hydrocarbon receptor. Free Radic. Biol. Med. *33*, 1268–1278.

Simsek, T., Kocabas, F., Zheng, J., DeBerardinis, R.J., Mahmoud, A.I., Olson, E.N., Schneider, J.W., Zhang, C.C., and Sadek, H.A. (2010a). The Distinct Metabolic Profile of Hematopoietic Stem Cells Reflects Their Location in a Hypoxic Niche. Cell Stem Cell *7*, 380–390.

Simsek, T., Kocabas, F., Zheng, J., DeBerardinis, R.J., Mahmoud, A.I., Olson, E.N., Schneider, J.W., Zhang, C.C., and Sadek, H.A. (2010b). The Distinct Metabolic Profile of Hematopoietic Stem Cells Reflects Their Location in a Hypoxic Niche. Cell Stem Cell *7*, 380–390.

Singh, K.P., Casado, F.L., Opanashuk, L.A., and Gasiewicz, T.A. (2009). The Aryl Hydrocarbon Receptor has a Normal Function in the Regulation of Hematopoietic and Other Stem/Progenitor Cell Populations. Biochem. Pharmacol. *77*, 577–587.

Singh, K.P., Garrett, R.W., Casado, F.L., and Gasiewicz, T.A. (2011). Aryl Hydrocarbon Receptor-Null Allele Mice Have Hematopoietic Stem/Progenitor Cells with Abnormal Characteristics and Functions. Stem Cells Dev. *20*, 769–784.

Singh, K.P., Bennett, J.A., Casado, F.L., Walrath, J.L., Welle, S.L., and Gasiewicz, T.A. (2014). Loss of aryl hydrocarbon receptor promotes gene changes associated with premature hematopoietic stem cell exhaustion and development of a myeloproliferative disorder in aging mice. Stem Cells Dev. *23*, 95–106.

Snoeck, H.-W. (2017). Mitochondrial regulation of hematopoietic stem cells. Curr. Opin. Cell Biol. *49*, 91–98.

Srivastava, A., Shinn, A.S., Lee, P.J., and Mannam, P. (2015). MKK3 mediates inflammatory response through modulation of mitochondrial function. Free Radic. Biol. Med. *83*, 139–148.

Suda, T., Takubo, K., and Semenza, G.L. (2011). Metabolic Regulation of Hematopoietic Stem Cells in the Hypoxic Niche. Cell Stem Cell *9*, 298–310.

Sudo, K., Ema, H., Morita, Y., and Nakauchi, H. (2000). Age-associated characteristics of murine hematopoietic stem cells. J. Exp. Med. *192*, 1273–1280.

Swedenborg, E., Rüegg, J., Mäkelä, S., and Pongratz, I. (2009). Endocrine disruptive chemicals: mechanisms of action and involvement in metabolic disorders. J. Mol. Endocrinol. *43*, 1–10.

Takubo, K., Nagamatsu, G., Kobayashi, C.I., Nakamura-Ishizu, A., Kobayashi, H., Ikeda, E., Goda, N., Rahimi, Y., Johnson, R.S., Soga, T., et al. (2013). Regulation of Glycolysis by Pdk Functions as a Metabolic Checkpoint for Cell Cycle Quiescence in Hematopoietic Stem Cells. Cell Stem Cell *12*, 49–61.

Tappenden, D.M., Lynn, S.G., Crawford, R.B., Lee, K., Vengellur, A., Kaminski, N.E., Thomas, R.S., and LaPres, J.J. (2011). The aryl hydrocarbon receptor interacts with ATP5α1, a subunit of the ATP synthase complex, and modulates mitochondrial function. Toxicol. Appl. Pharmacol. *254*, 299–310.

Tappenden, D.M., Hwang, H.J., Yang, L., Thomas, R.S., and LaPres, J.J. (2013). The Aryl-Hydrocarbon Receptor Protein Interaction Network (AHR-PIN) as Identified by Tandem Affinity Purification (TAP) and Mass Spectrometry. J. Toxicol. *2013*, e279829.

Tavian, M., and Peault, B. (2005). Embryonic development of the human hematopoietic system. Int. J. Dev. Biol. *49*, 243–250.

Thomsen, J.S., Kietz, S., Ström, A., and Gustafsson, J.-\AAke (2004). HES-1, a novel target gene for the aryl hydrocarbon receptor. Mol. Pharmacol. *65*, 165–171.

Vaidyanathan, B., Chaudhry, A., Yewdell, W.T., Angeletti, D., Yen, W.-F., Wheatley, A.K., Bradfield, C.A., McDermott, A.B., Yewdell, J.W., Rudensky, A.Y., et al. (2017). The aryl hydrocarbon receptor controls cell-fate decisions in B cells. J. Exp. Med. *214*, 197–208.

Vannini, N., Girotra, M., Naveiras, O., Nikitin, G., Campos, V., Giger, S., Roch, A., Auwerx, J., and Lutolf, M.P. (2016). Specification of haematopoietic stem cell fate via modulation of mitochondrial activity. Nat. Commun. *7*, 13125.

Vásquez-Vivar, J. (2009). Tetrahydrobiopterin, Superoxide and Vascular Dysfunction. Free Radic. Biol. Med. *47*, 1108–1119.

Veldhoen, M., Hirota, K., Westendorf, A.M., Buer, J., Dumoutier, L., Renauld, J.-C., and Stockinger, B. (2008). The aryl hydrocarbon receptor links TH17-cell-mediated autoimmunity to environmental toxins. Nature *453*, 106–109.

Venezia, T.A., Merchant, A.A., Ramos, C.A., Whitehouse, N.L., Young, A.S., Shaw, C.A., and Goodell, M.A. (2004). Molecular Signatures of Proliferation and Quiescence in Hematopoietic Stem Cells. PLoS Biol. *2*.

Villa, M., Gialitakis, M., Tolaini, M., Ahlfors, H., Henderson, C.J., Wolf, C.R., Brink, R., and Stockinger, B. (2017). Aryl hydrocarbon receptor is required for optimal B-cell proliferation. EMBO J. *36*, 116–128.

Vorderstrasse, B.A., and Lawrence, B.P. (2006). Protection against lethal challenge with Streptococcus pneumoniae is conferred by aryl hydrocarbon receptor activation but is not associated with an enhanced inflammatory response. Infect. Immun. *74*, 5679–5686.

Vorderstrasse, B.A., Cundiff, J.A., and Lawrence, B.P. (2004). Developmental exposure to the potent aryl hydrocarbon receptor agonist 2,3,7,8-tetrachlorodibenzo-p-dioxin Impairs the cell-mediated immune response to infection with influenza a virus, but enhances elements of innate immunity. J. Immunotoxicol. *1*, 103–112.

Wahlström, D. (2008). Molecular mechanisms of AhR mediated endocrine disruption of estrogen and retinoic acid signalling pathways (Institutet för miljömedicin (IMM) / Institute of Enviromental Medicine).

Weber, H., and Birnbaum, L.S. (1985). 2,3,7,8-Tetrachlorodibenzo-p-dioxin (TCDD) and 2,3,7,8-tetrachlorodibenzofuran (TCDF) in pregnant C57BL/6N mice: distribution to the embryo and excretion. Arch. Toxicol. *57*, 159–162.

Wernet, M.F., Mazzoni, E.O., Çelik, A., Duncan, D.M., Duncan, I., and Desplan, C. (2006). Stochastic spineless expression creates the retinal mosaic for colour vision. Nature *440*, 174–180.

Wilson, A., Laurenti, E., Oser, G., van der Wath, R.C., Blanco-Bose, W., Jaworski, M., Offner, S., Dunant, C.F., Eshkind, L., Bockamp, E., et al. (2008). Hematopoietic Stem Cells Reversibly Switch from Dormancy to Self-Renewal during Homeostasis and Repair. Cell *135*, 1118–1129.

Winkler, I.G., Barbier, V., Wadley, R., Zannettino, A.C.W., Williams, S., and Levesque, J.-P. (2010). Positioning of bone marrow hematopoietic and stromal cells relative to blood flow in vivo: serially reconstituting hematopoietic stem cells reside in distinct nonperfused niches. Blood *116*, 375–385.

Xu, C.-X., Krager, S.L., Liao, D.-F., and Tischkau, S.A. (2010). Disruption of CLOCK-BMAL1 Transcriptional Activity Is Responsible for Aryl Hydrocarbon Receptor–Mediated Regulation of Period1 Gene. Toxicol. Sci. *115*, 98–108.

Yilmaz, Ö.H., Kiel, M.J., and Morrison, S.J. (2006). SLAM family markers are conserved among hematopoietic stem cells from old and reconstituted mice and markedly increase their purity. Blood *107*, 924–930.

Yoshimoto, M., Montecino-Rodriguez, E., Ferkowicz, M.J., Porayette, P., Shelley, W.C., Conway, S.J., Dorshkind, K., and Yoder, M.C. (2011). Embryonic day 9 yolk sac and intra-embryonic hemogenic endothelium independently generate a B-1 and marginal zone progenitor lacking B-2 potential. Proc. Natl. Acad. Sci. U. S. A. *108*, 1468–1473.

Yoshimoto, M., Porayette, P., Glosson, N.L., Conway, S.J., Carlesso, N., Cardoso, A.A., Kaplan, M.H., and Yoder, M.C. (2012). Autonomous murine T-cell progenitor production in the extra-embryonic yolk sac before HSC emergence. Blood *119*, 5706–5714.

Yu, W.-M., Liu, X., Shen, J., Jovanovic, O., Pohl, E.E., Gerson, S.L., Finkel, T., Broxmeyer, H.E., and Qu, C.-K. (2013). Metabolic Regulation by the Mitochondrial Phosphatase PTPMT1 Is Required for Hematopoietic Stem Cell Differentiation. Cell Stem Cell *12*, 62–74.

Zhou, Y., Li, S., Huang, L., Yang, Y., Zhang, L., Yang, M., Liu, W., Ramasamy, K., Jiang, Z., Sundaresan, P., et al. (2018). A splicing mutation in aryl hydrocarbon receptor associated with retinitis pigmentosa. Hum. Mol. Genet. *27*, 2563–2572.

Everett Tate

Education

Ph.D. Environmental Health Science
December 2019
Joseph J. Zilber School of Public Health

B.A. Ancient Philosophy
December 2004
Marquette University

Publications

1. Yu F, Molino S, Sikora J, Rasmussen S, Rybova J, Tate E, Geurts A, Turner P, McKillop WM, Medin J. Hepatic pathology and altered gene transcription in a murine model of acid ceramidase deficiency. *Laboratory Investigation*. (Accepted for publication)

2. Molino S, Tate E, McKillop WM, Medin JA. Sphingolipid pathway enzymes modulate cell fate and immune responses. *Immunotherapy*. 2017 Nov 9

3. Laiosa MD, Tate ER, Ahrenhoerster LS, Chen Y, Wang D. Effects of Developmental Activation of the Aryl Hydrocarbon Receptor by 2,3,7,8-Tetrachlorodibenzo-*p*-dioxin on Long-Term Self-Renewal of Murine Hematopoietic Stem Cells. *Environ Health Perspect*. 2015 Oct 23.

4. Laiosa MD, Tate ER. Fetal Hematopoietic Stem Cells Are the Canaries in the Coal Mine That Portend Later Life Immune Deficiency. *Endocrinology*. 2015 Oct;156(10):3458-65.

5. Ahrenhoerster L.S., Leuthner T.C., Tate E.R., Lakatos P.A., Laiosa M.D. (2014)

Developmental Exposure To 2,3,7,8 Tetrachlorodibenzo-p-Dioxin Attenuates Later-Life Notch1-Mediated T Cell Development and Leukemogenesis. *Toxicology and Applied Pharmacology,* 2015 Mar 1;283(2):99-108.

6. Rymaszewski AL, Tate E, Yimbesalu JP, Gelman AE, Jarzembowski JA, Zhang H, Pritchard KA Jr, Vikis HG. The role of neutrophil myeloperoxidase in models of lung tumor development. Cancers (Basel). 2014 May 9;6(2):1111-27.

7. Ahrenhoerster LS, Tate ER, Lakatos PA, Wang X, Laiosa MD. Developmental exposure to 2,3,7,8 tetrachlorodibenzo-p-dioxin attenuates capacity of hematopoietic stem cells to undergo lymphocyte differentiation. Toxicol Appl Pharmacol. 2014 Jun 1;277(2):172-82.

8. James MA, Vikis HG, Tate E, Rymaszewski AL, You M. CRR9/CLPTM1L regulates cell survival signaling and is required for Ras transformation and lung tumorigenesis. Cancer Res. 2014 Feb 15;74(4):1116-27.

9. Menden H, Tate E, Hogg N, Sampath V. LPS-mediated endothelial activation in pulmonary endothelial cells: role of Nox2-dependent IKK-β phosphorylation. Am J Physiol Lung Cell Mol Physiol. 2013 Mar 15;304(6):L445-55.

Research Experience

2013-2019 Graduate Research Assistant (PhD Candidate)

Laboratory for Developmental Immunotoxicology,

Dr. Michael Laiosa

2016-2018 Research Associate

Department of Pediatrics

Dr. Jeffrey Medin

2013-2013 Research Specialist

Laboratory for Developmental Immunotoxicology

Dr. Michael Laiosa

2011-2013 Research Technologist II

Department of Pharmacology and Toxicology

Carcinogenesis and Chemoprevention

Dr. Haris Vikis

2010-2011 Research Technologist II

Department of Pediatrics, Neonatology

Dr. Venkatesh Sampath

2008-2010 Research Technologist I

Department of Biophysics/Redox Biology

Dr. Jeanette Vasquez-Vivar